Sluch a rovnováha

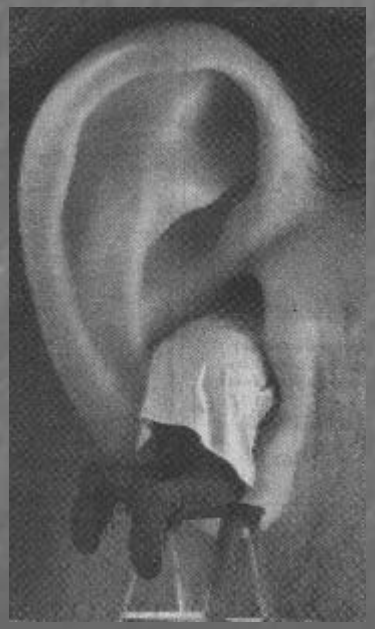

Vlásková buňka:
Mimořádný mechanoreceptor obratlovců (10^{-10} – 10^{-12}m)

postranní čára
vestibulární aparát
Cortiho orgán

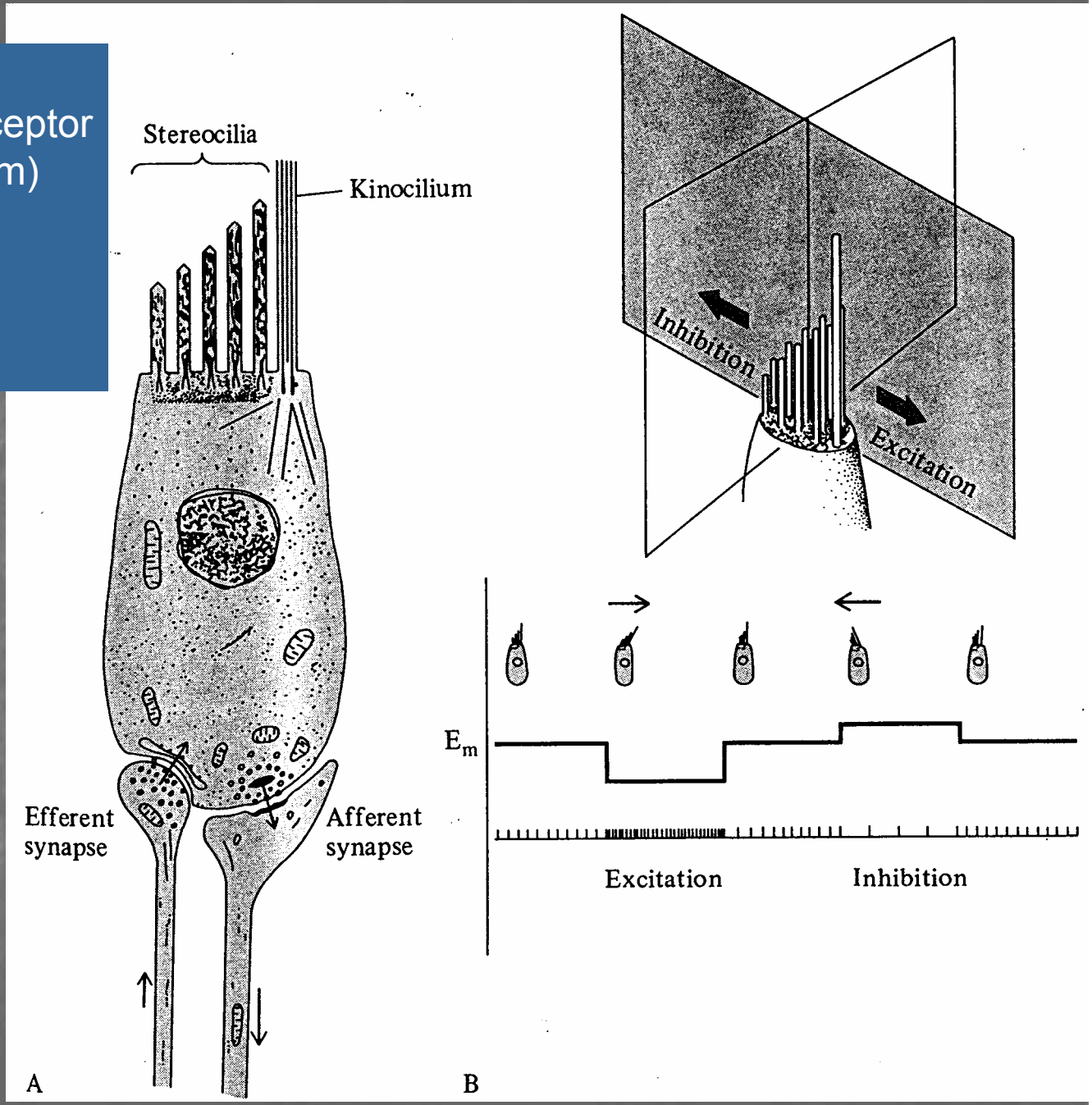

Anatomie a terminologie

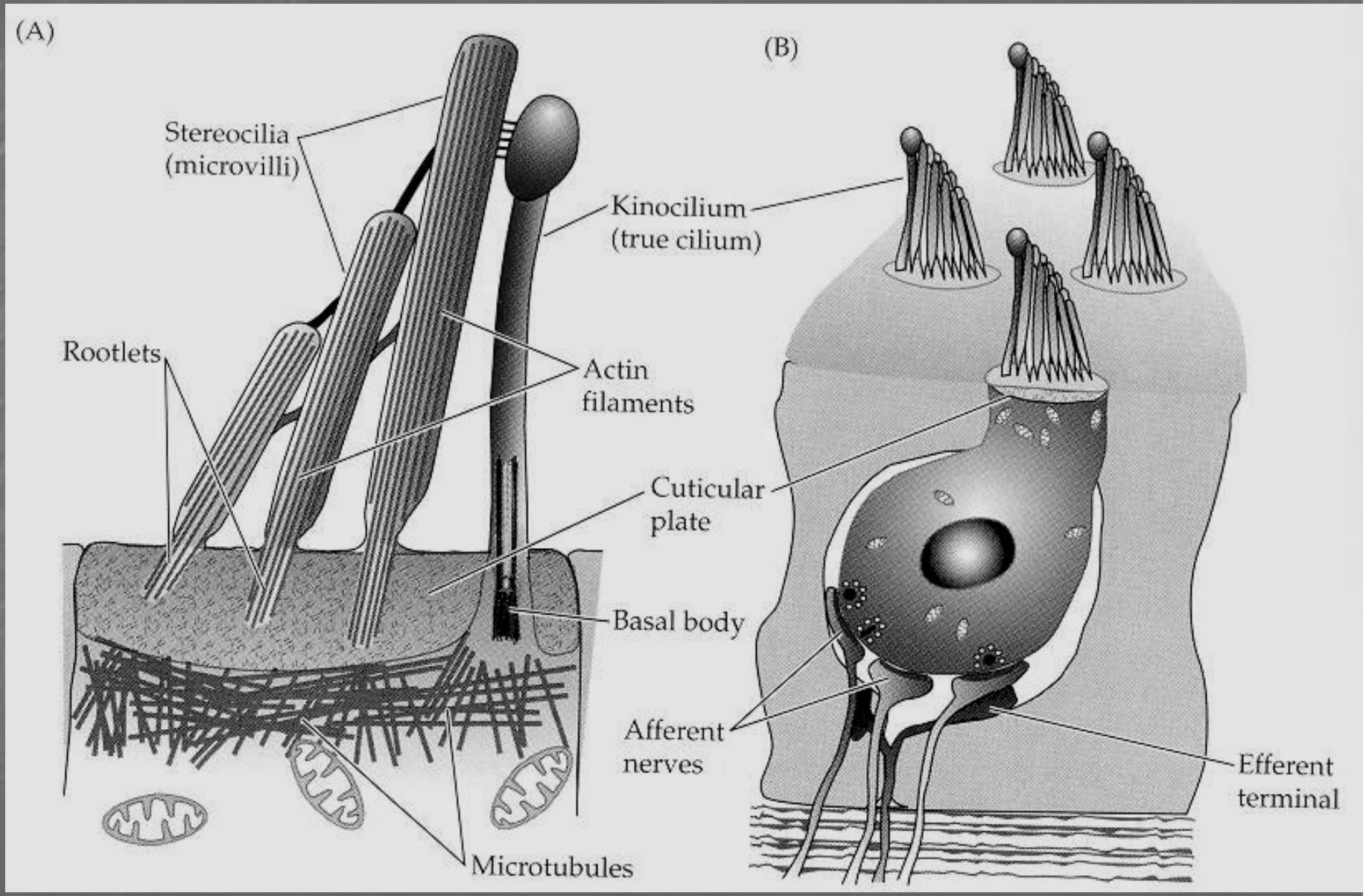

Mikrovily

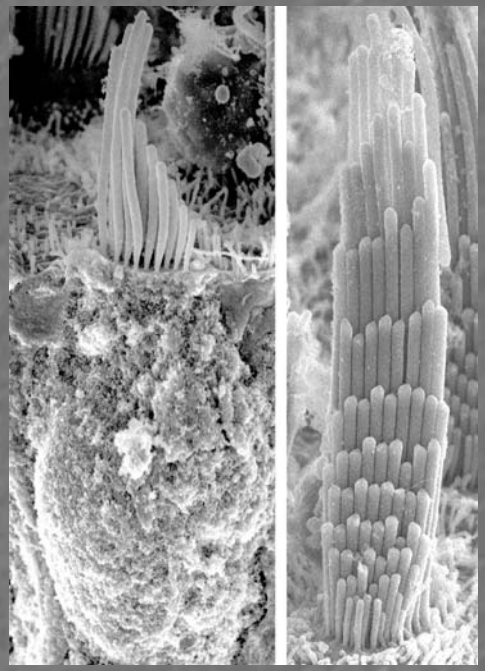

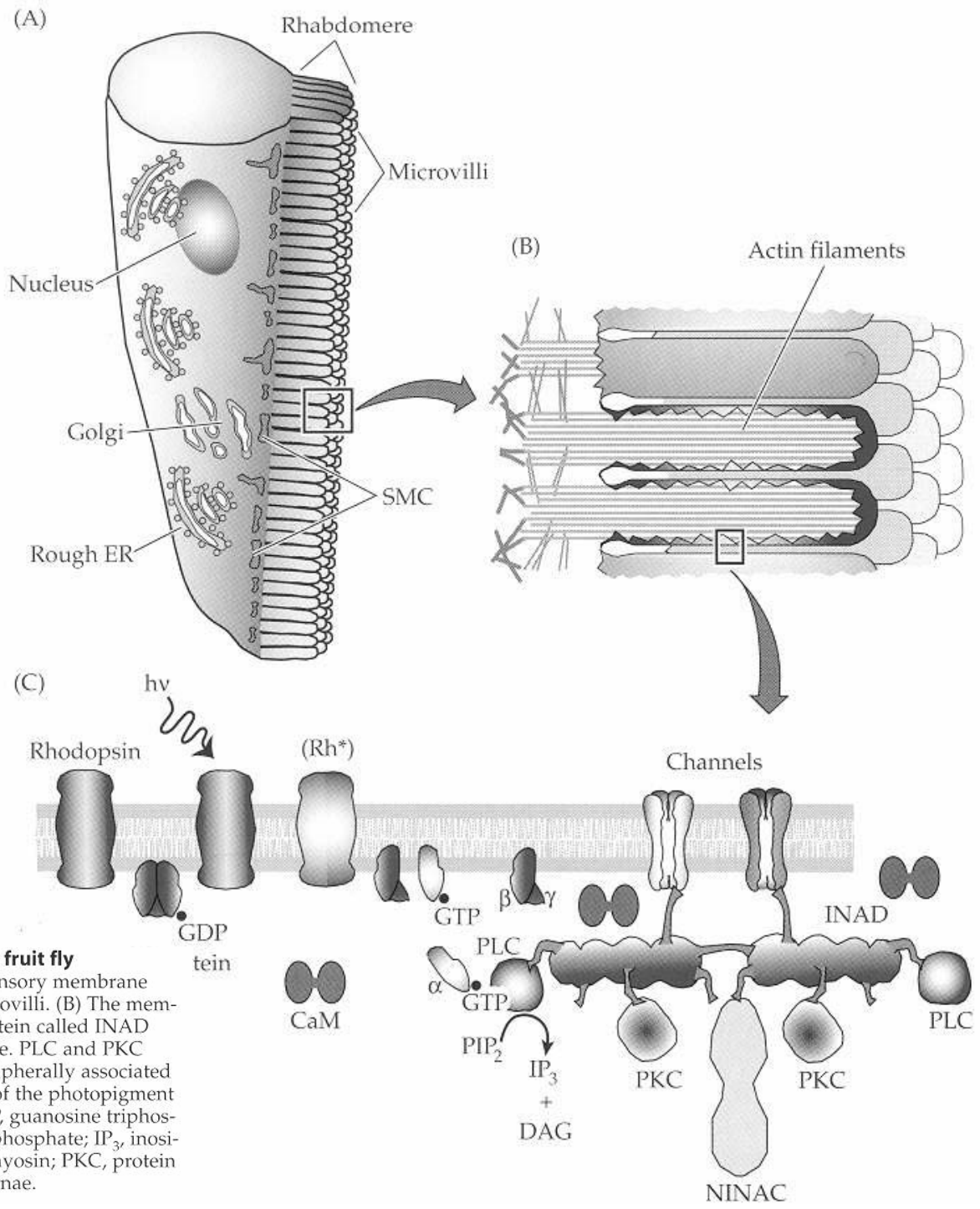

Organization of sensory membrane of a photoreceptor in the fruit fly *Drosophila* (A) Anatomy of a *Drosophila* photoreceptor. The sensory membrane forms a structure, called a rhabdomere, composed of 50,000 microvilli. (B) The membrane of the microvillus is highly organized by a scaffolding protein called INAD (C), which binds to proteins in the cytosol and plasma membrane. PLC and PKC proteins are shown as if cytosolic but are likely to be at least peripherally associated with the plasma membrane. Abbreviations: Rh^*, activated form of the photopigment rhodopsin; GDP, guanosine diphosphate; CaM, calmodulin; GTP, guanosine triphosphate; PLC, phospholipase C; PIP_2, phosphatidylinositol 4,5-bisphosphate; IP_3, inositol 1,4,5-triphosphate; DAG, diacylglycerol; NINAC, a form of myosin; PKC, protein kinase C; ER, endoplasmic reticulum; SMC, submicrovillar cisternae.

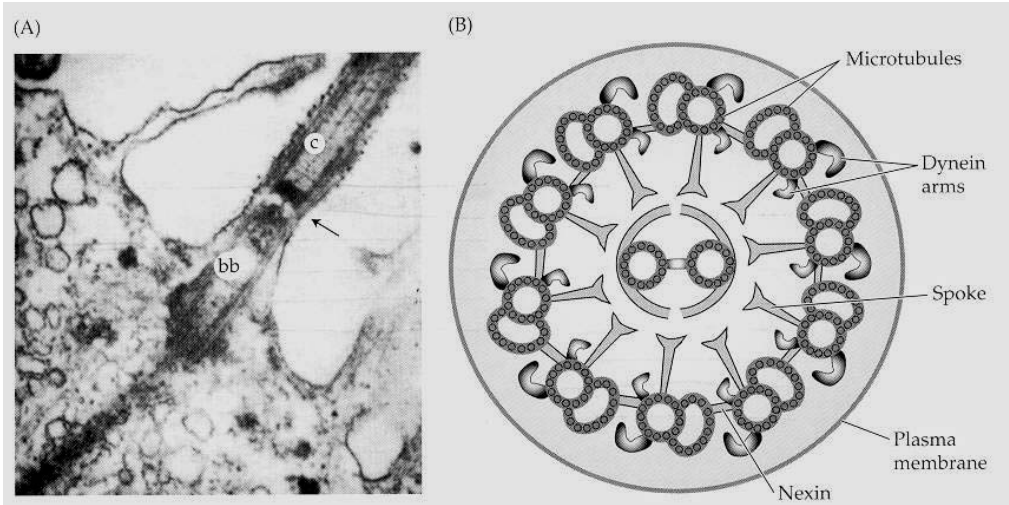

Figure 2.3
Cilium (A) Structure of a cilium from a sea urchin embryo. Note the basal body (bb) at the base of the cilium (c). Magnification 22,000×. (B) Schematic drawing of a cross section of cilium. (A from Chakrabarti et. al., 1998.)

Cilie

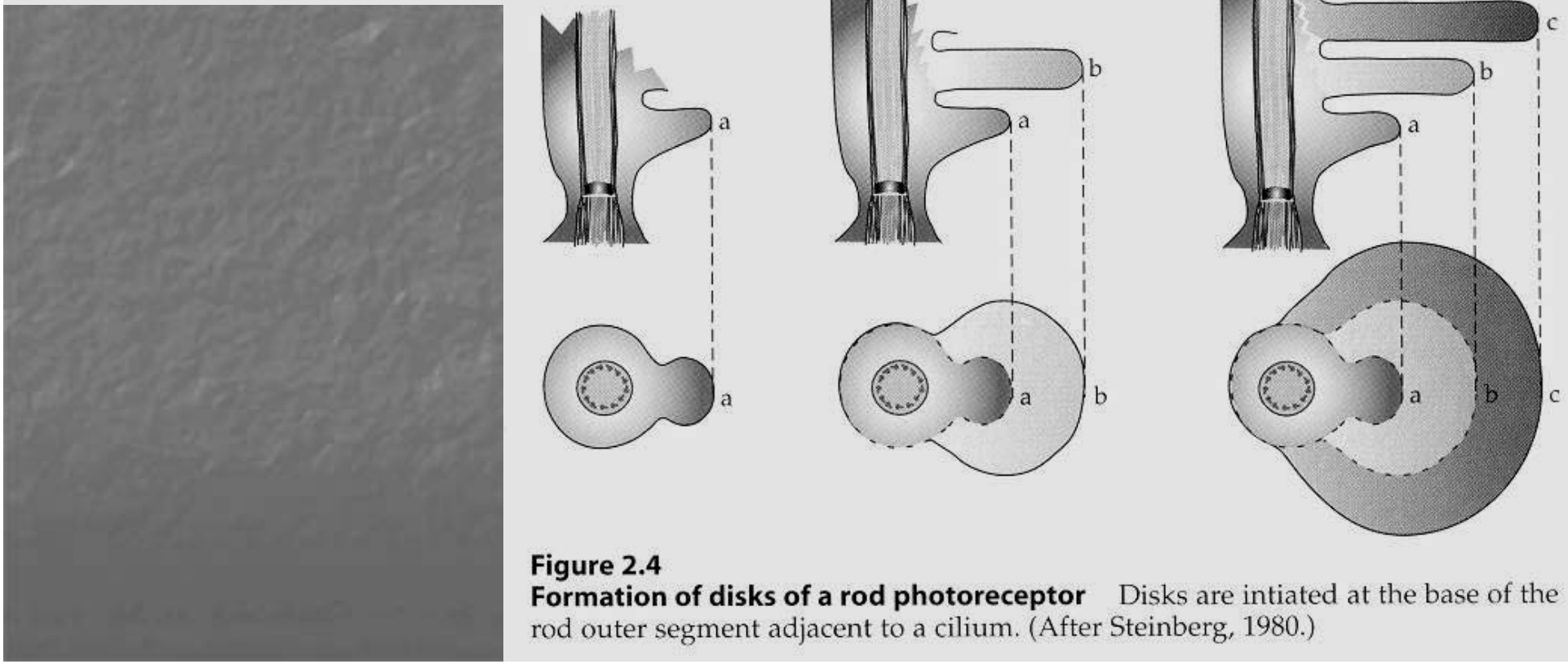

Figure 2.4
Formation of disks of a rod photoreceptor Disks are intiated at the base of the rod outer segment adjacent to a cilium. (After Steinberg, 1980.)

Tip links

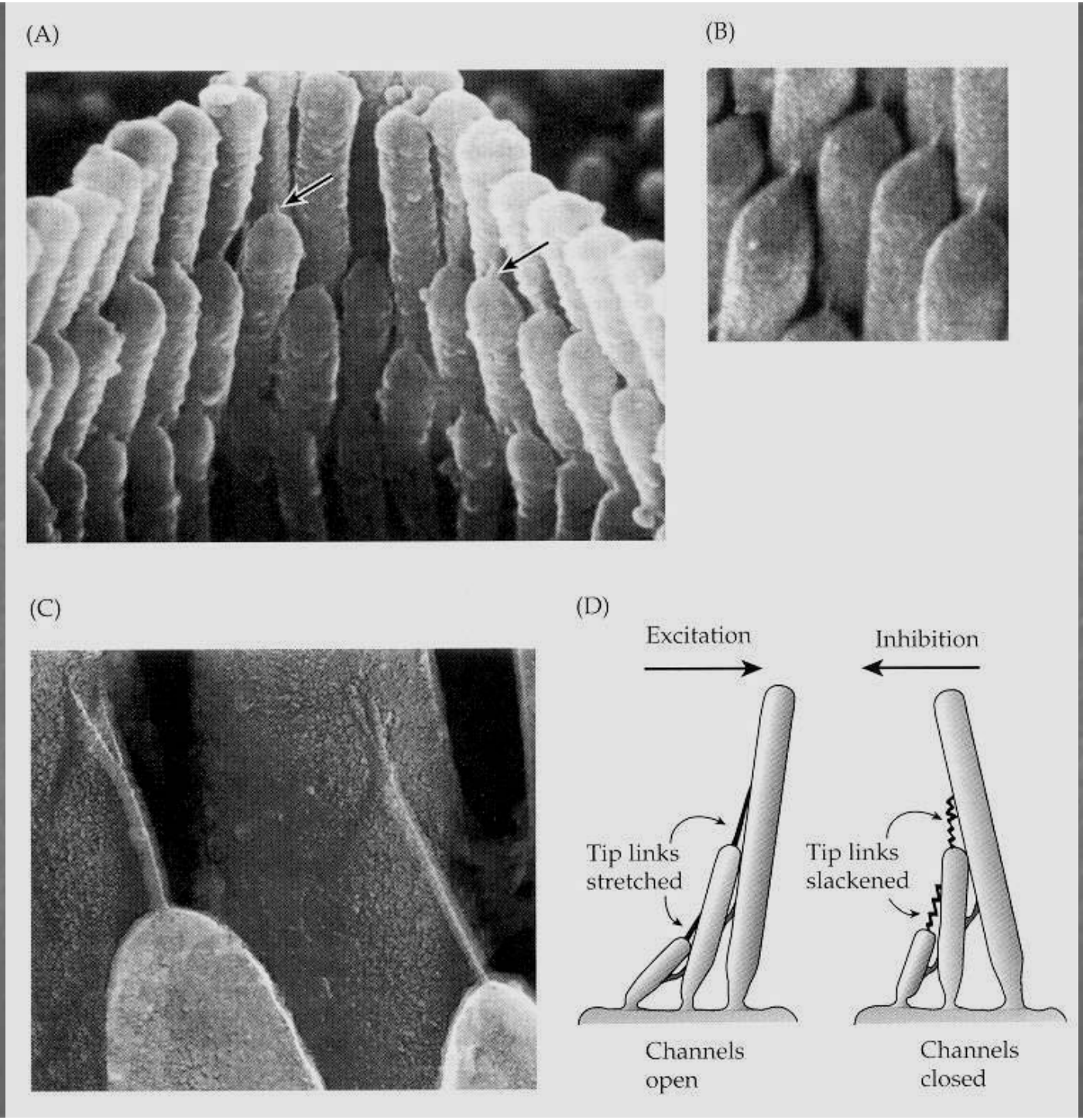
(A)
(B)
(C)
(D)
Excitation
Inhibition
Tip links stretched
Tip links slackened
Channels open
Channels closed

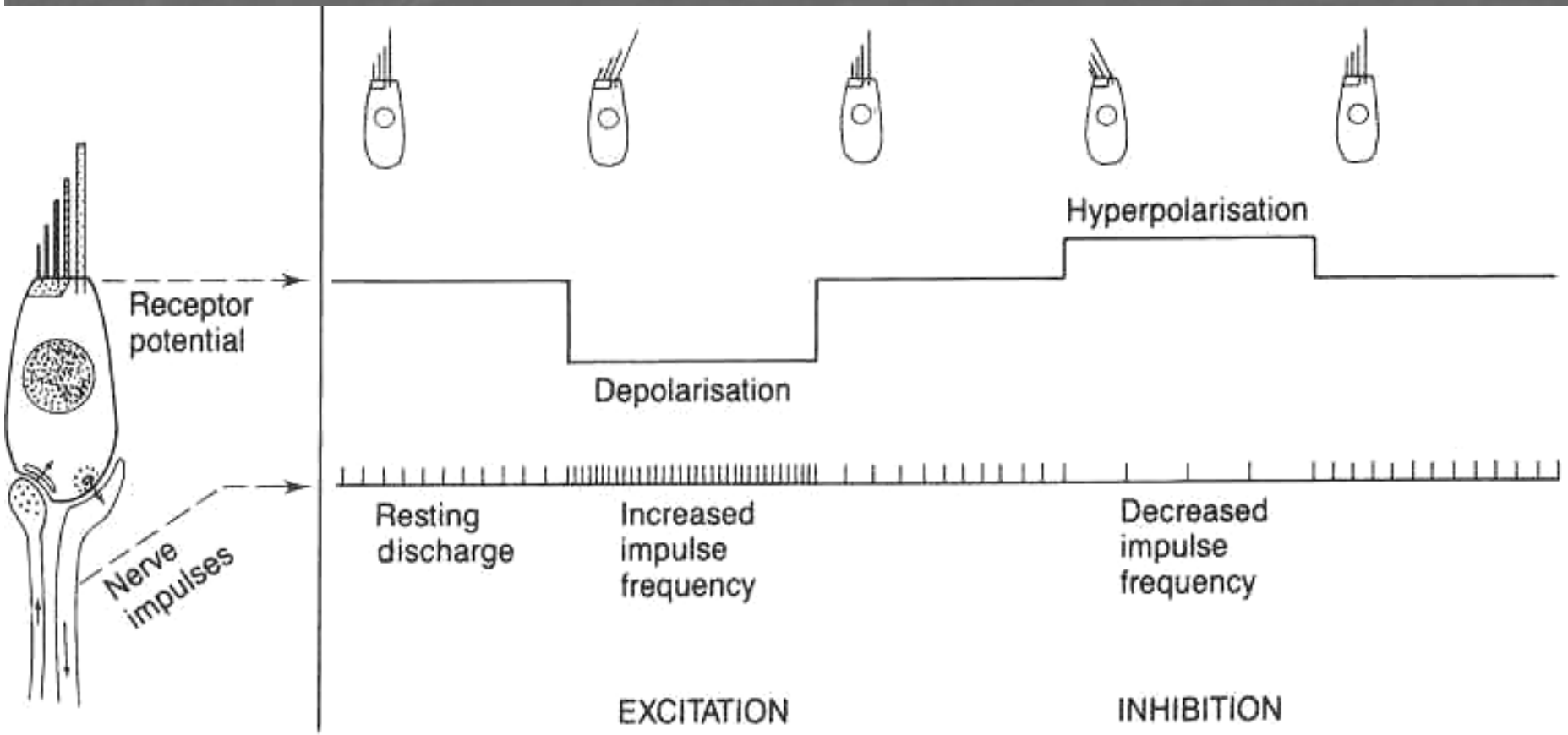
Receptor potential
Nerve impulses
Hyperpolarisation
Depolarisation
Resting discharge
Increased impulse frequency
Decreased impulse frequency
EXCITATION
INHIBITION

Statokinetické čidlo – vestibulární aparát
Obratlovci: evolučně staré
2 typy informací, 2 principy detekce

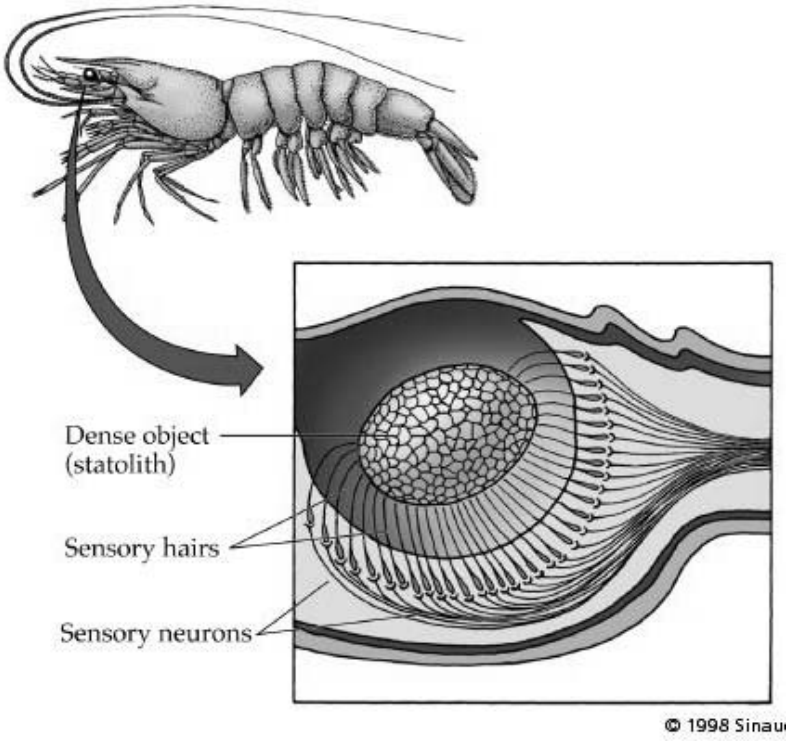

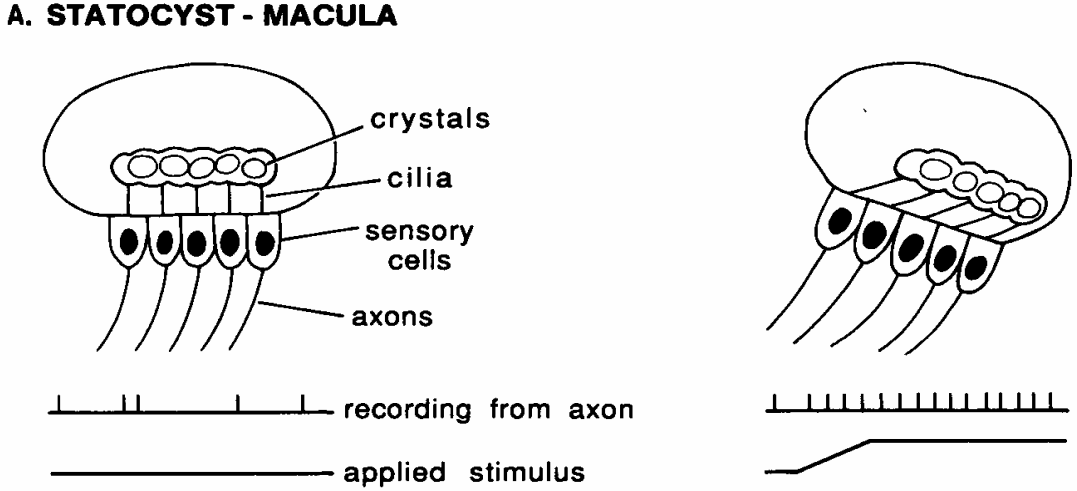

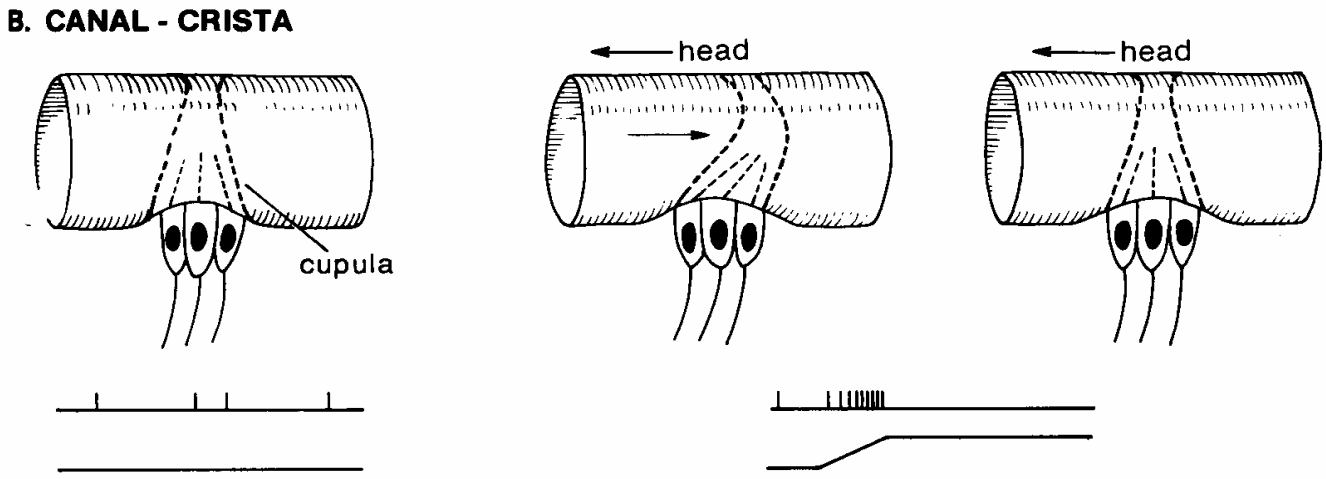

Orgán postranní čáry

Video

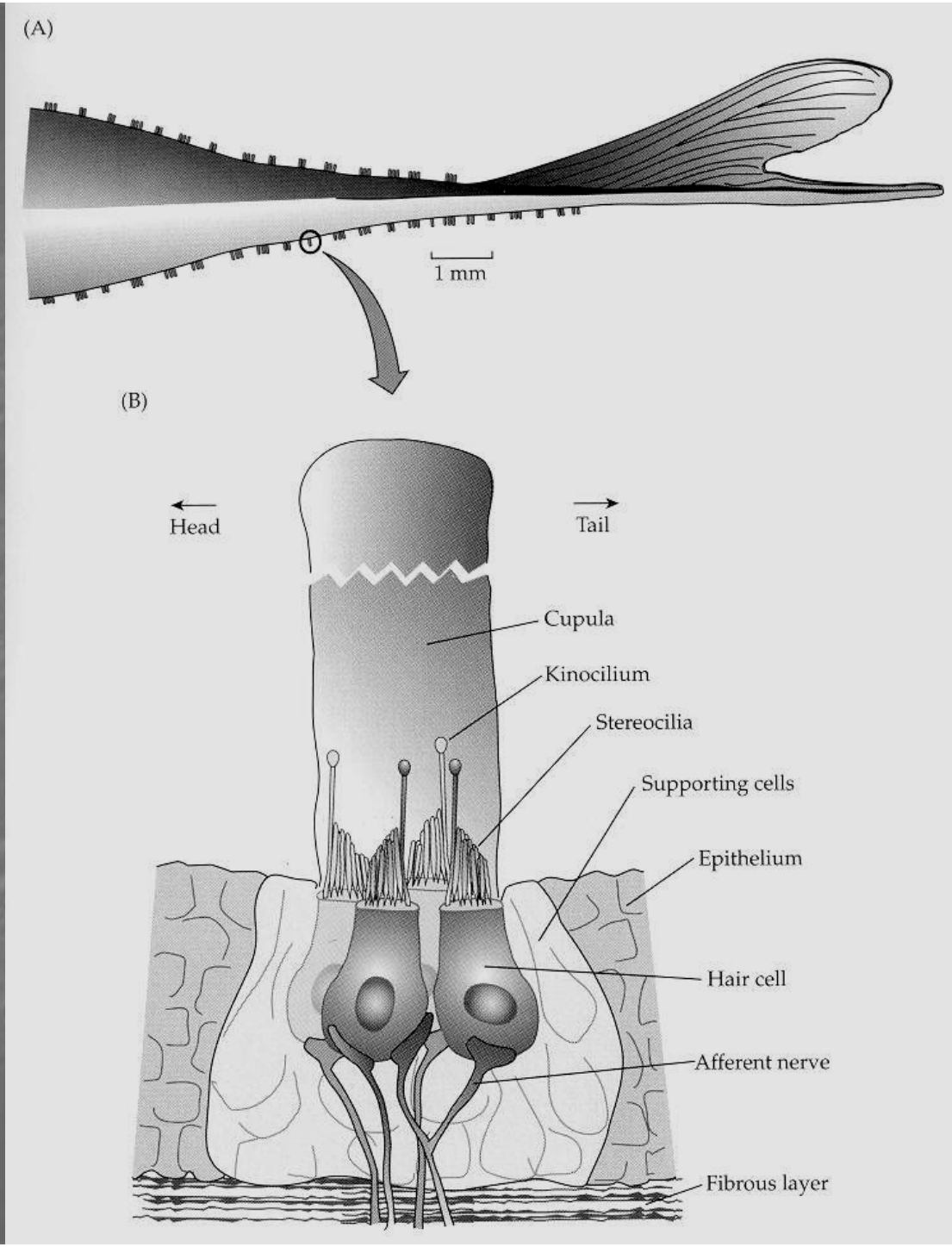

Primárně statokinetické čidlo – vestibulární aparát
Sekundárně lagena se sluchovou funkcí

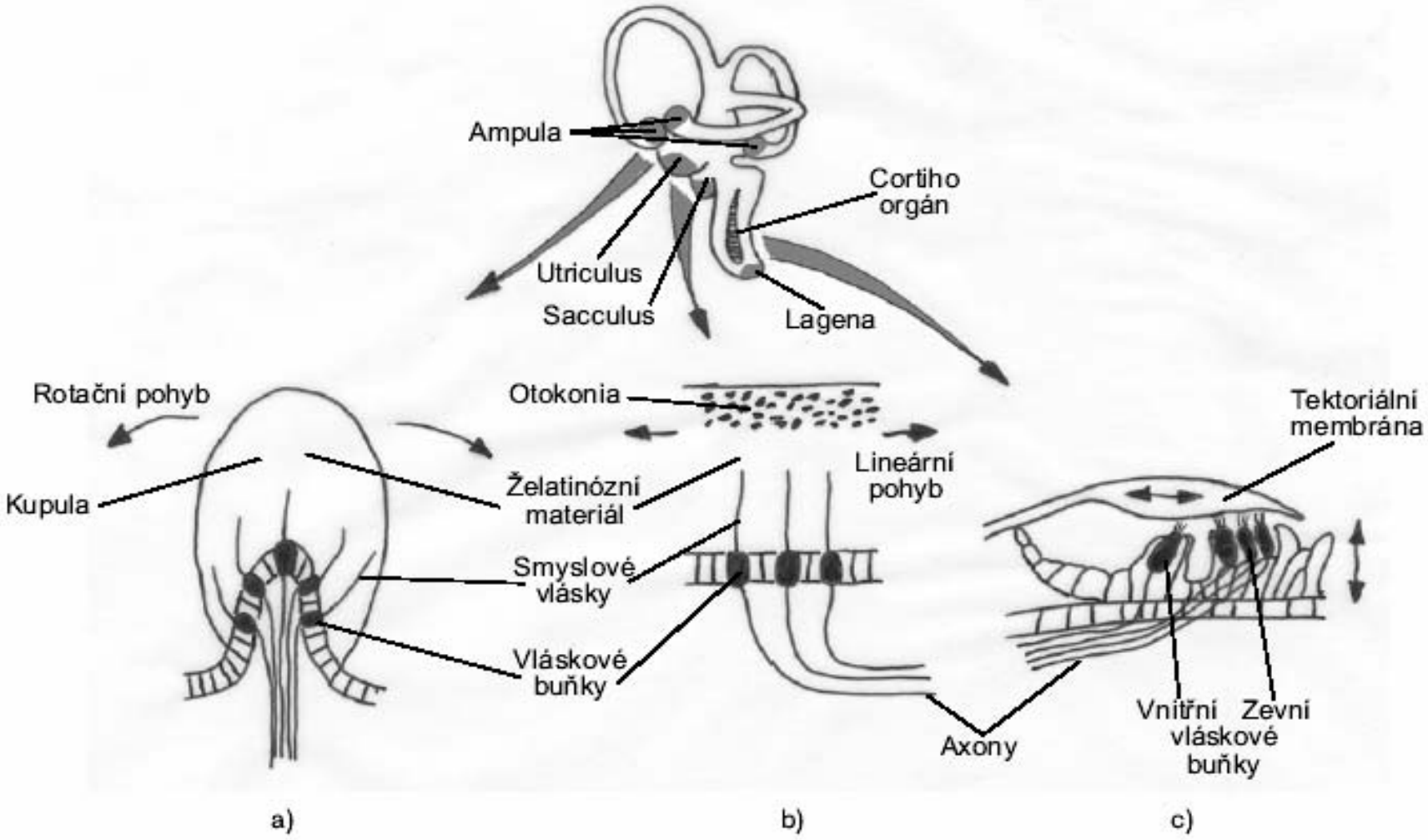

Obr. 16.4. Vláskové buňky a stavba vnitřního ucha obratlovců (ptáka). Sluchové ústrojí je ve spojení se statokinetickým. Polokruhovité chodby s váčky (ampulami), v nichž se pohybuje želatinózní kupula, detekují rotační zrychlení (a). Lineární zrychlení a gravitaci detekují tři políčka vláskových buněk (utriculus, sacculus, lagena) s krystalky v želatinózní čepičce (b). Třetí orgán – Cortiho – slouží jako sluchový (c).

Primárně statokinetické čidlo – vestibulární aparát
Sekundárně lagena se sluchovou funkcí

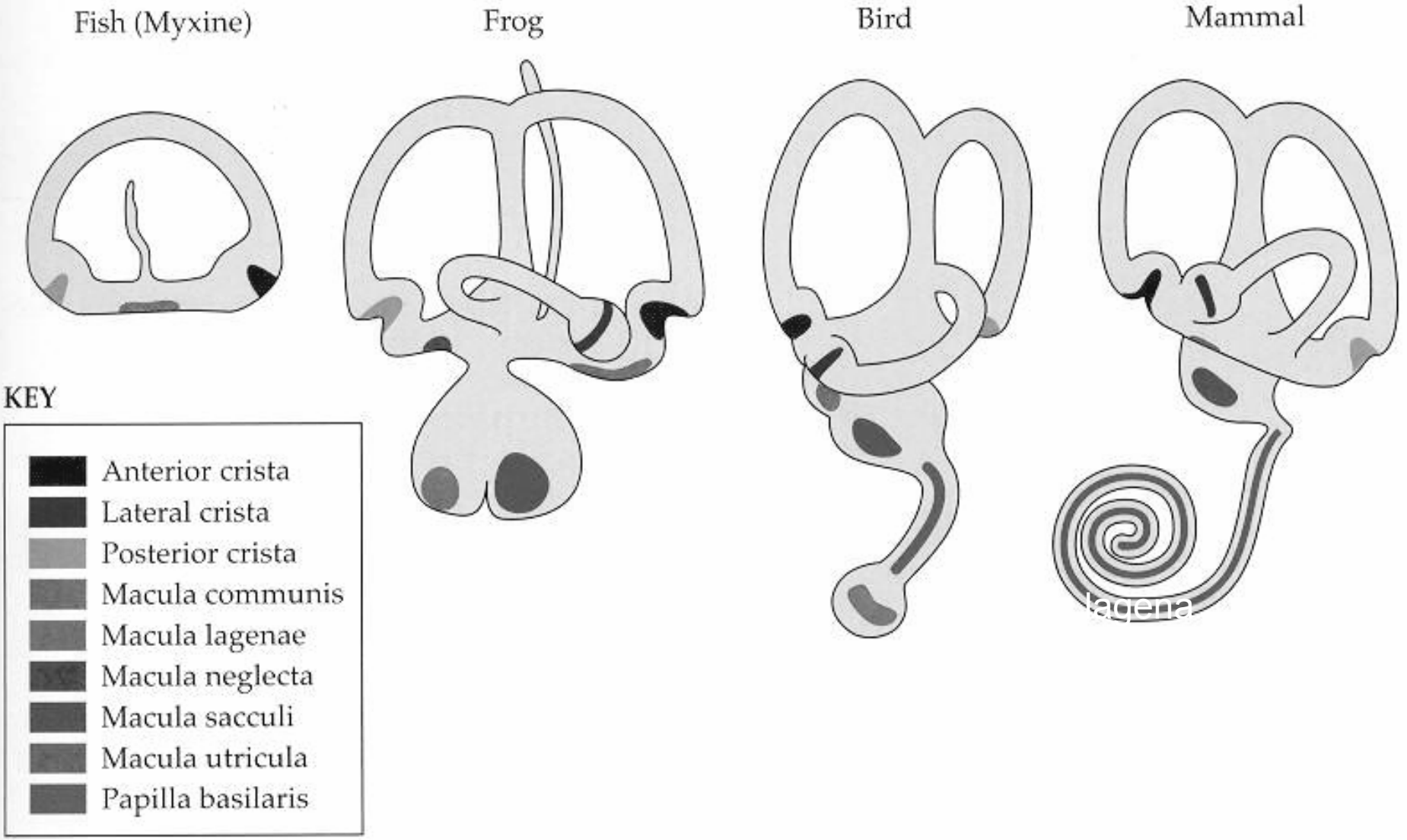

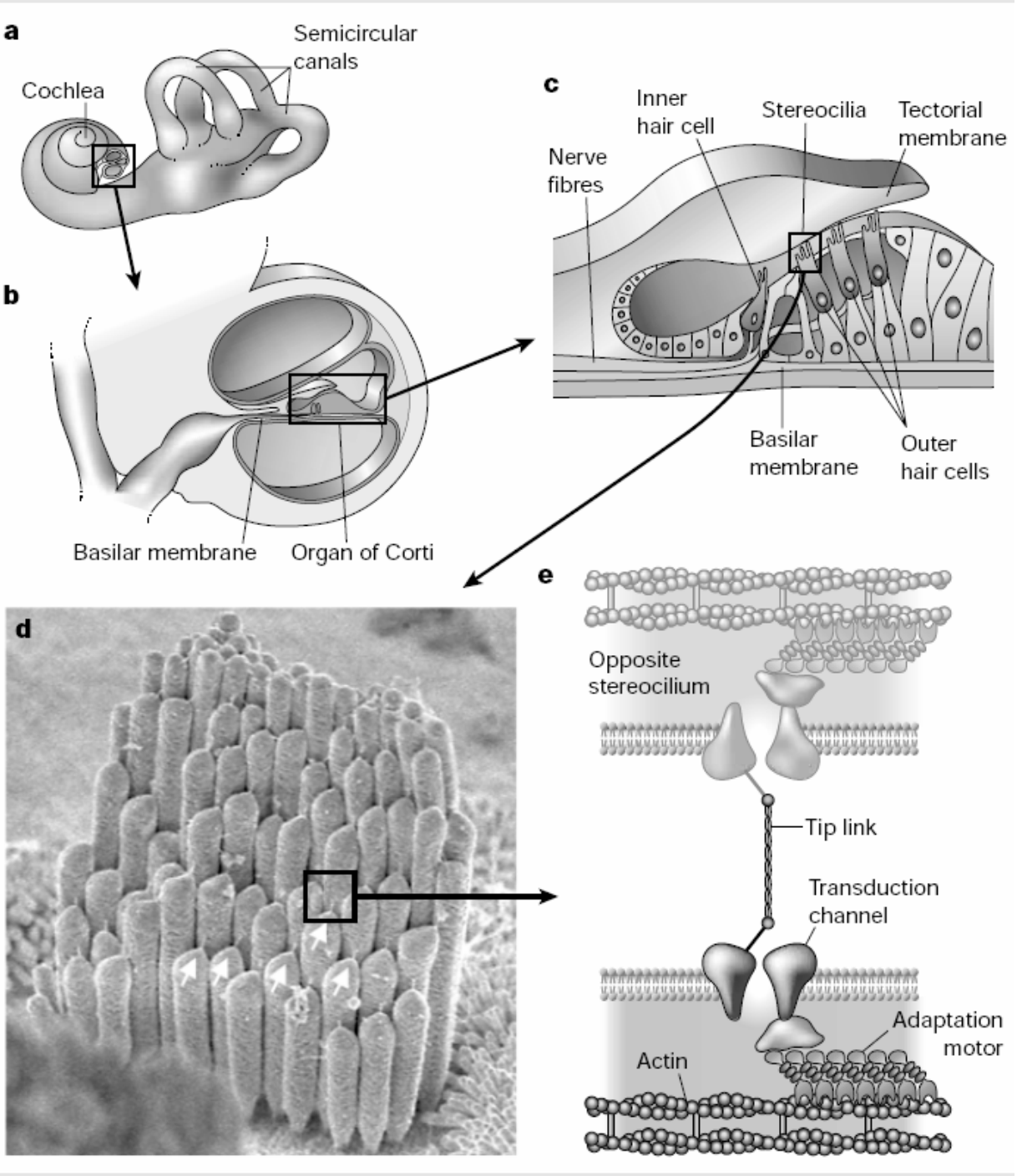

Figure 4 Inner-ear structure and hair-cell transduction model. **a**, Gross view of part of the inner ear. Sound is transmitted through the external ear to the tympanic membrane; the stimulus is transmitted through the middle ear to the fluid-filled inner ear. Sound is transduced by the coiled cochlea. **b**, Cross-section through the cochlear duct. Hair cells are located in the organ of Corti, resting on the basilar membrane. **c**, Sound causes vibrations of the basilar membrane of the organ of Corti; because flexible hair-cell stereocilia are coupled to the overlying tectorial membrane, oscillations of the basilar membrane cause back-and-forth deflection of the hair bundles. **d**, Scanning electron micrograph of hair bundle (from chicken cochlea). Note tip links (arrows). **e**, Proposed molecular model for hair-cell transduction apparatus.

Sluch kaprovitých ryb

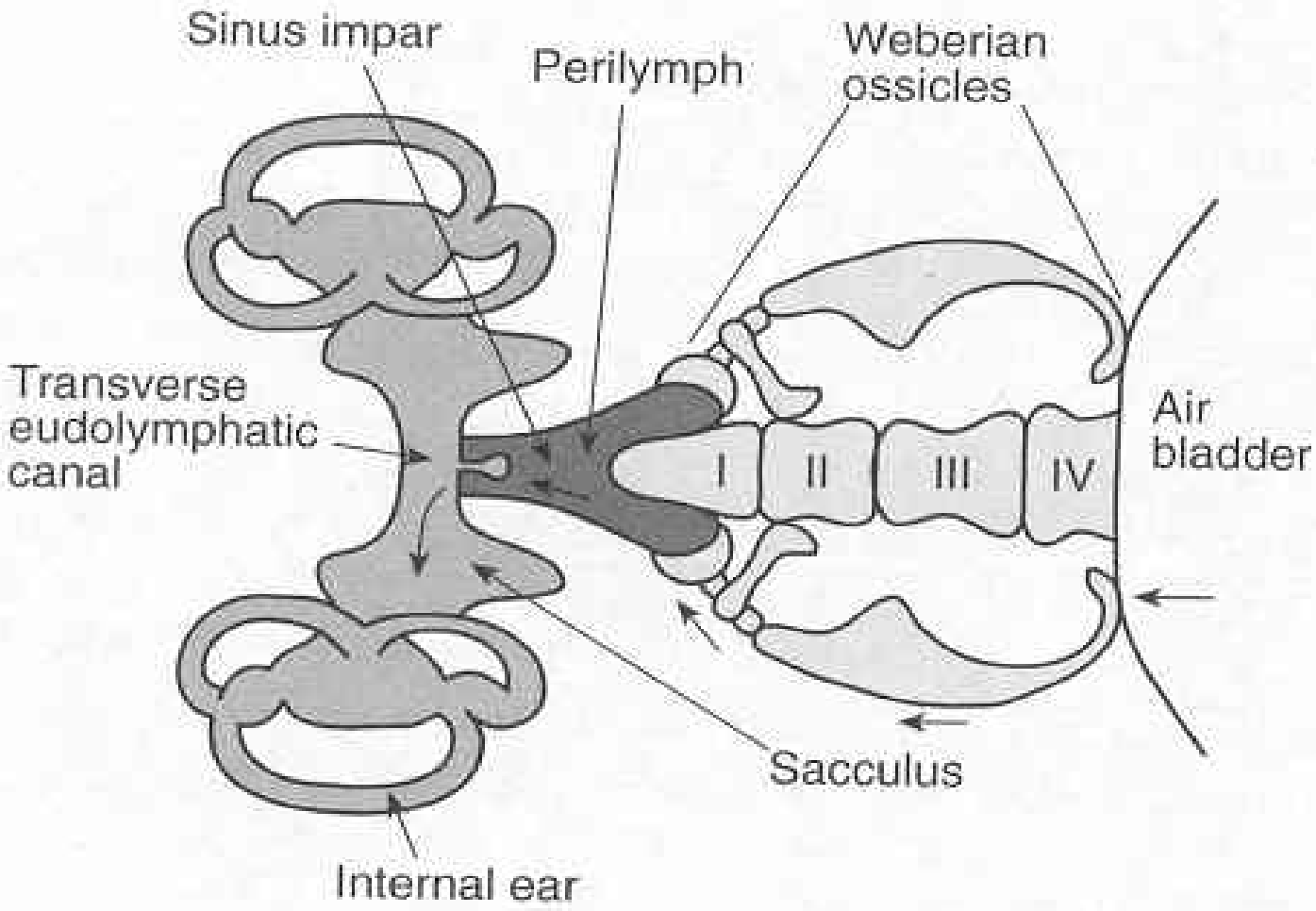

Figure 8.10 Weberian ossicles. The figure shows a horizontal section through the anterior region of the body of a carp (*Cyprinus carpio*). The arrows indicate the direction of vibrations from the swim bladder to the sacculus. I, II, III, and IV indicate the four vertebrae from which the ossicles are derived. Modified from Romer, 1970

Sluch
ptáků a savců

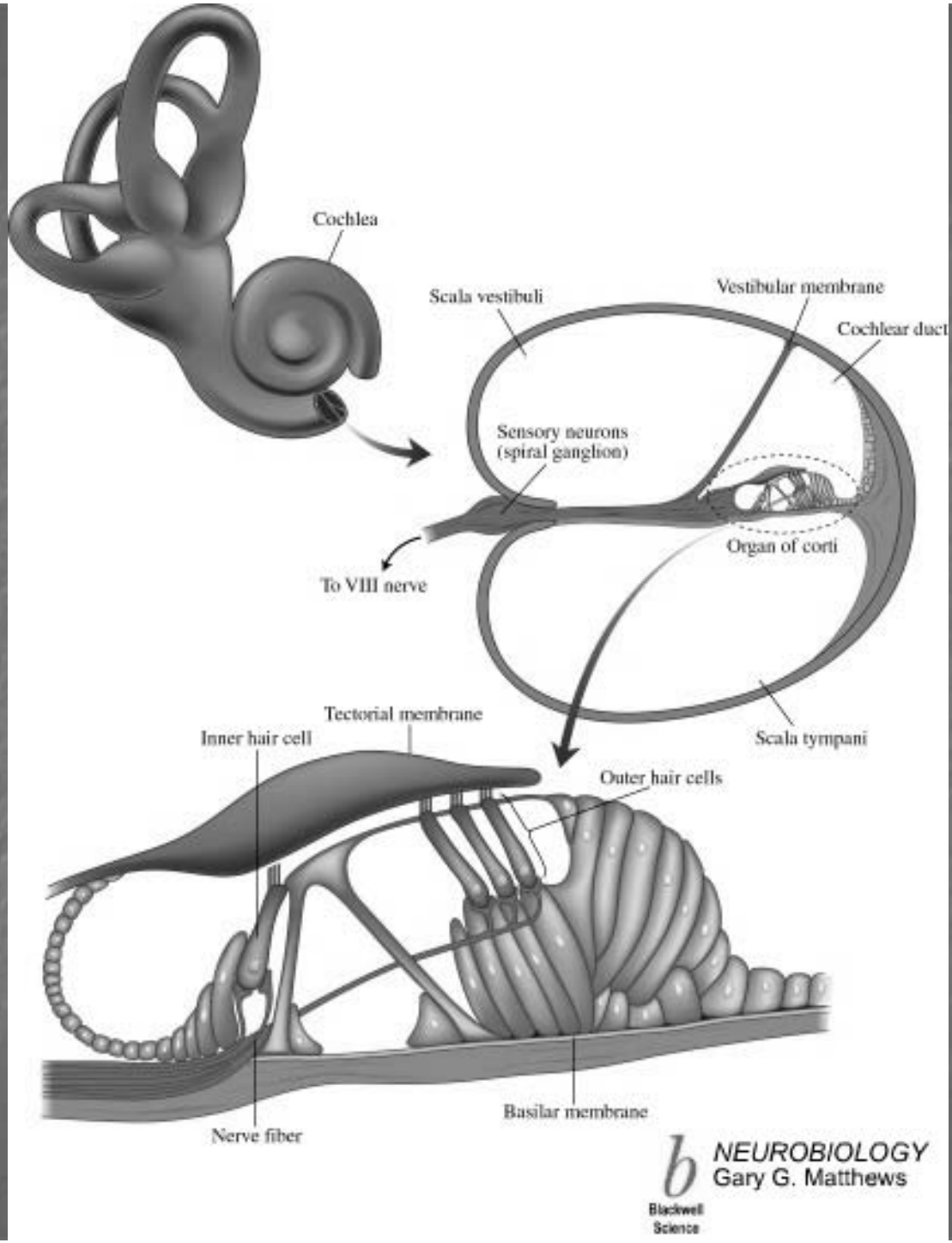

Sluch
ptáků a savců

Kůstky: převod ze vzduchu do kapaliny. 22x silnější
Svaly: m.tensor tympani a m.stapedius

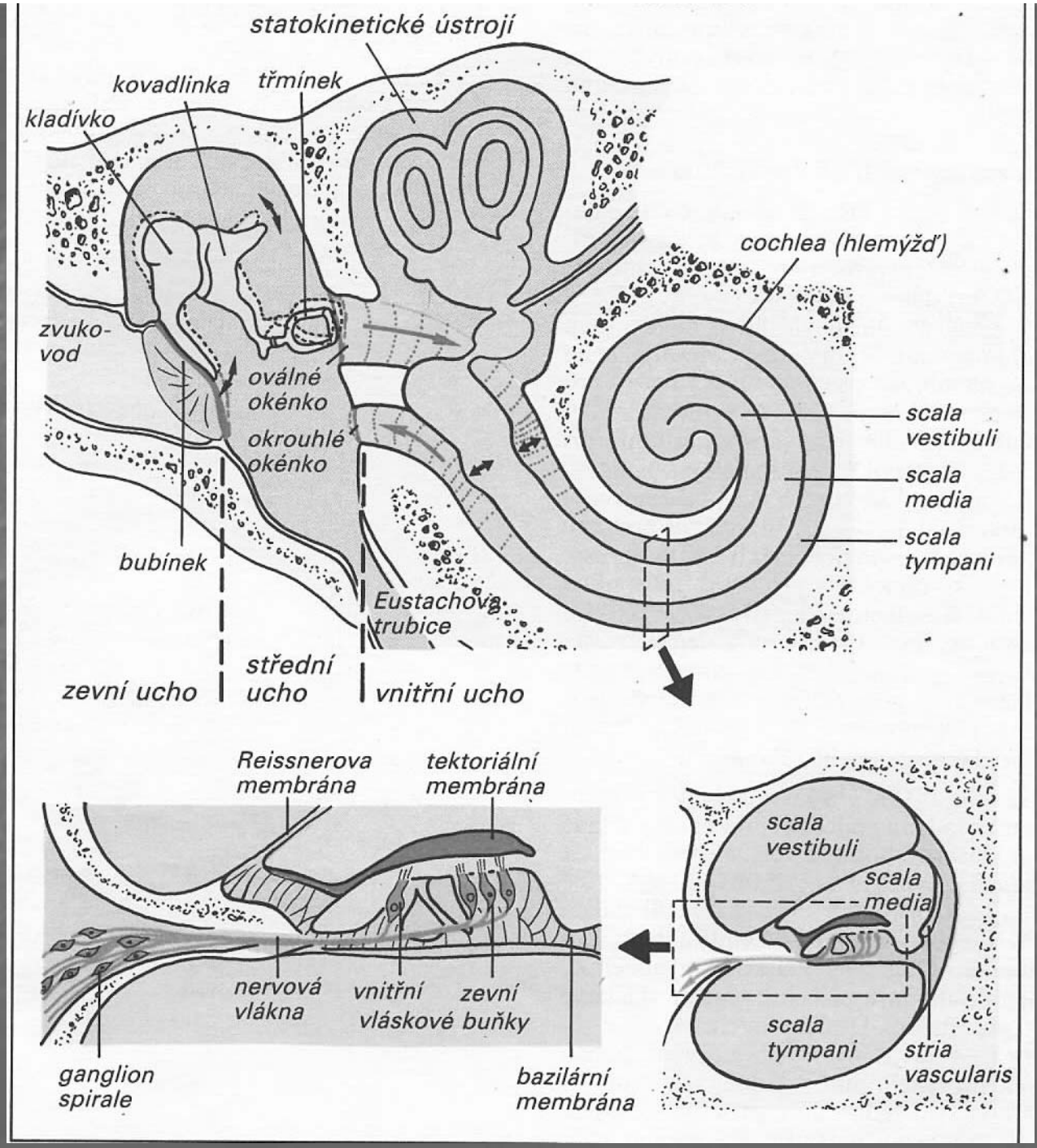

Sluch
ptáků a savců

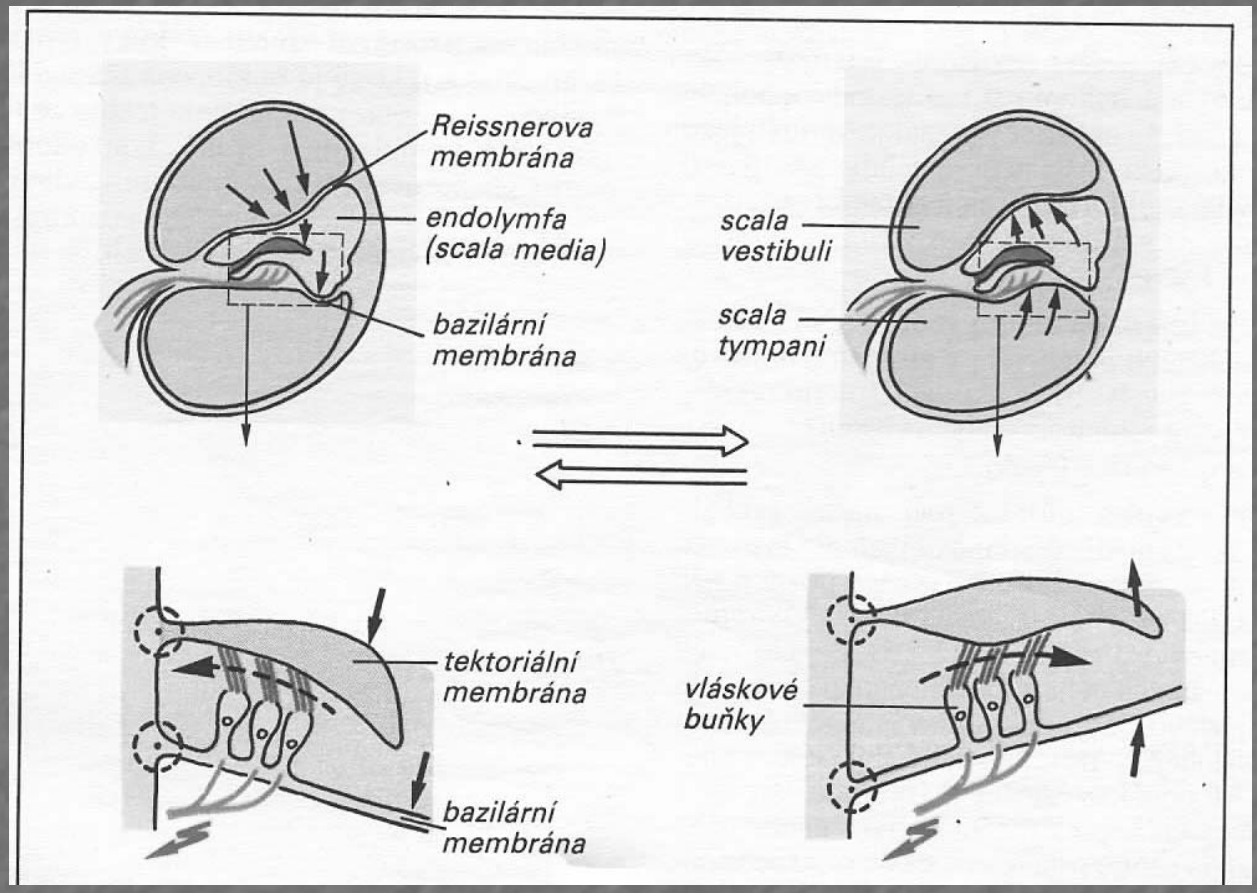

Pohyb anim.

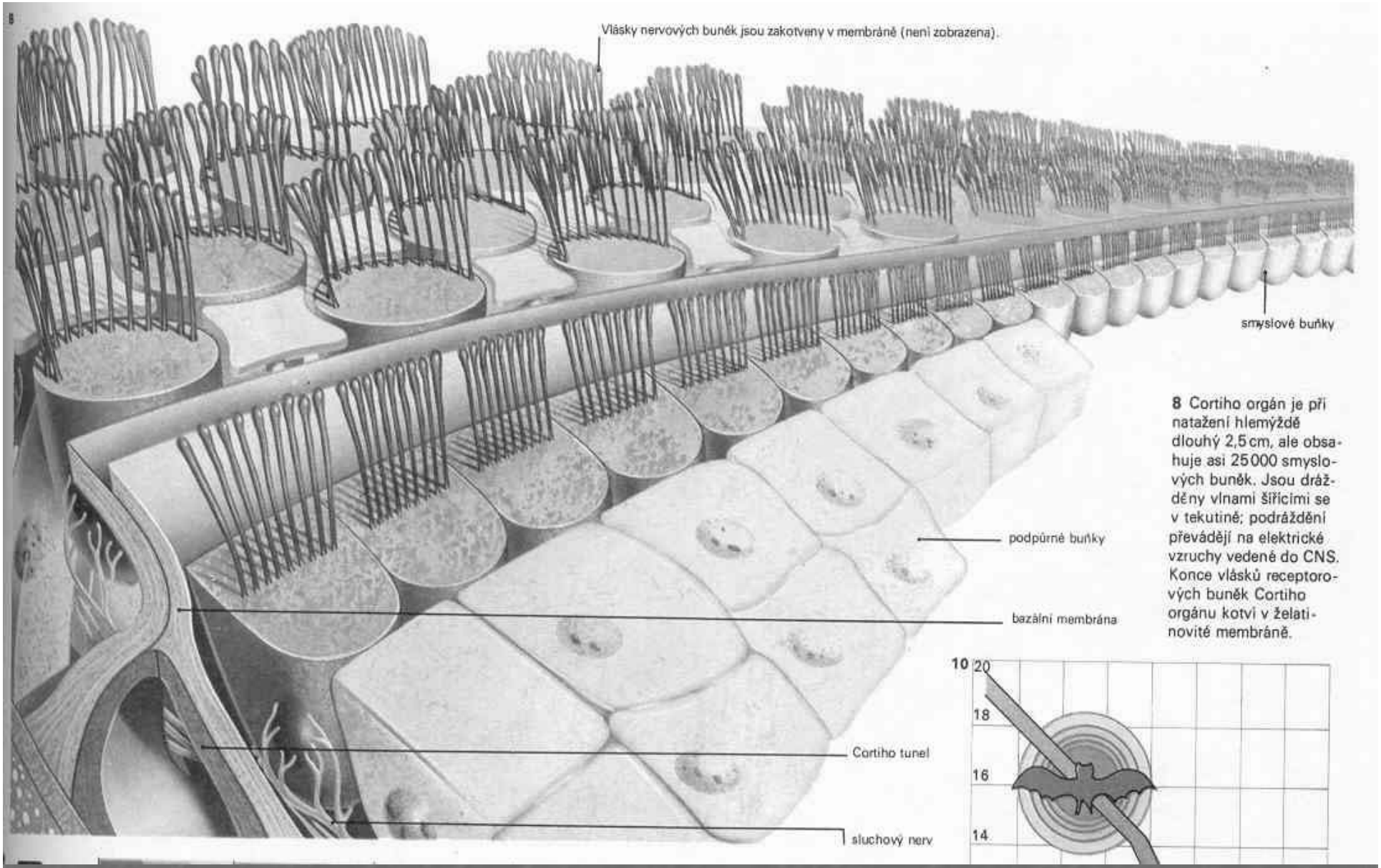

Cortiho orgán: 25.000 vláskových buněk ve dvou řadách

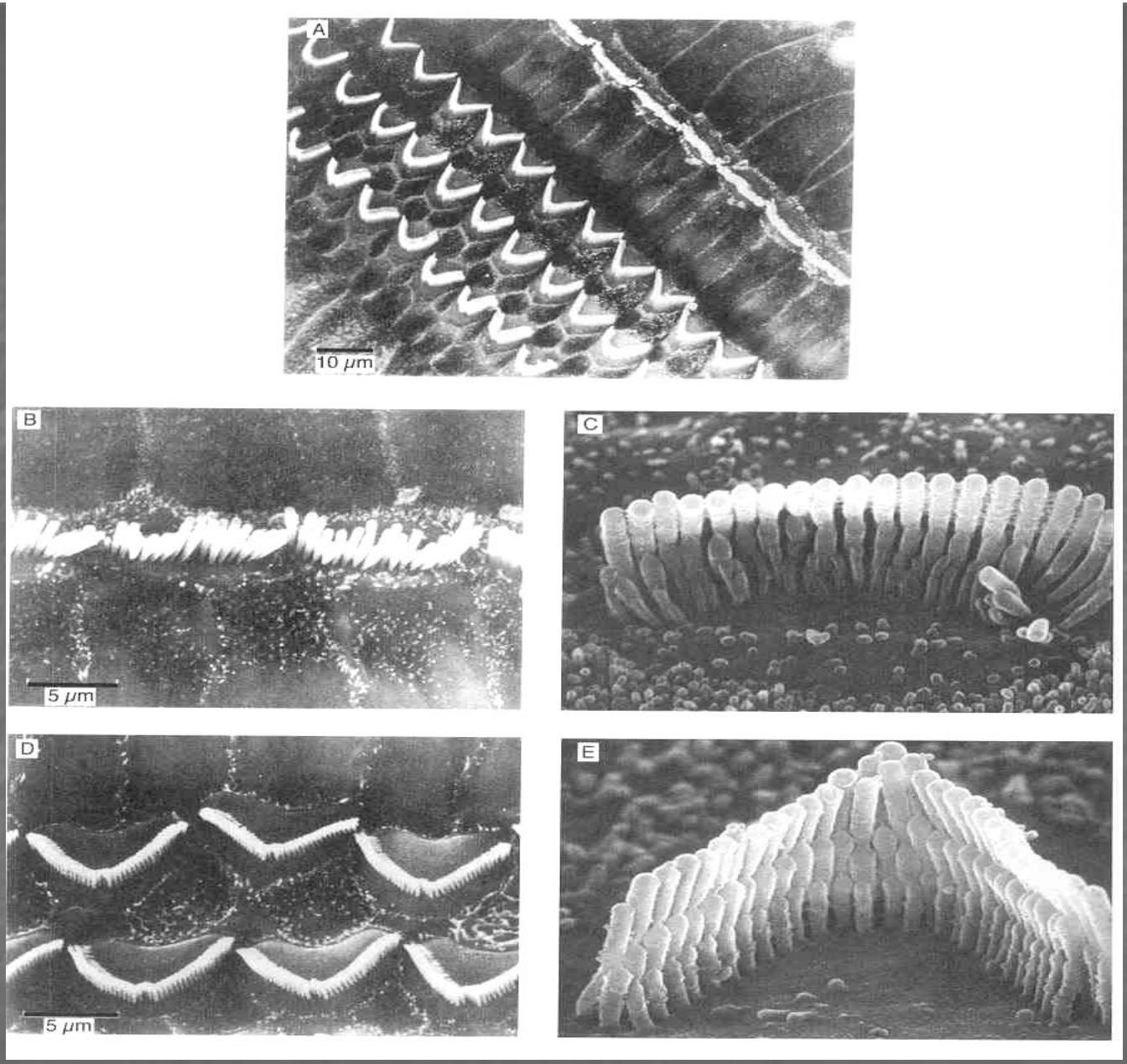

Cortiho orgán: 25.000 vláskových buněk ve dvou řadách

Zobrazení frekvence

Problém: max frekvence AP je mnohem nižší než max. frekvence zvuku

Člověk rozliší 1000Hz
Od 1003Hz

JSB v uchu

Video

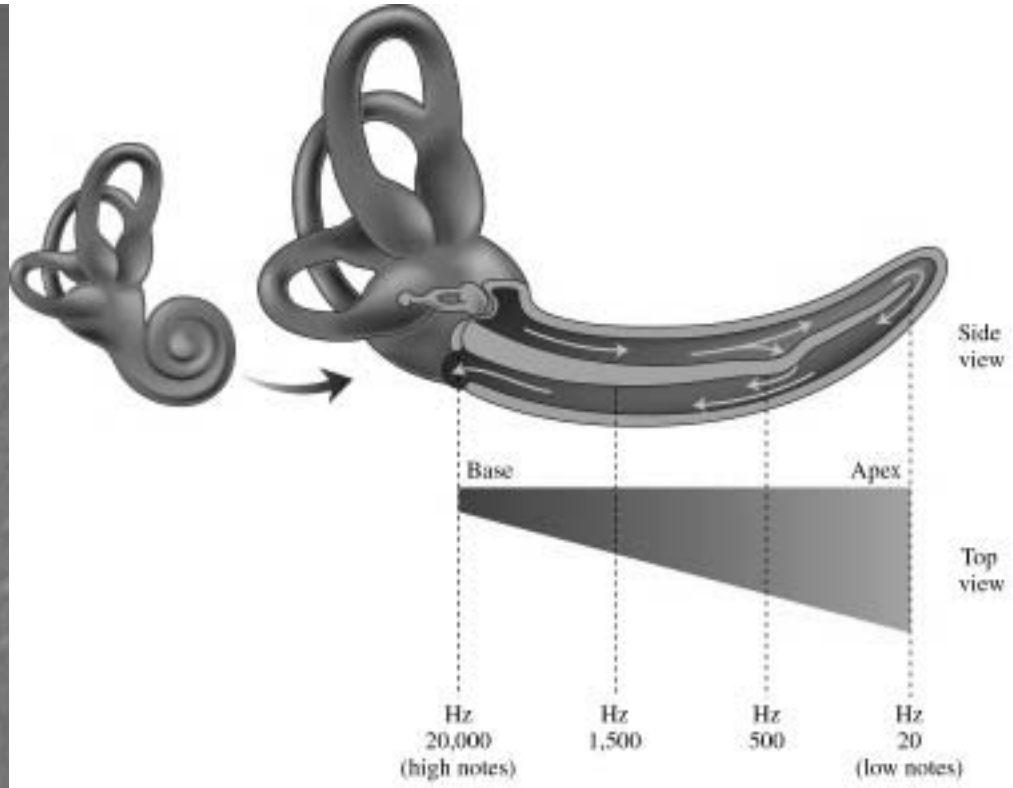

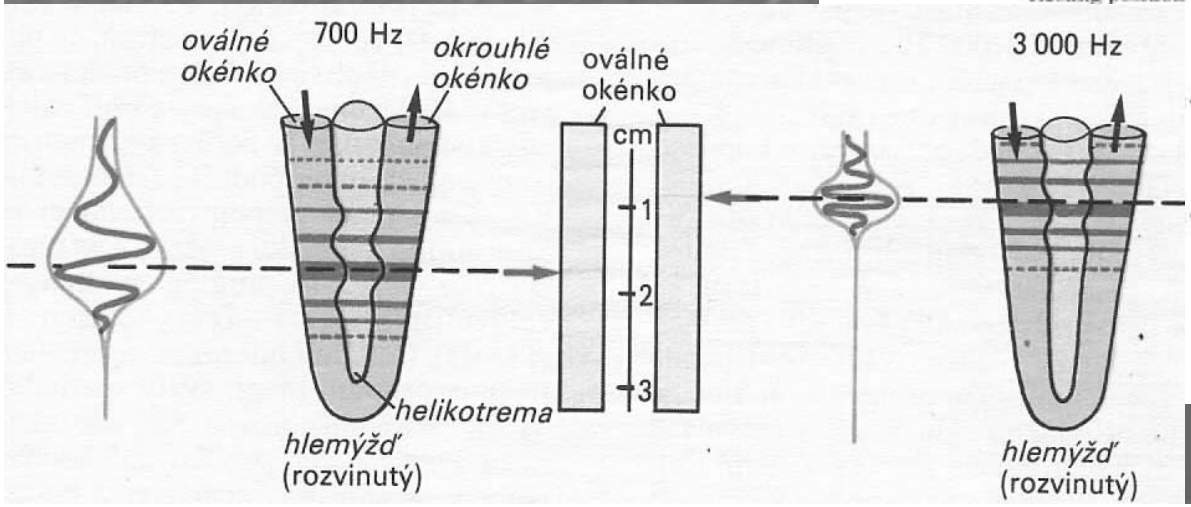

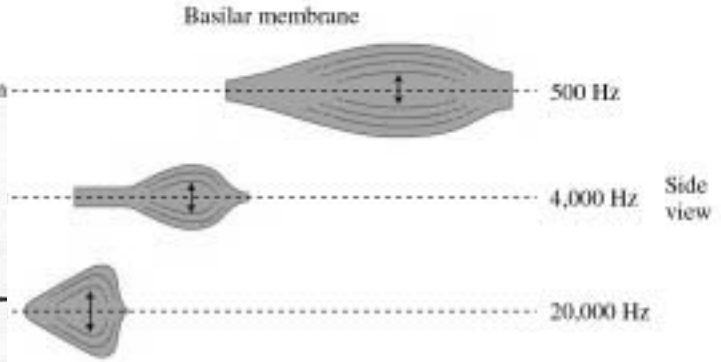

VNITŘNÍ VNĚJŠÍ
„mlčící většina“

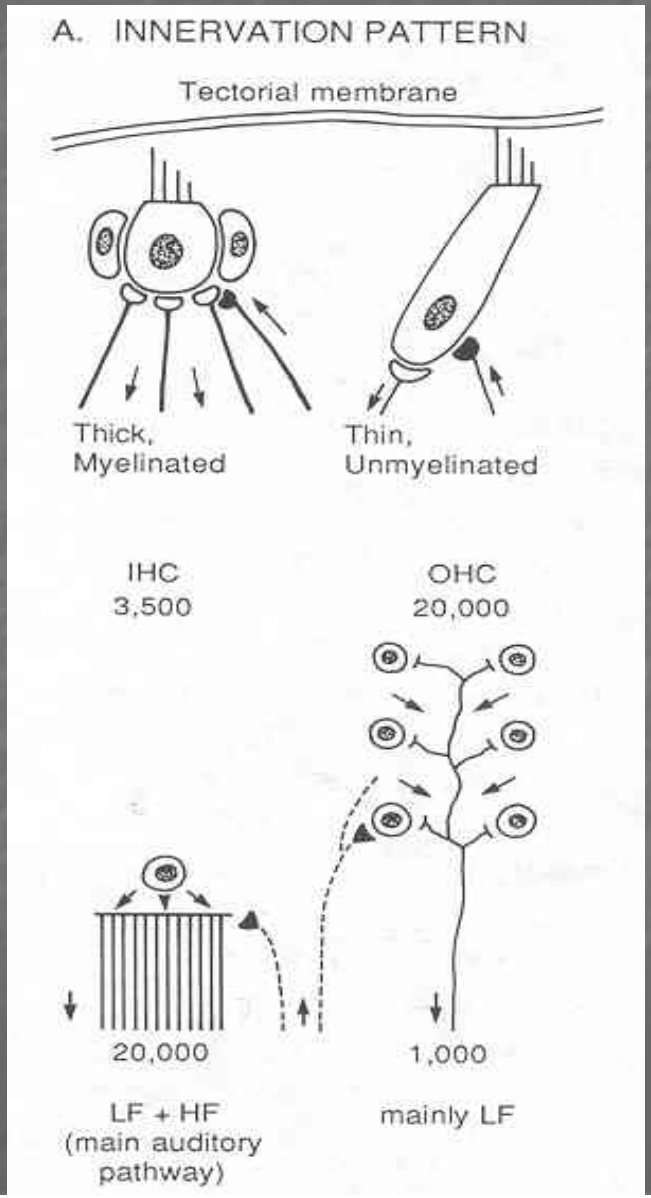

VNITŘNÍ VNĚJŠÍ

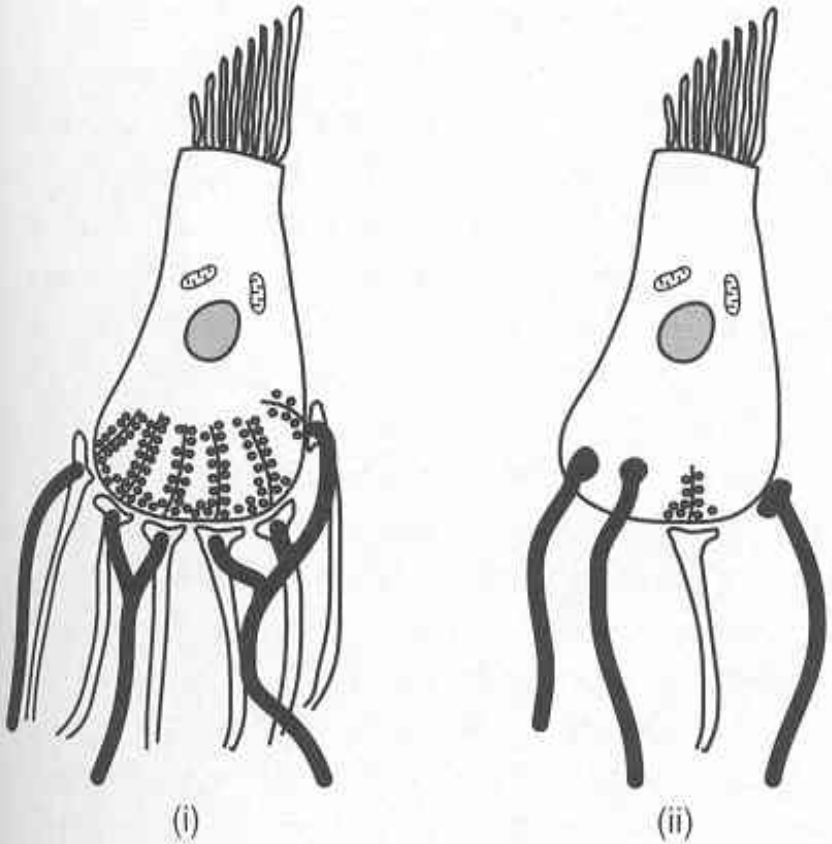

Figure 8.16 Innervation of inner and outer hair cells in the organ of Corti. The schematic figure shows afferent fibres (white) and efferent fibres (black). (i) Inner hair cell. The efferent fibres make synaptic contact with the dendritic endings of the afferent fibres. (ii) Outer hair cell. The efferent fibres synapse directly on the hair cell which makes rather few synapses (only one shown) with sensory (afferent) fibres

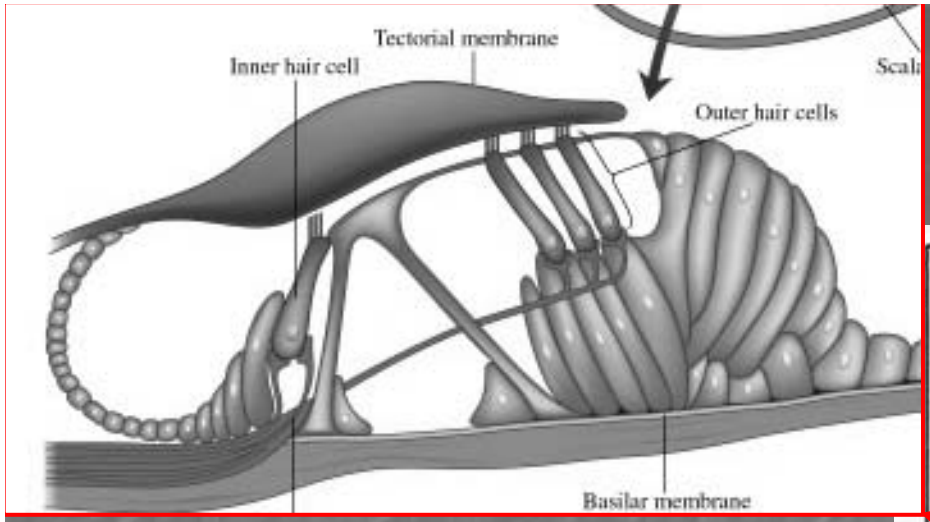

Potenciál v kochlei
Velká hnací síla 140mV pro kationty
– snadný vznik receptorové odezvy

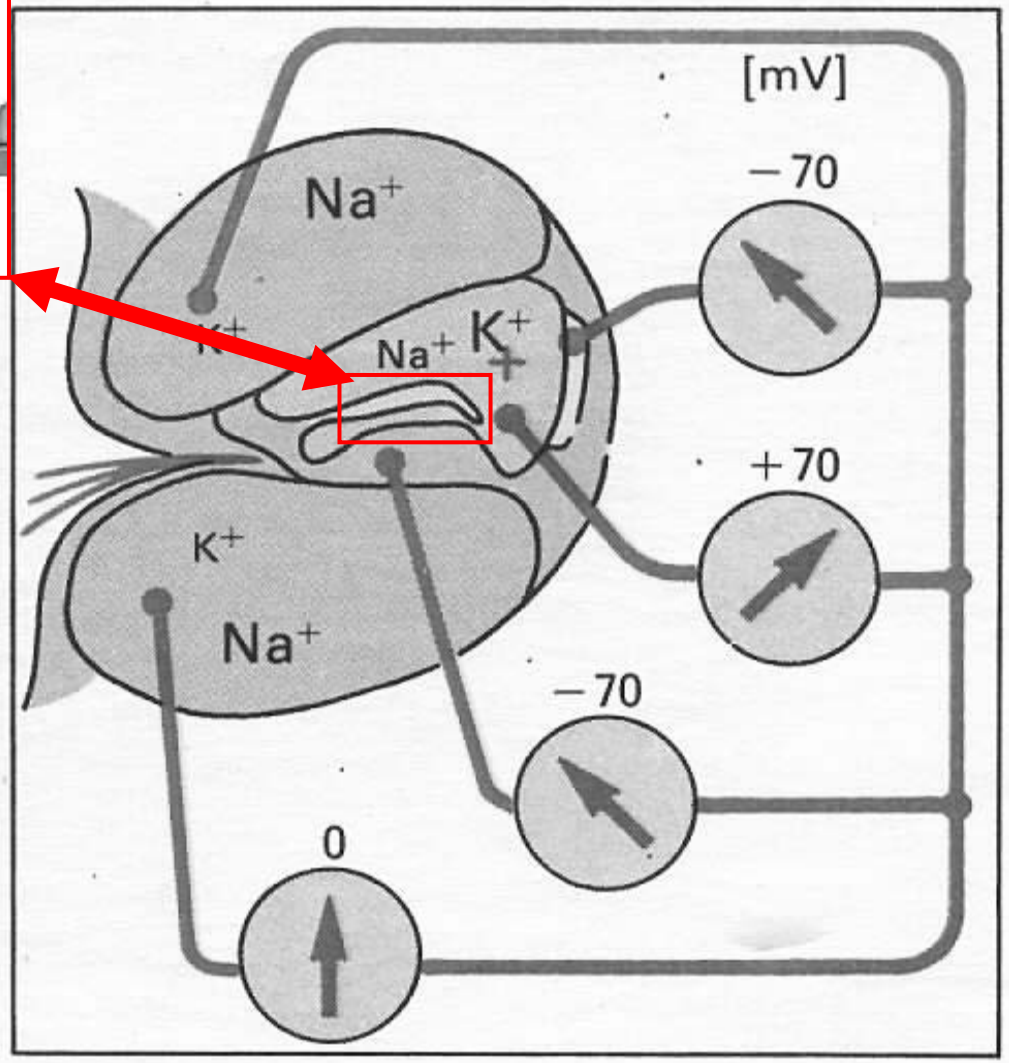

C. Kochleární potenciály a rozložení elektrolytů v oddílech hlemýždě

Nemáme mutantní linie vláskových buněk jako u háďátka.

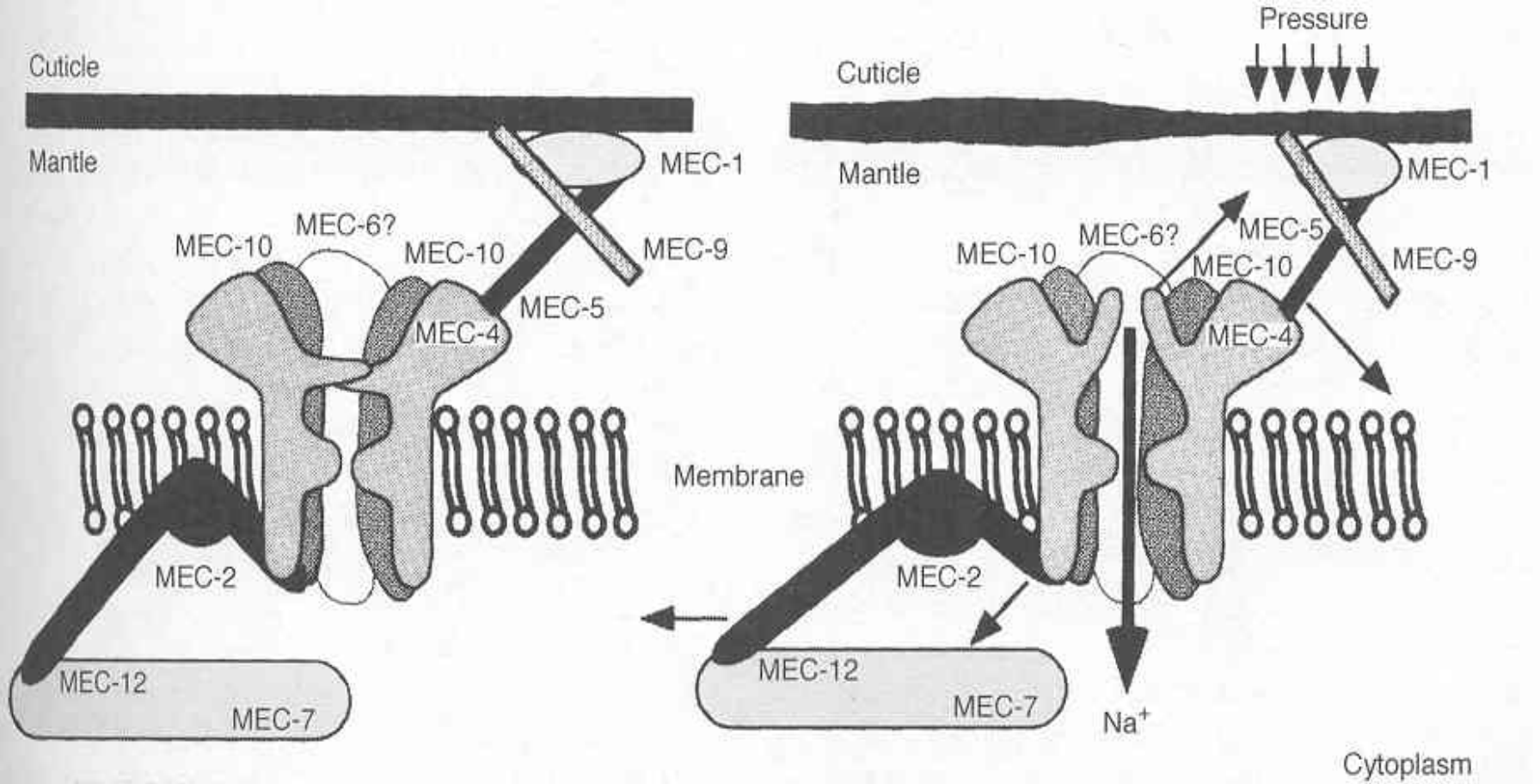

Figure 7.6 Conceptual model of *C. elegans* touch receptor. Explanation and nomenclature in text. From N. Tavernarakis and M. Driscoll, 1997, 'Molecular modelling of mechanotransduction in the nematode *Caenorhabditis elegans*', *Annual Review of Physiology*, **59**, 679. With permission, from the *Annual Review of Physiology*, Volume 59, ©1997, by Annual Reviews www.annualreviews.org

Analýza vrozených vad dokázala příbuznost proteinů vl. buněk a bezobratlých

Figure 4 Inner-ear structure and hair-cell transduction model. **a**, Gross view of part of the inner ear. Sound is transmitted through the external ear to the tympanic membrane; the stimulus is transmitted through the middle ear to the fluid-filled inner ear. Sound is transduced by the coiled cochlea. **b**, Cross-section through the cochlear duct. Hair cells are located in the organ of Corti, resting on the basilar membrane. **c**, Sound causes vibrations of the basilar membrane of the organ of Corti; because flexible hair-cell stereocilia are coupled to the overlying tectorial membrane, oscillations of the basilar membrane cause back-and-forth deflection of the hair bundles. **d**, Scanning electron micrograph of hair bundle (from chicken cochlea). Note tip links (arrows). **e**, Proposed molecular model for hair-cell transduction apparatus.

Obecný molekulární
Princip mechanorecepce

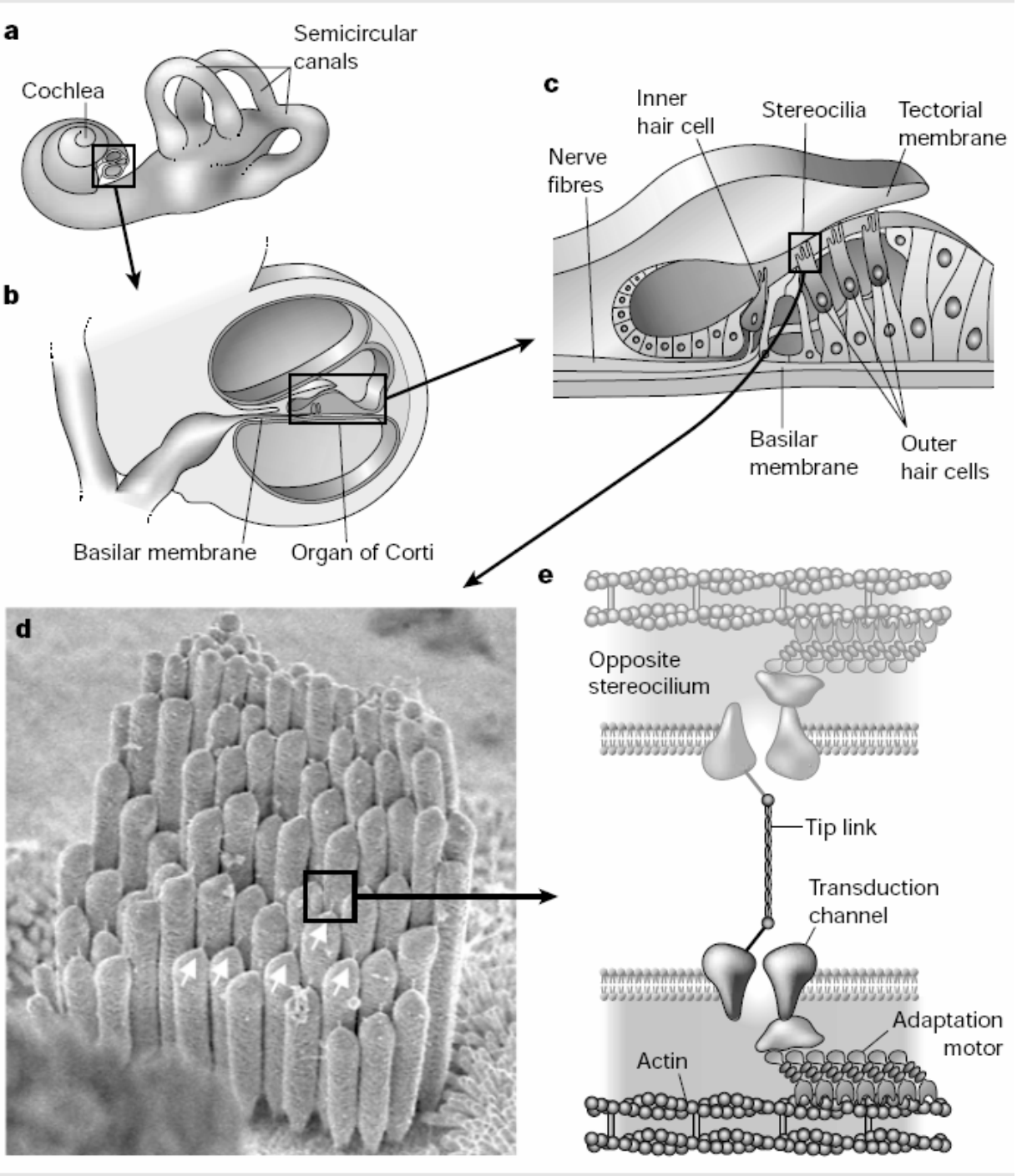

Obrovská citlivost - pohyby v kochlei

- Dva druhy adaptace
- Kochleární zesilovač – vnější buňky savců

Testy tuhosti
a měření pohybu
vlásků

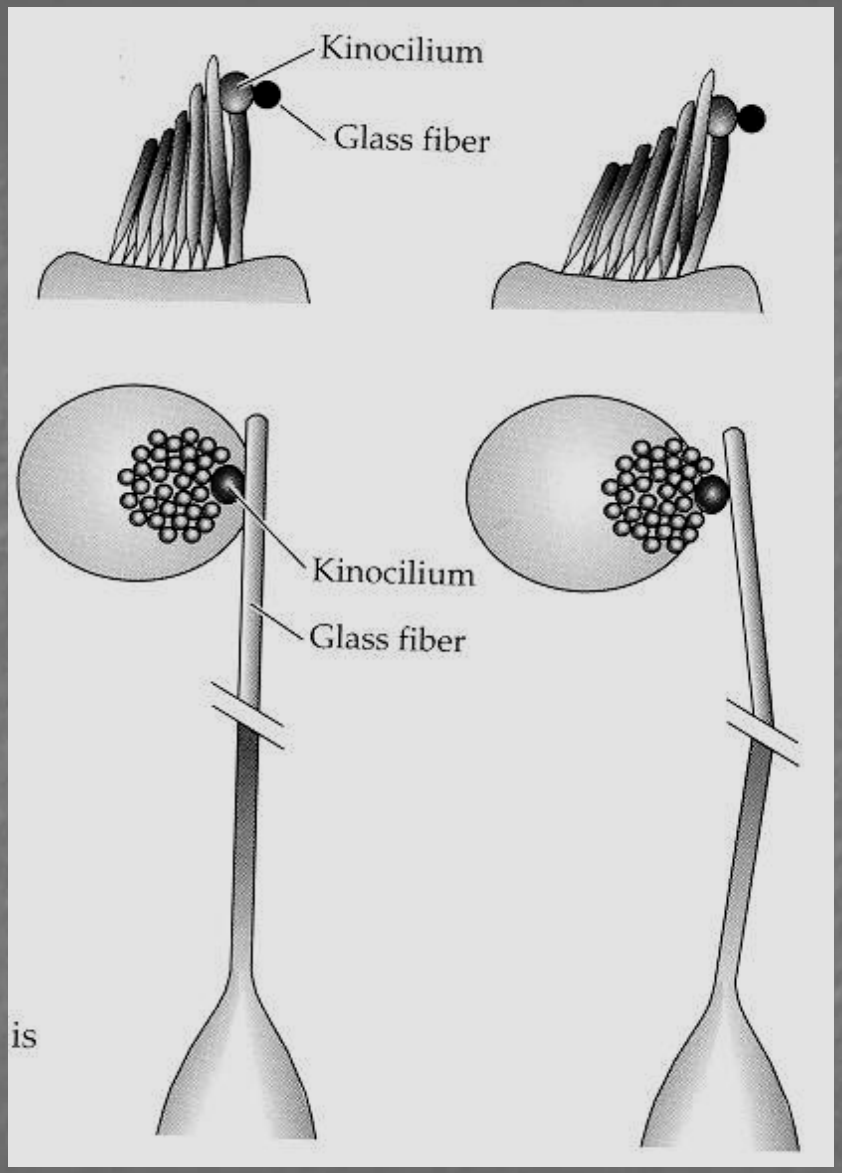

Otevření kanálů
vyvolá pohyb celého svazku
a influx kationtů. Depolarizace.
Ca pak kanály inhibuje.

Platí i obráceně: depolarizace
vede k pohybu vlásků – základ
pro aktivní pohyby svazku.

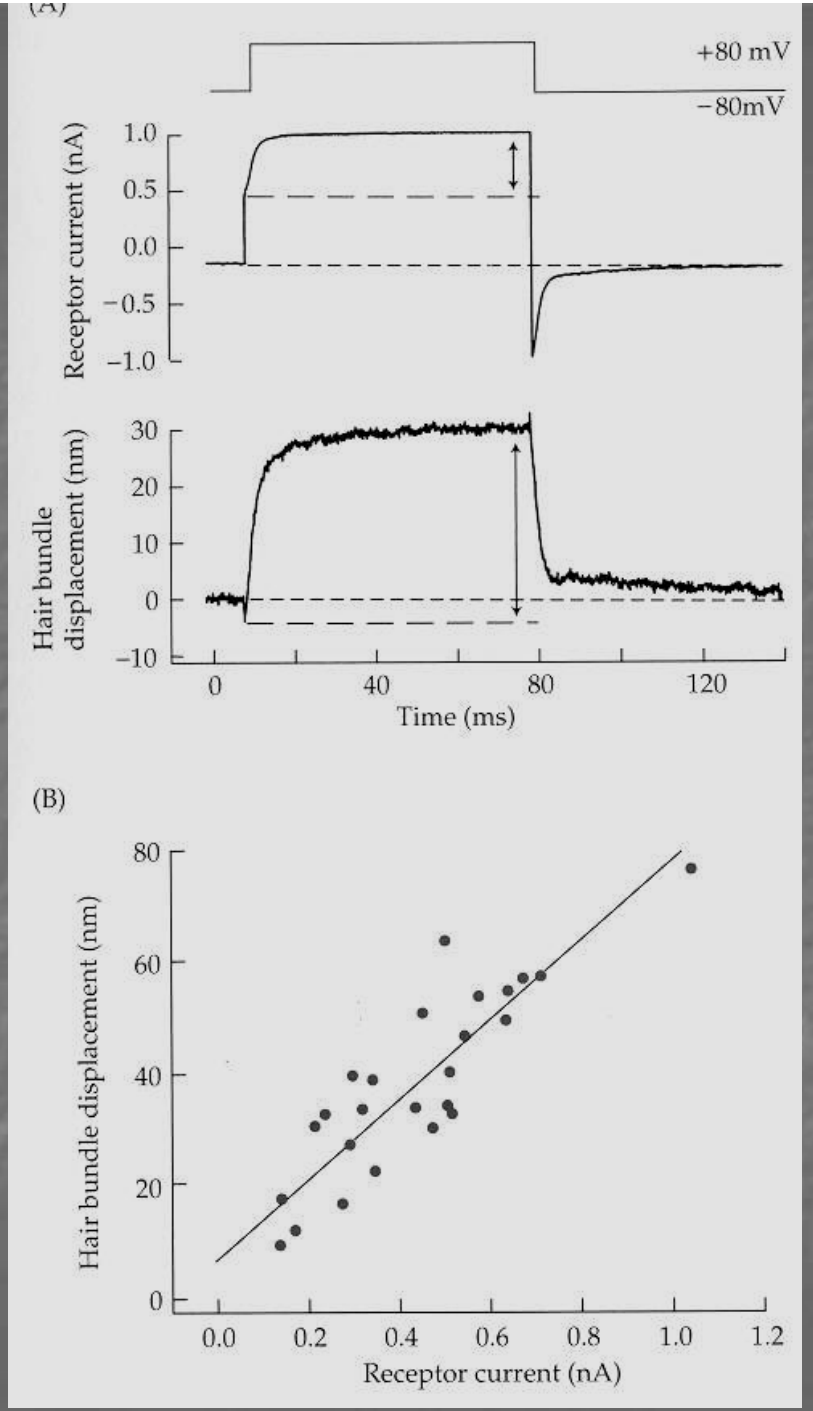

Rychlá adaptace:
Protipohyb uzavírající kanály a tlačící svazek zpět.

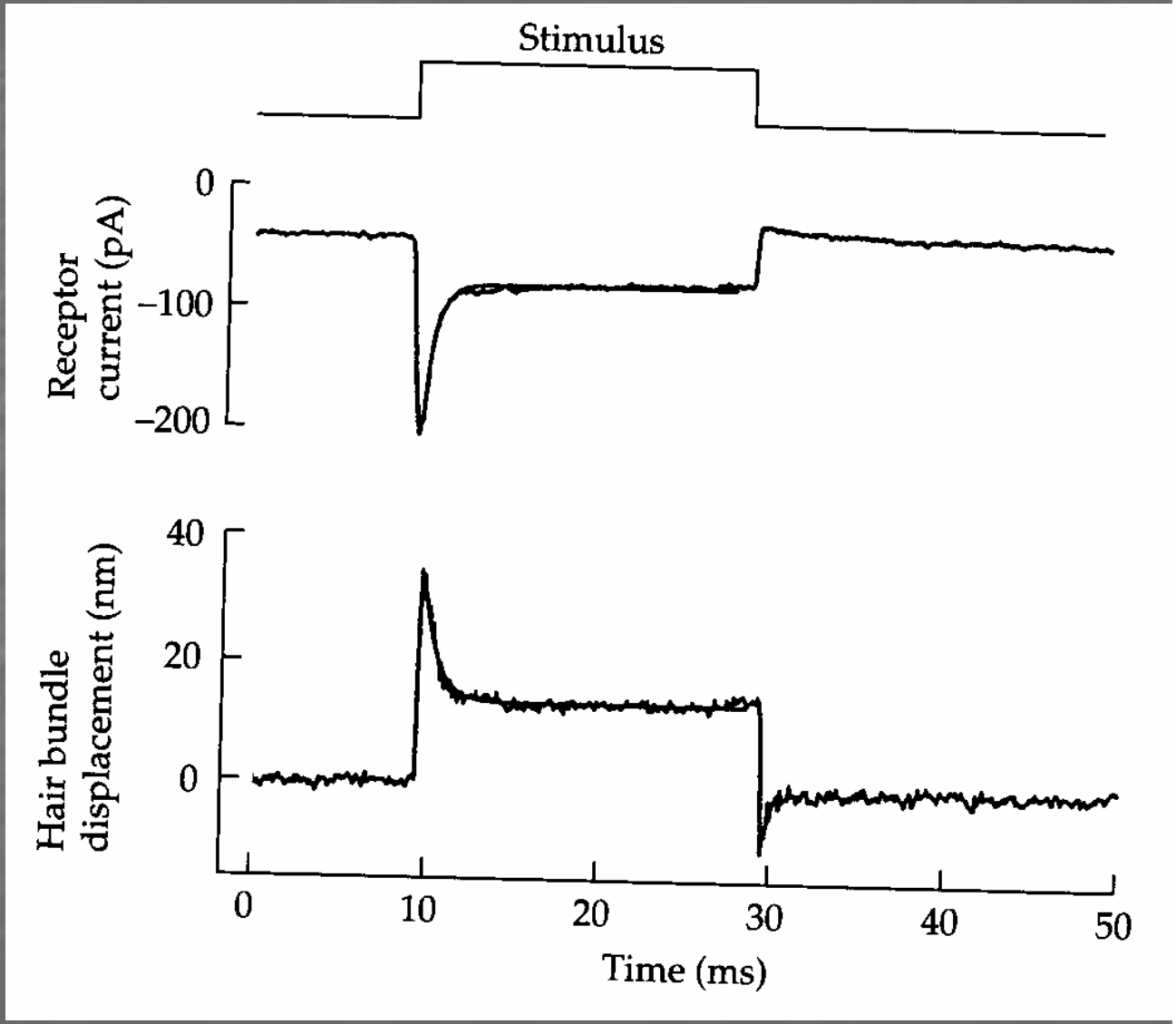

Rychlá – Ca do buňky,
Část kanálů se zavře,
Svazek se pohne zpět
Od kinocilie

Pomalá – uvolnění tenze vrátkovacích spojů

Obě závislé na Ca^{2+}

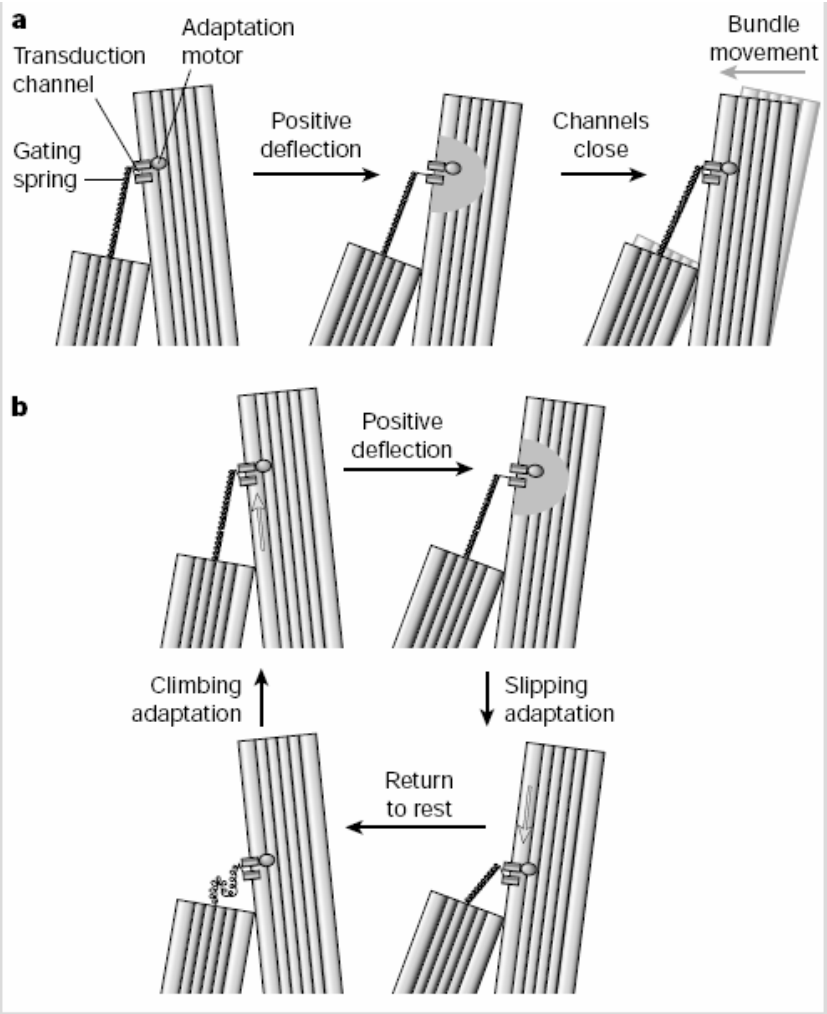

Box 2 Figure Hair-cell transduction and adaptation. **a**, Transduction and fast adaptation. At rest (left panel), transduction channels spend ~5% of the time open, allowing a modest Ca^{2+} entry (pink shading). A positive deflection (middle) stretches the gating spring (drawn here as the tip link); the increased tension propagates to the gate of the transduction channel, and channels open fully. The resulting Ca^{2+} flowing in through the channels shifts the channels' open probability to favour channel closure (right). As the gates close, they increase force in the gating spring, which moves the bundle back in the direction of the original stimulus. **b**, Transduction and slow adaptation. Slow adaptation ensues when the motor (green oval) slides down the stereocilium (lower right), allowing channels to close. After the bundle is returned to rest (lower left), gating-spring tension is very low; adaptation re-establishes tension and returns the channel to the resting state.

Pomalá adaptace
Řízená Ca

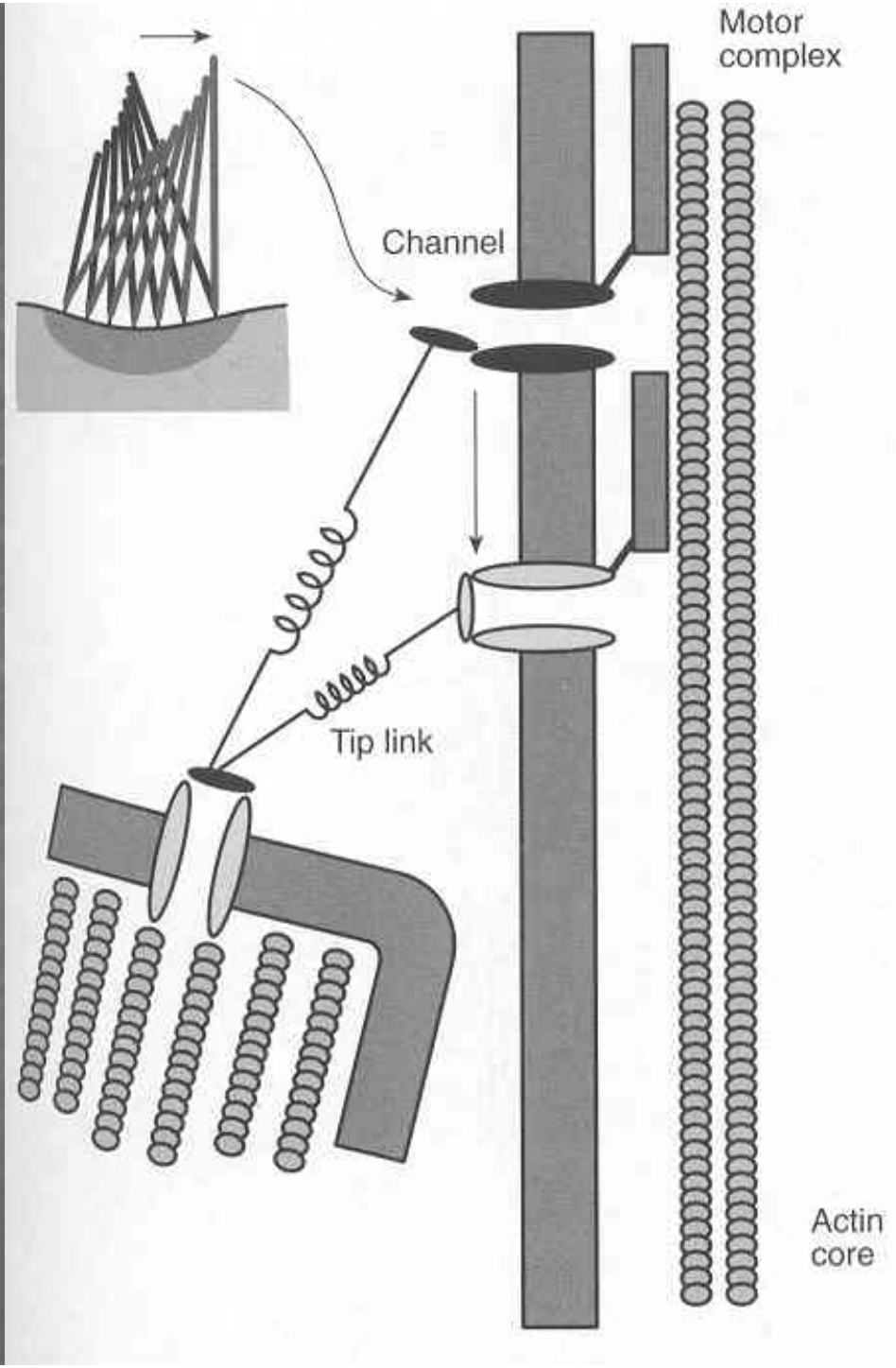

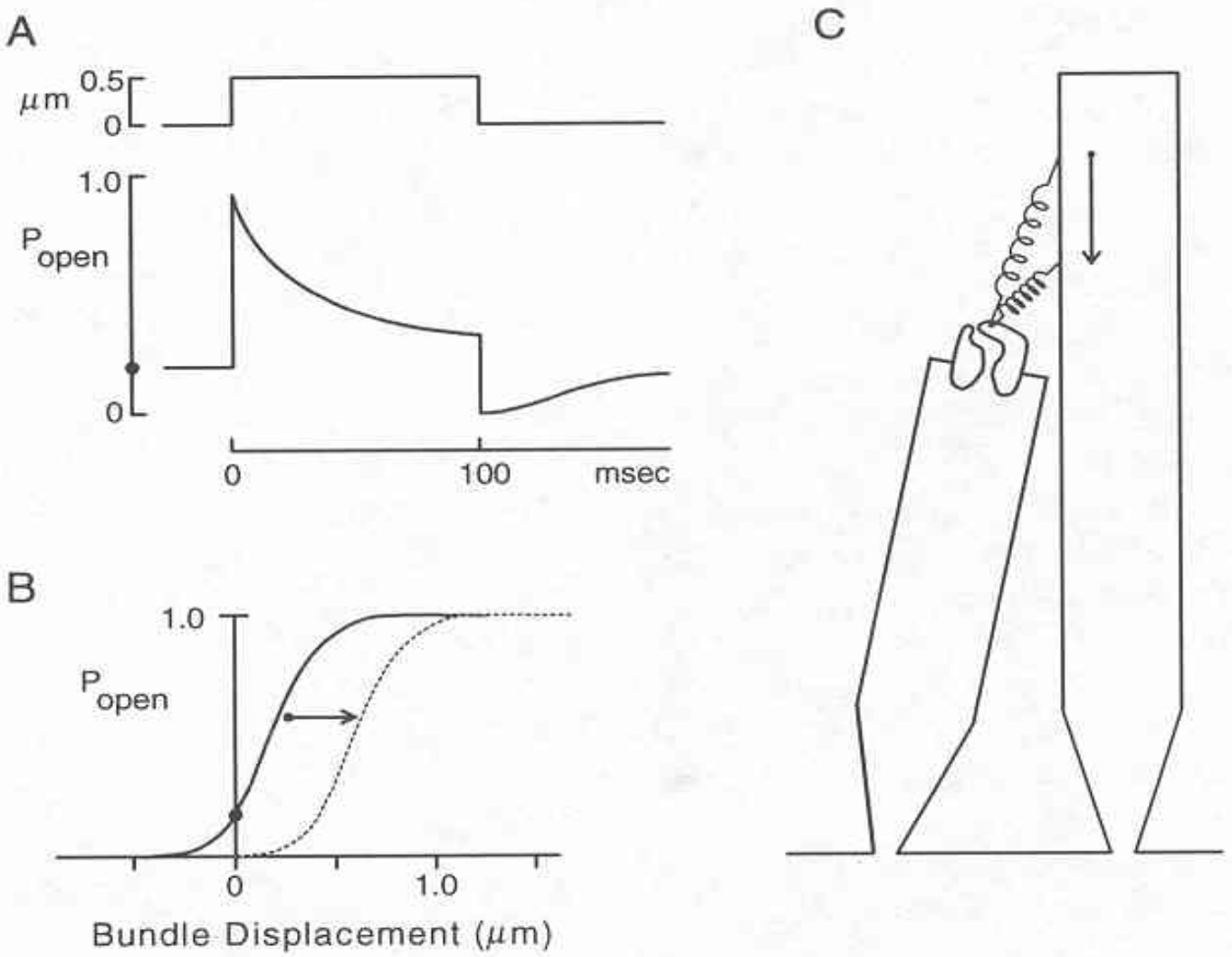

Fig. 14.7 Adaptation in hair cells. **A.** Deflection of the hair bundle toward the tallest stereocilia causes a large increase in the open probability of the transduction channels, followed by a rapid decline toward the resting value. Upon cessation of the stimulus, the channels initially close, then return to the resting value for open probability. **B.** The sensitivity curve shifts during adaptation to accommodate the shift in bundle position. **C.** A model for the mechanism of adaptation, consistent with the tip-links model for sensory transduction. The changes in tension in the tip links are effected by the movement of the upper insertion point of the tip link. (From Pickles and Corey, 1992)

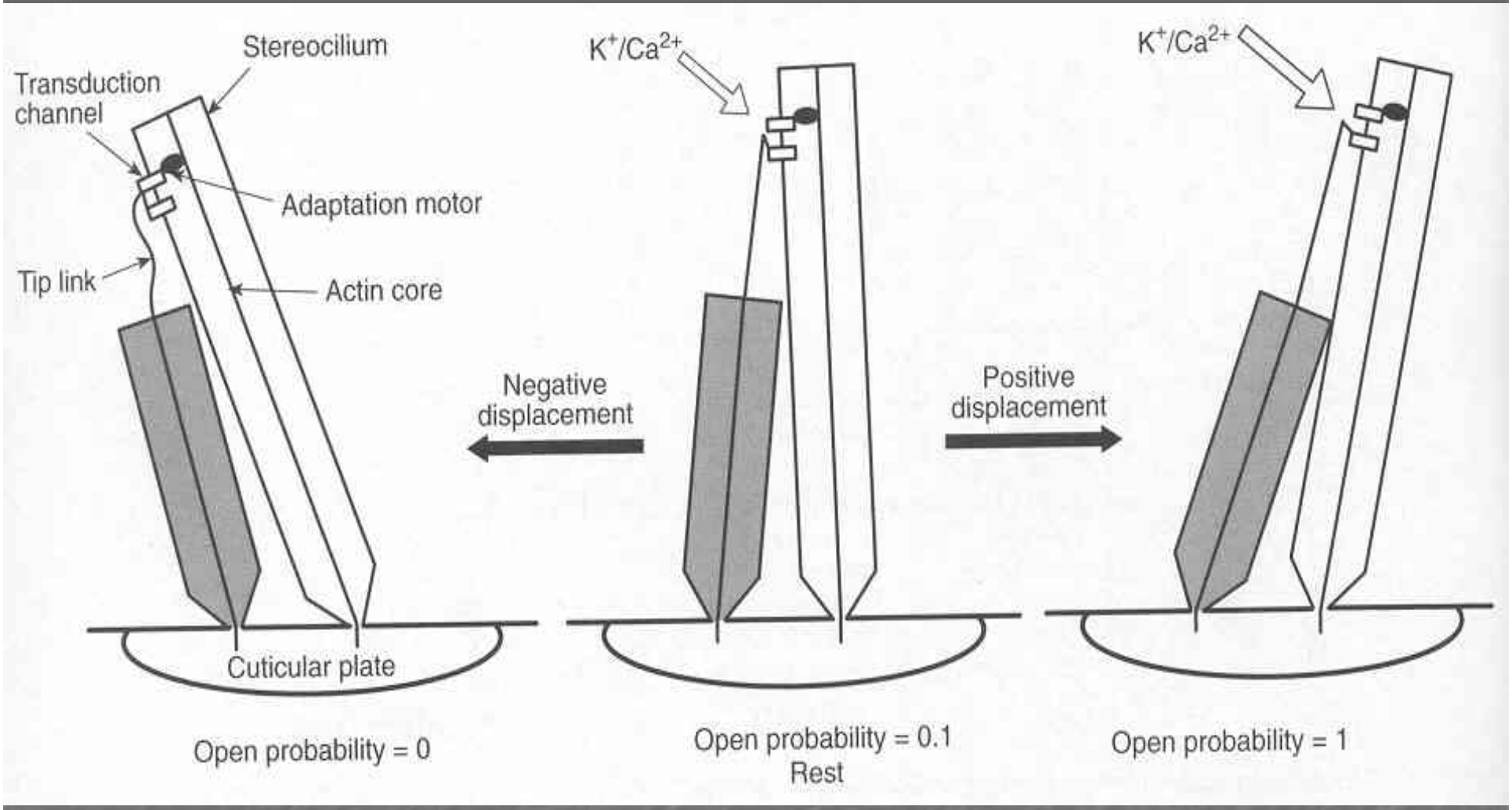
Stereocilium
Transduction channel
Adaptation motor
Tip link
Actin core
Cuticular plate
K^+/Ca^{2+}
K^+/Ca^{2+}
Negative displacement
Positive displacement
Open probability = 0
Open probability = 0.1
Rest
Open probability = 1

Kochleární zesilovač vnějších buněk
Kempovy otoaskutické emise

a) Membrána s **prestinem** –
pohyb celých buněk

b) Pohyb svazků sterocílií
díky mechanismu „rychlé adaptace“

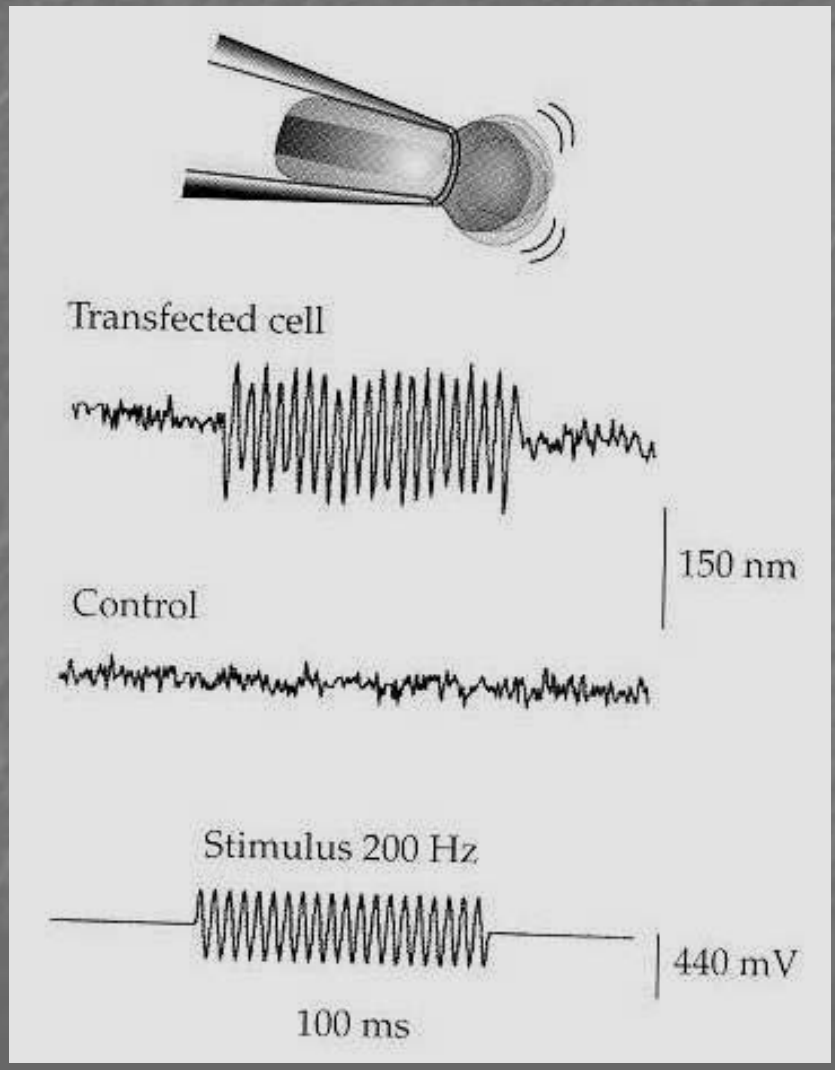

„Tancující“ membrána

a) Membrána s **prestinem** – pohyb celých buněk“

Elektro-mechanické spřažení

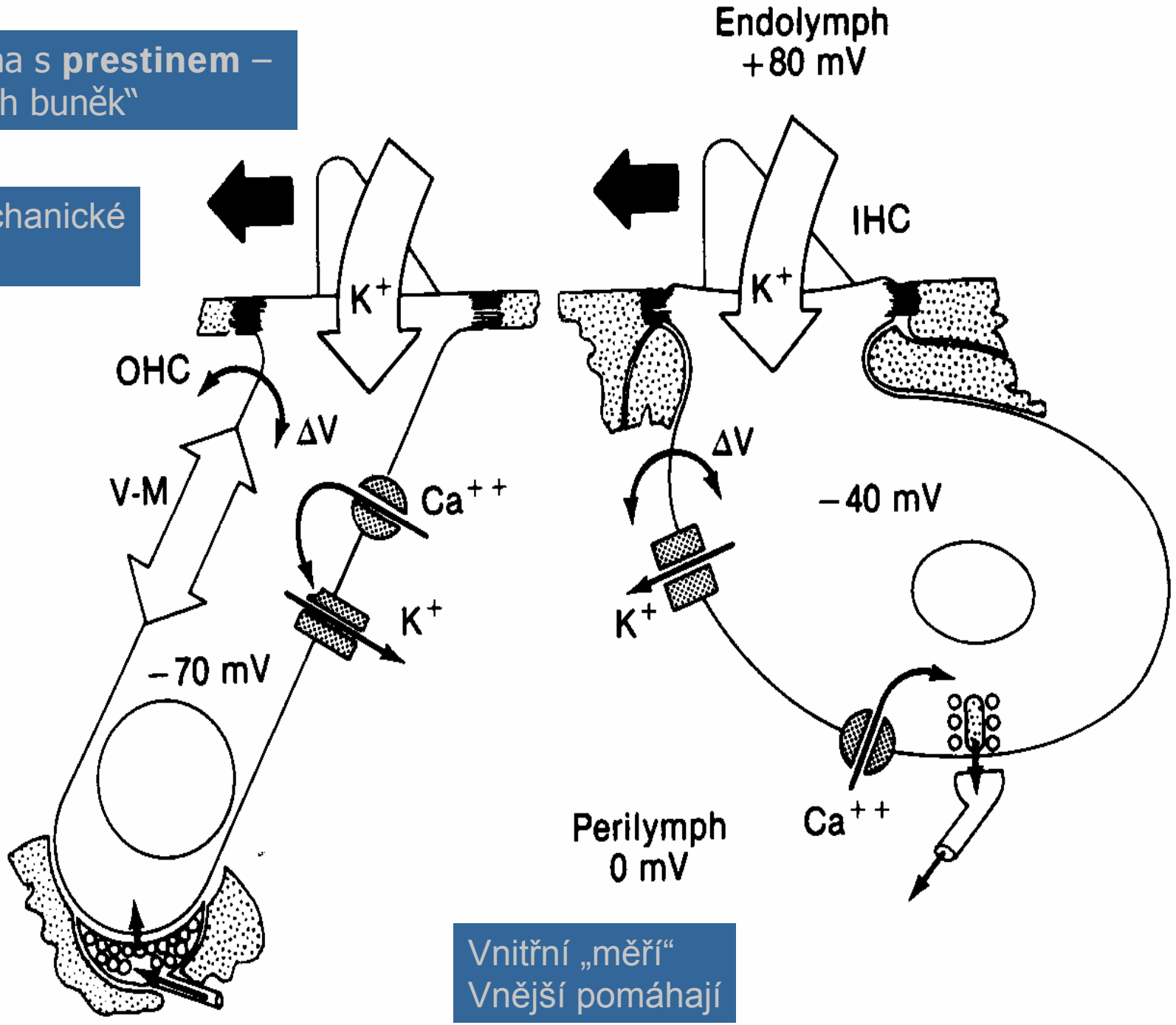

Vnitřní „měří“
Vnější pomáhají

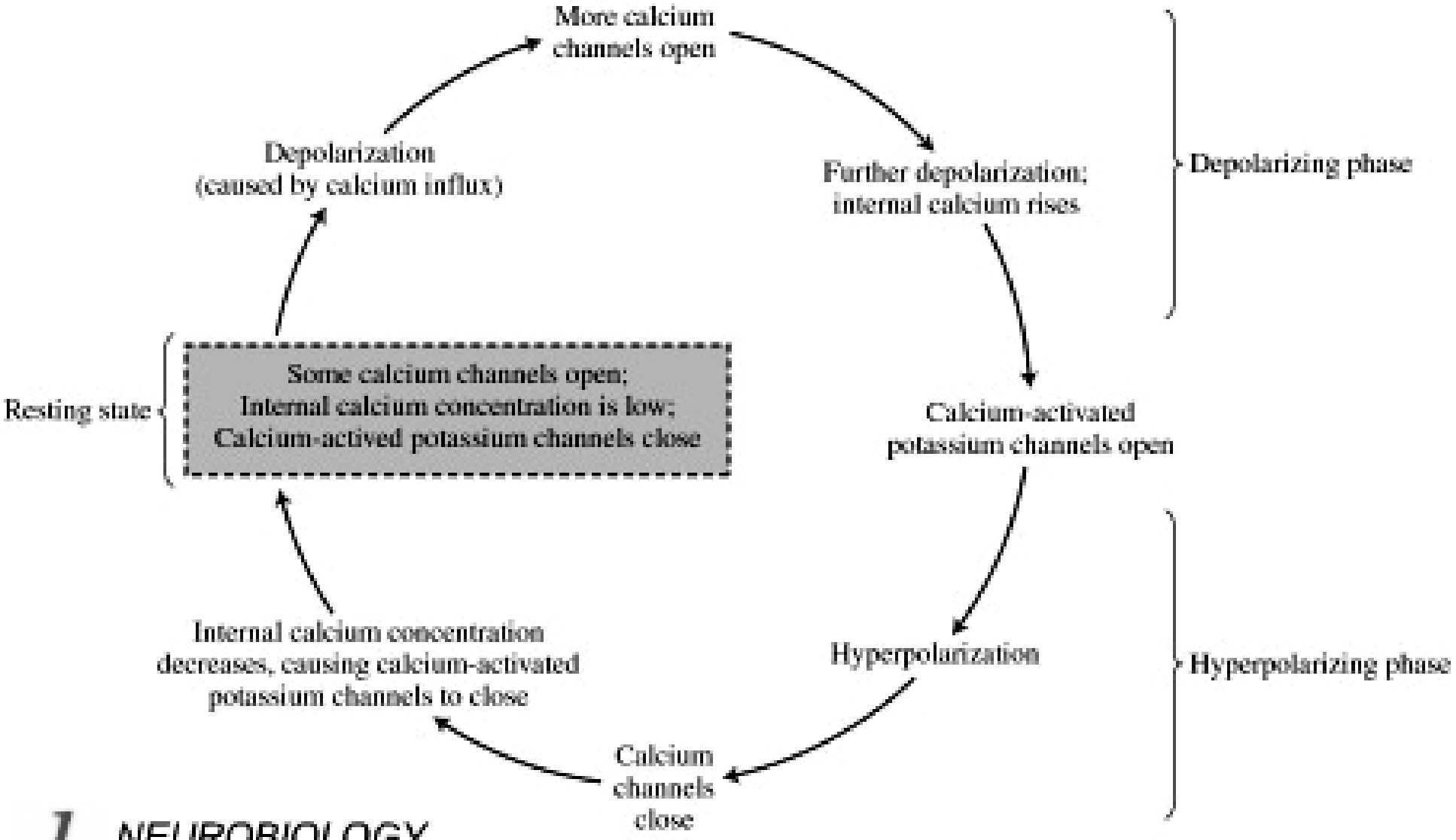

NEUROBIOLOGY
Gary G. Matthews
Blackwell Science

Vnitřní „měří“
Vnější pomáhají

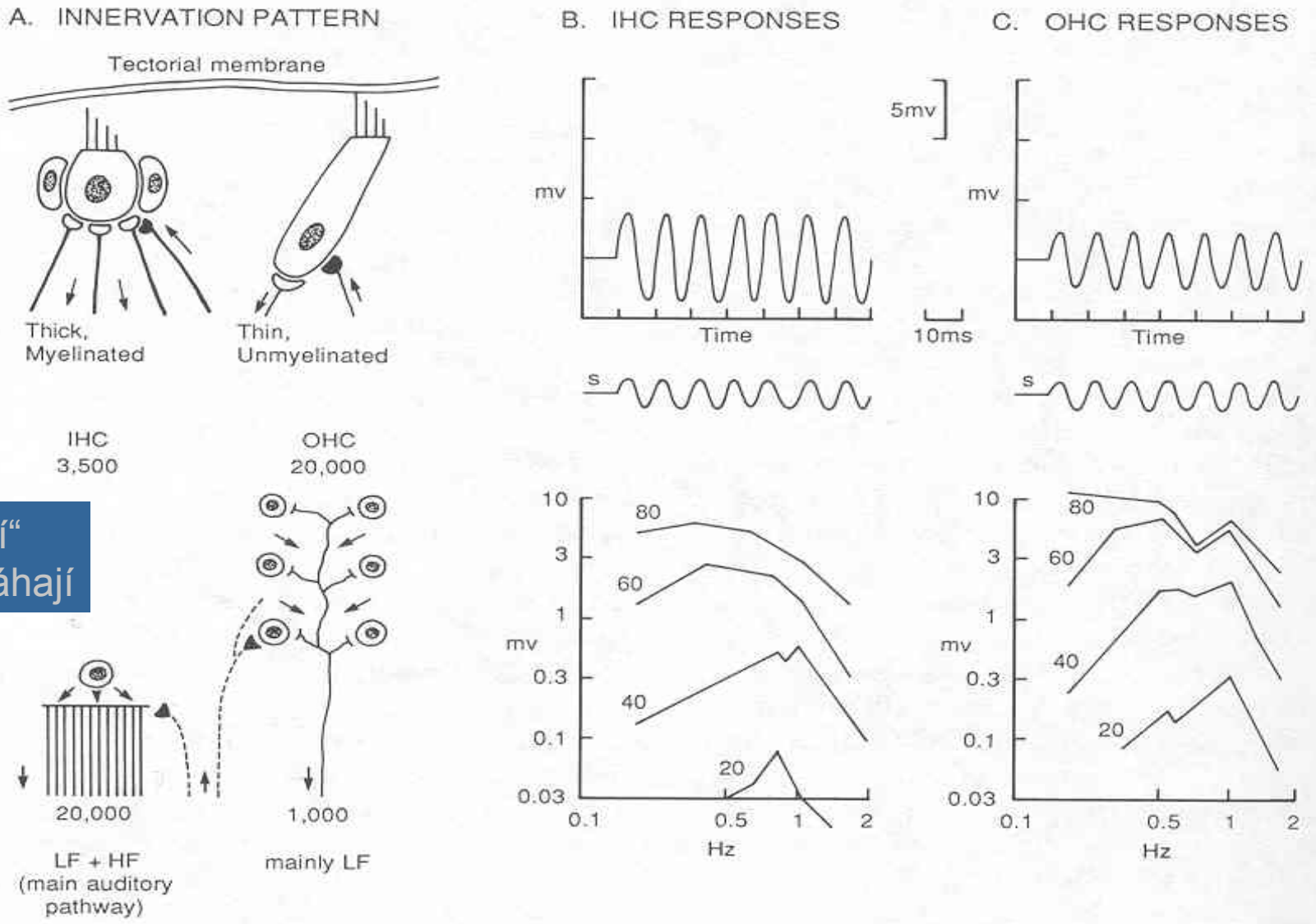

Fig. 15.5 Comparison of the organization and properties of inner hair cells (IHC) and outer hair cells (OHC). **A.** Innervation pattern. In the lower diagrams, the numbers of hair cells are given above and the numbers of auditory nerve fibers below. HF, high-frequency fibers; LF, low-frequency fibers. **B.** IHC response properties. *(Above)* Intracellular responses to tone stimulus (s). *(Below)* Response magnitude (as above) for different stimulus frequencies (abscissa) and at different stimulus intensities (20–80 dB). **C.** OHC response properties. (A based on Spoendlin, 1969; B,C based on Dallos, 1985)

Elektrická rezonance
Bez nutnosti mechanické

Vlastnosti kanálů určují rezonanční frekvenci

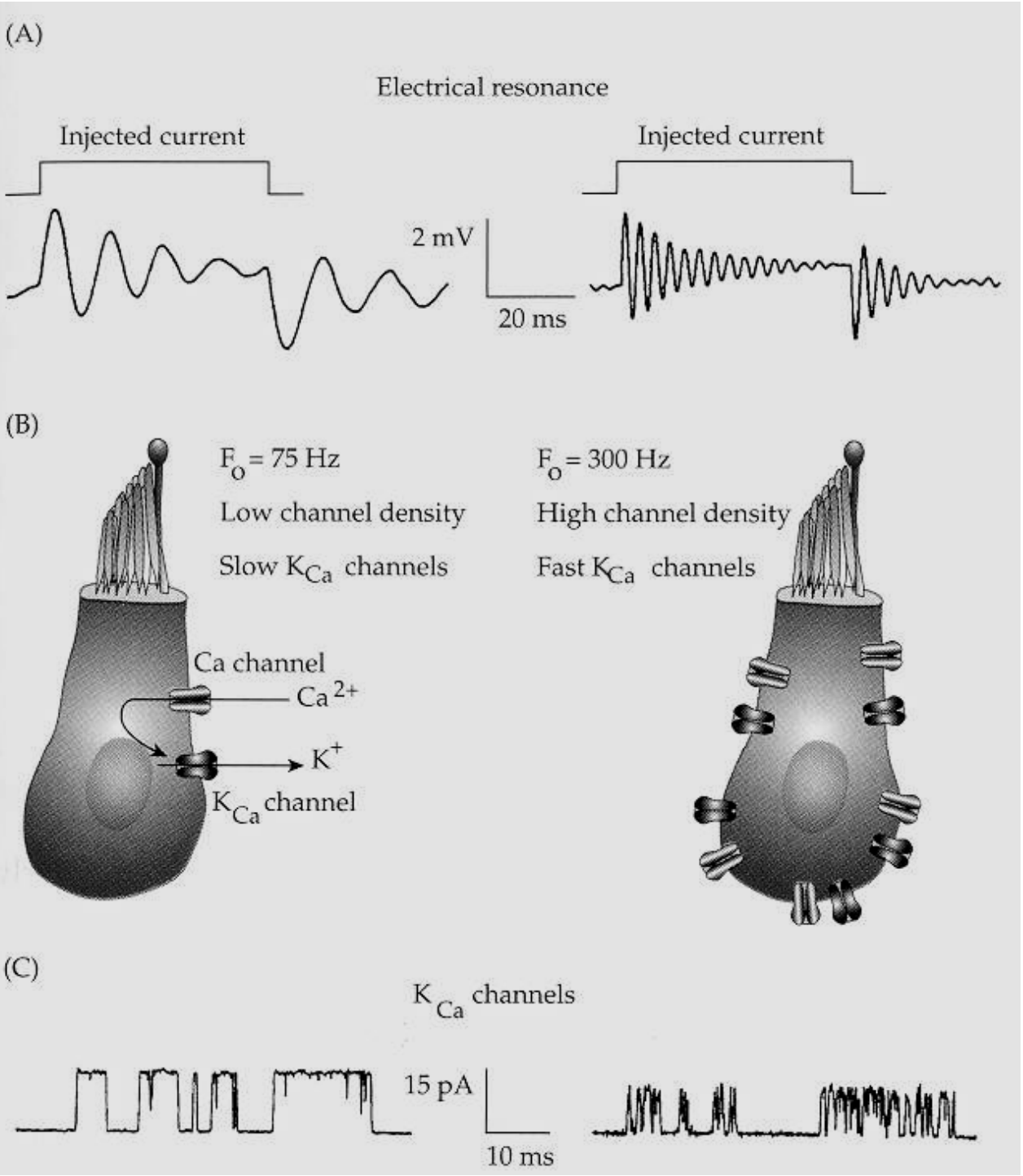

Elektrická rezonance
Bez nutnosti mechanické

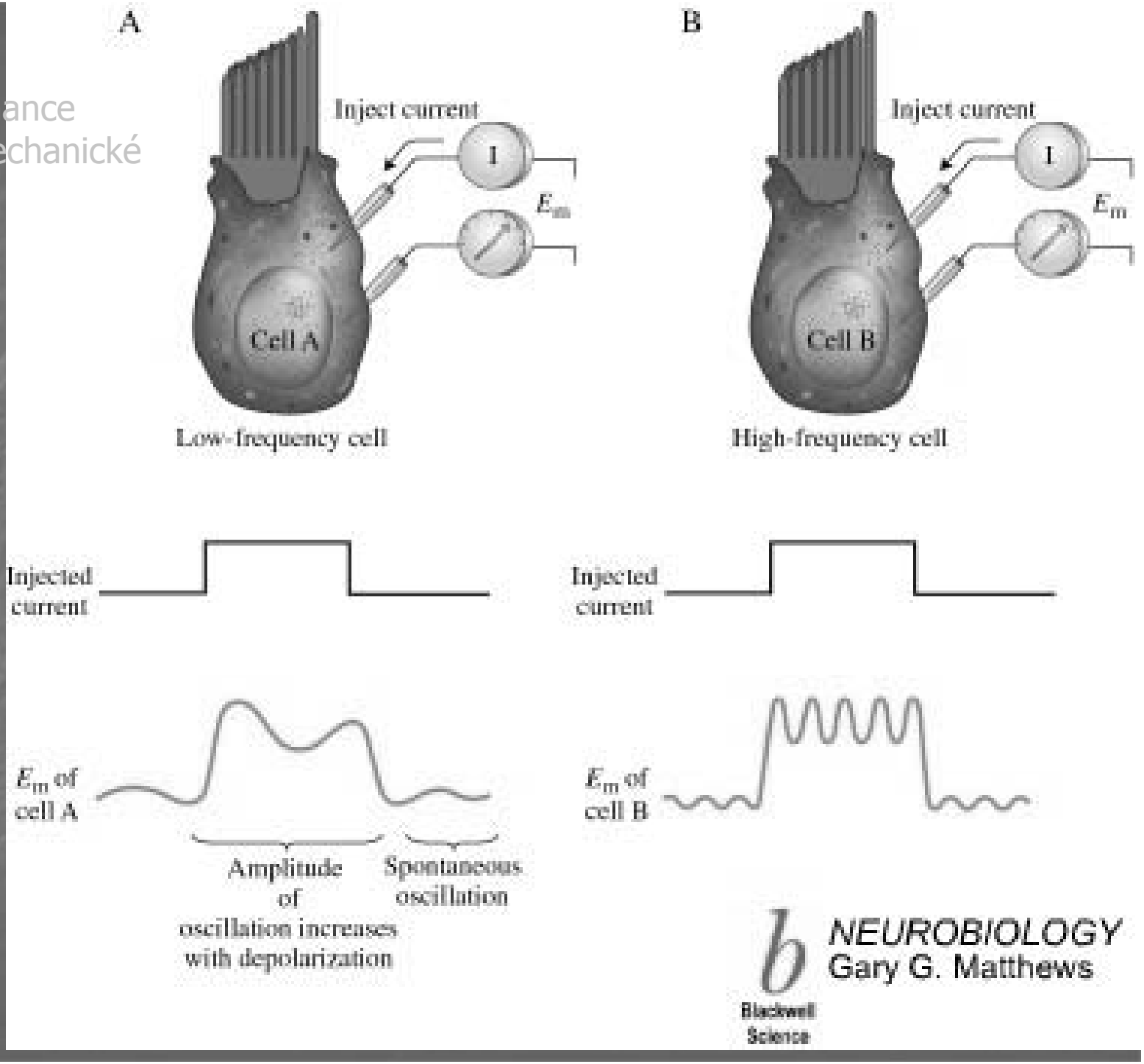

Hraniční spektrální citlivost pro
různá vlákna sluchového nervu
- Každý má své frekvenční optimum

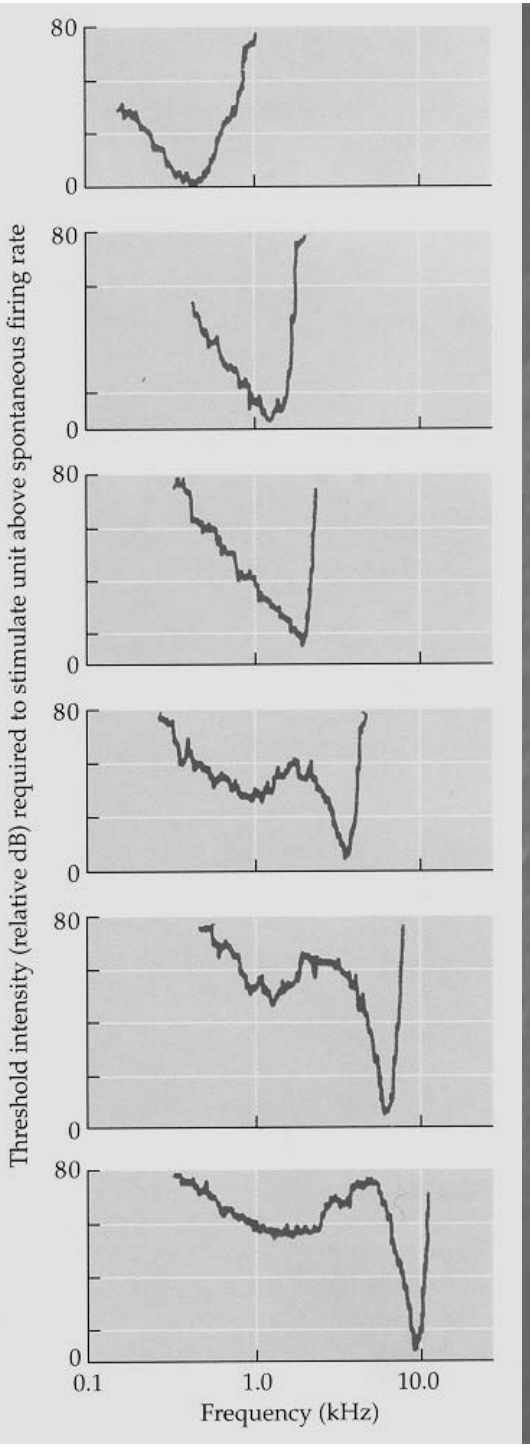

Frekvenčně naladěné buňky

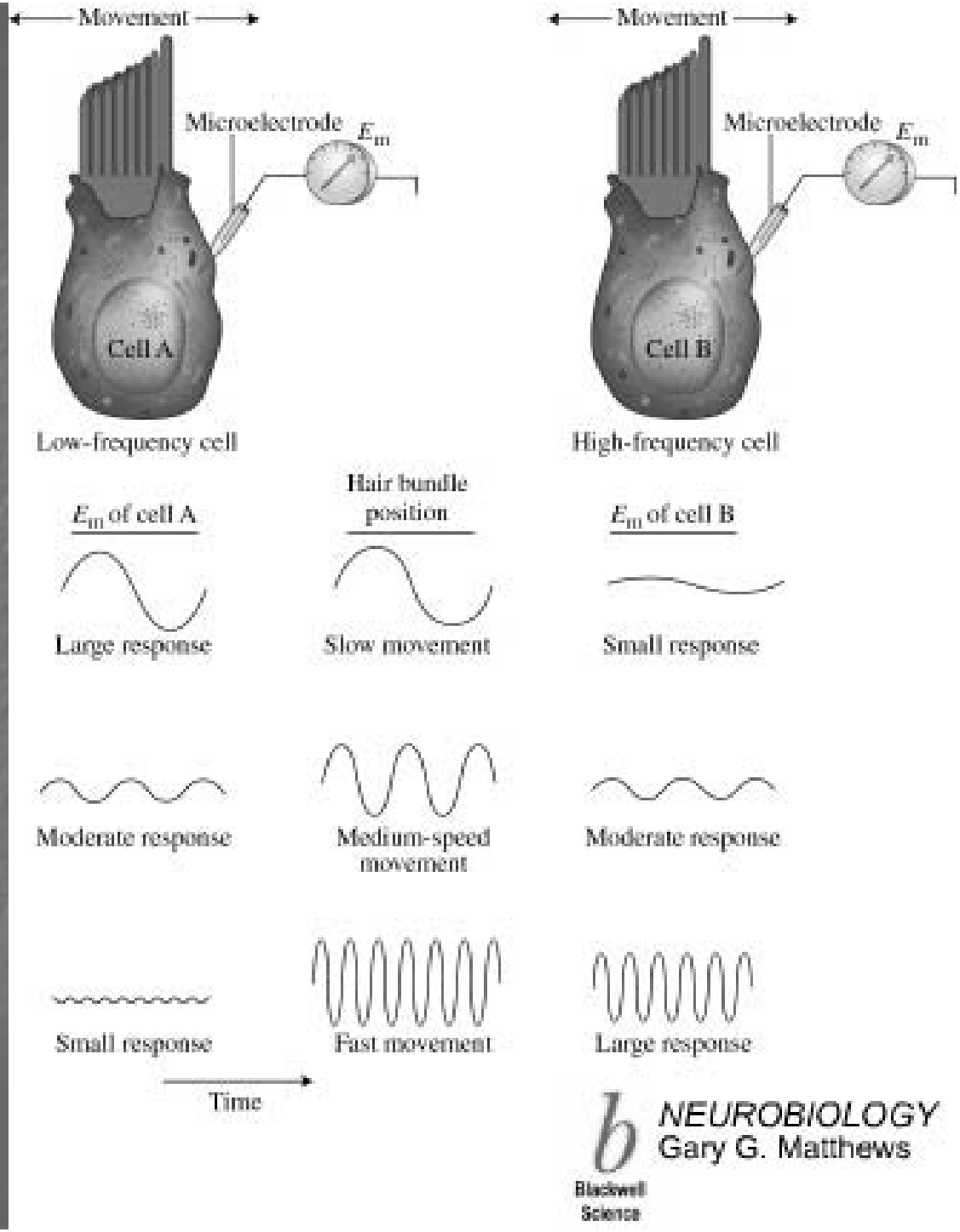

Kromě lokalizace k kochlei existuje i Časový kód
Neuron může „poznat“ fázi nízkých frekvencí –
Omezeno ale refrakterní periodou
pod 1 kHz

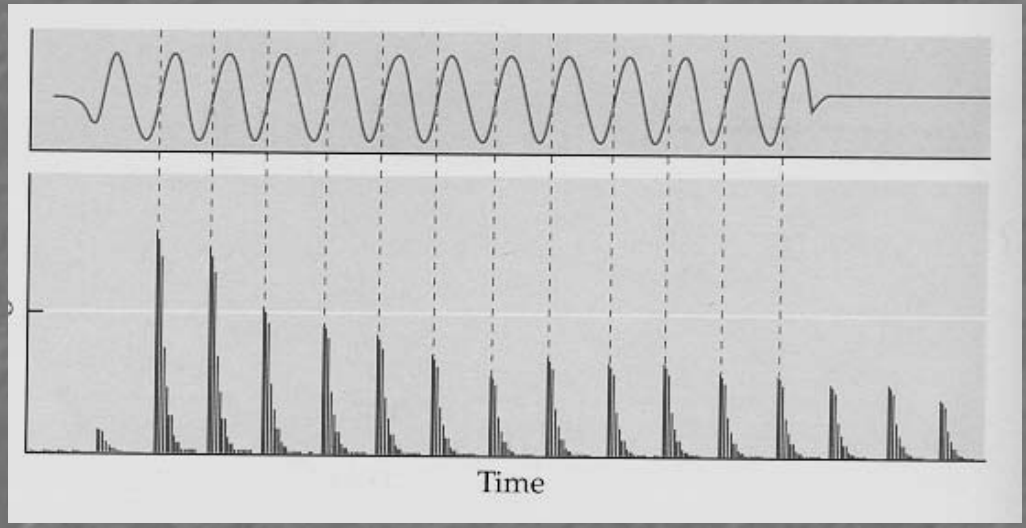

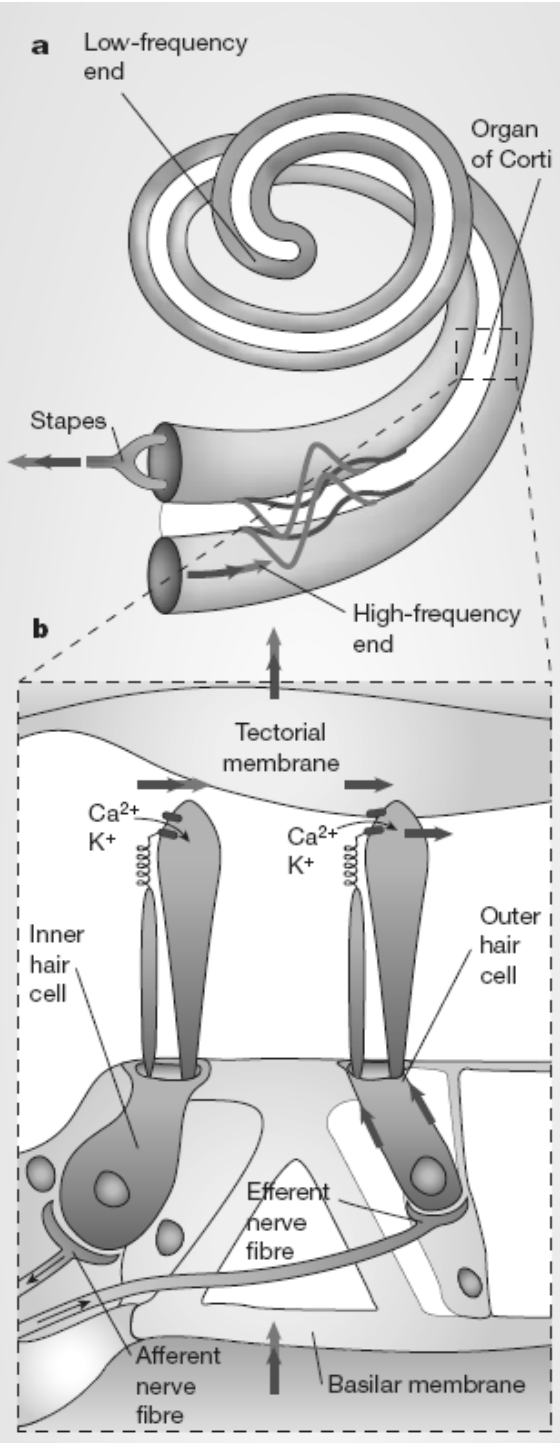
a
Low-frequency end
Organ of Corti
Stapes
High-frequency end
b
Tectorial membrane
Ca2+
K+
Ca2+
K+
Inner hair cell
Outer hair cell
Efferent nerve fibre
Afferent nerve fibre
Basilar membrane

Rovnováha
Vedení a zpracování signálu

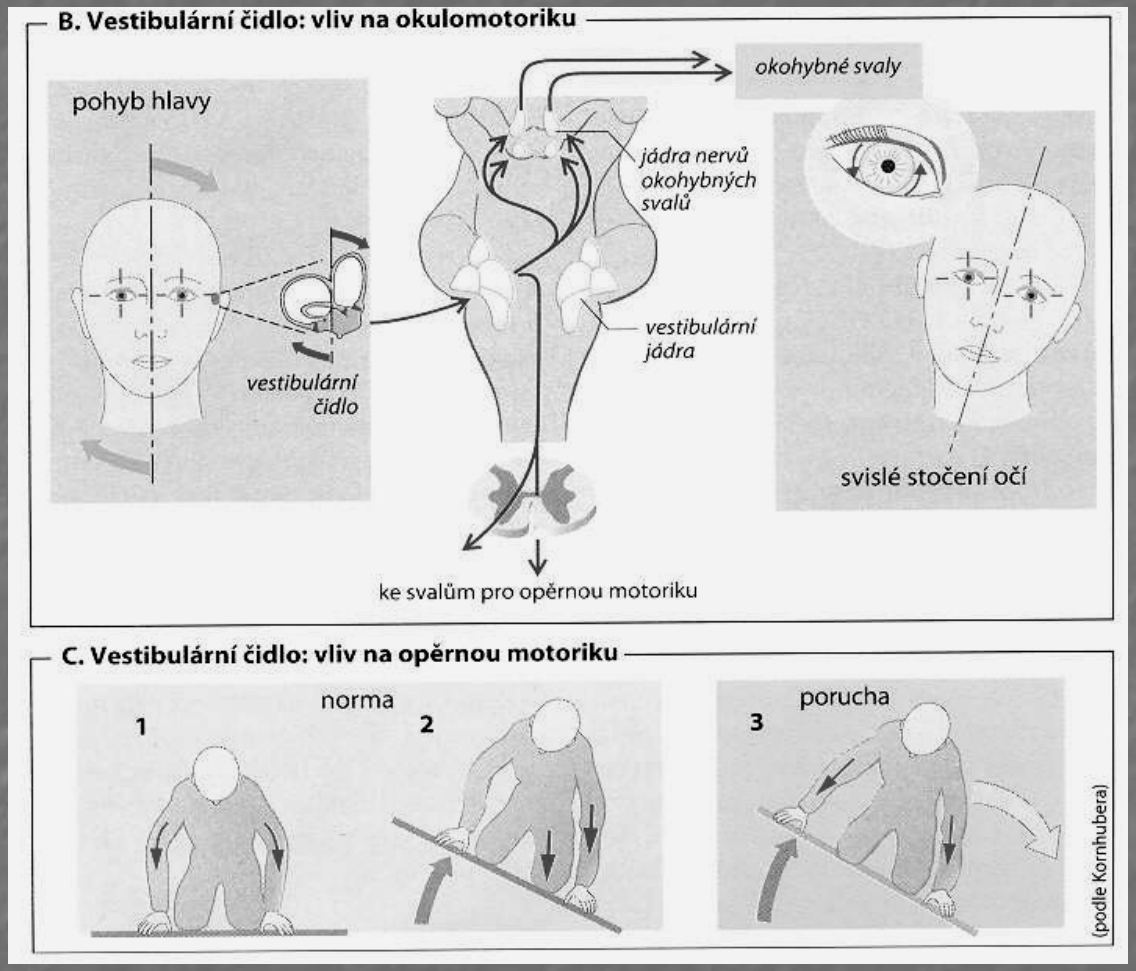

Sluchová dráha

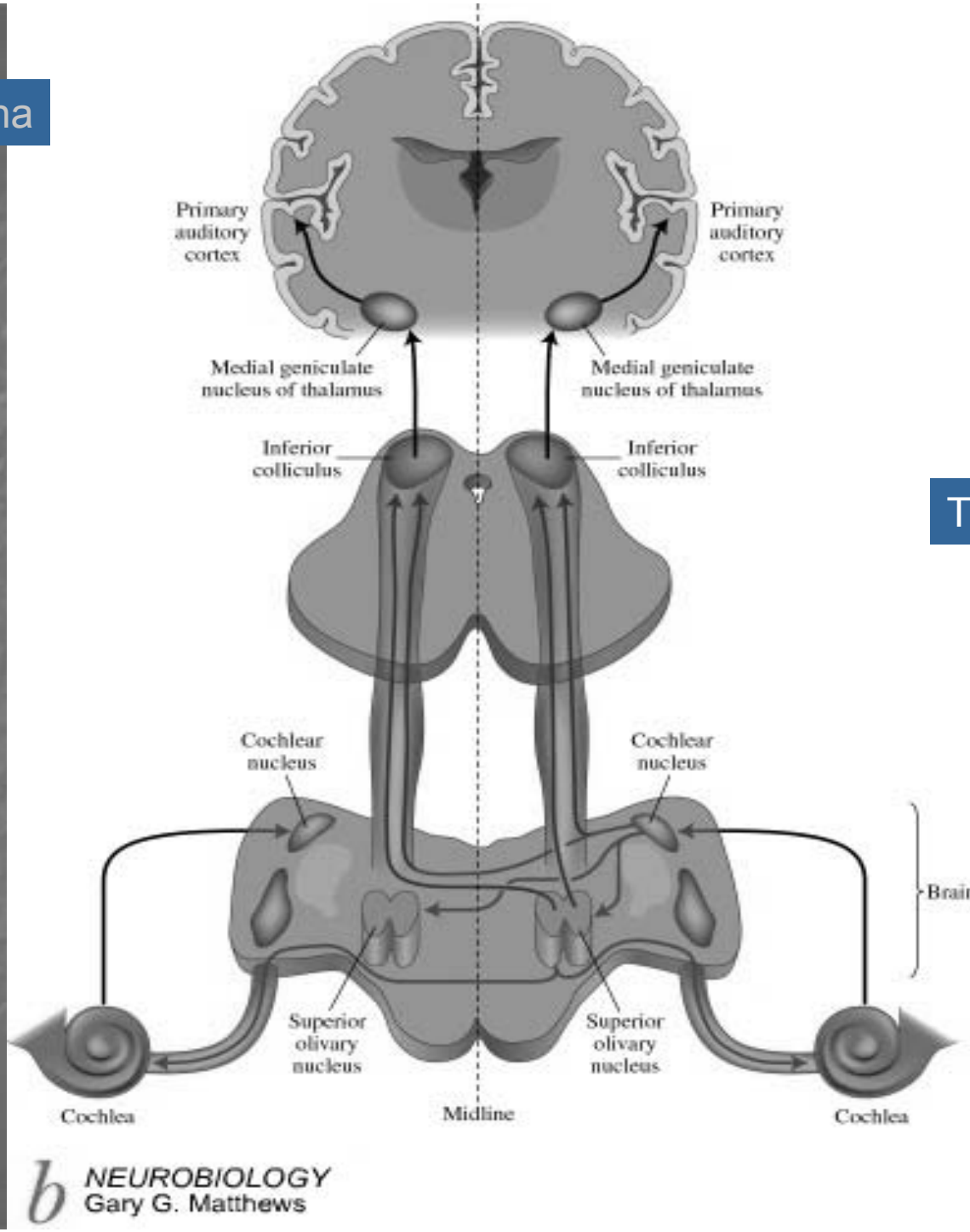

Tektum

Pons Varoli

Sluchová dráha
1.Kochleární jádra
Některé neurony citlivé na výšku, nástup, jiné na série. Laterální inhibice. Šum/signál.
2. Horní oliva – křížení nutné pro Lokalizaci. Analýza koincidence
3. Inf. coll. – spodní hrbolek Tekta
4. Geniculate komplex – poslední před kůrou. Mnoho eferentních vláken.
5. Prim a sec. Kůra

Ve srovnání se zrakem mnoho práce ještě před kůrou ve kmeni –
Savci nejprve pouze noční .
Až řeč lokalizována do kůry.

FIGURE 9.20 Schematic of auditory system pathways. Not all pathways are shown. Although there are two parallel pathways, note that information from both ears comes together very early in the auditory system, at the superior olives.

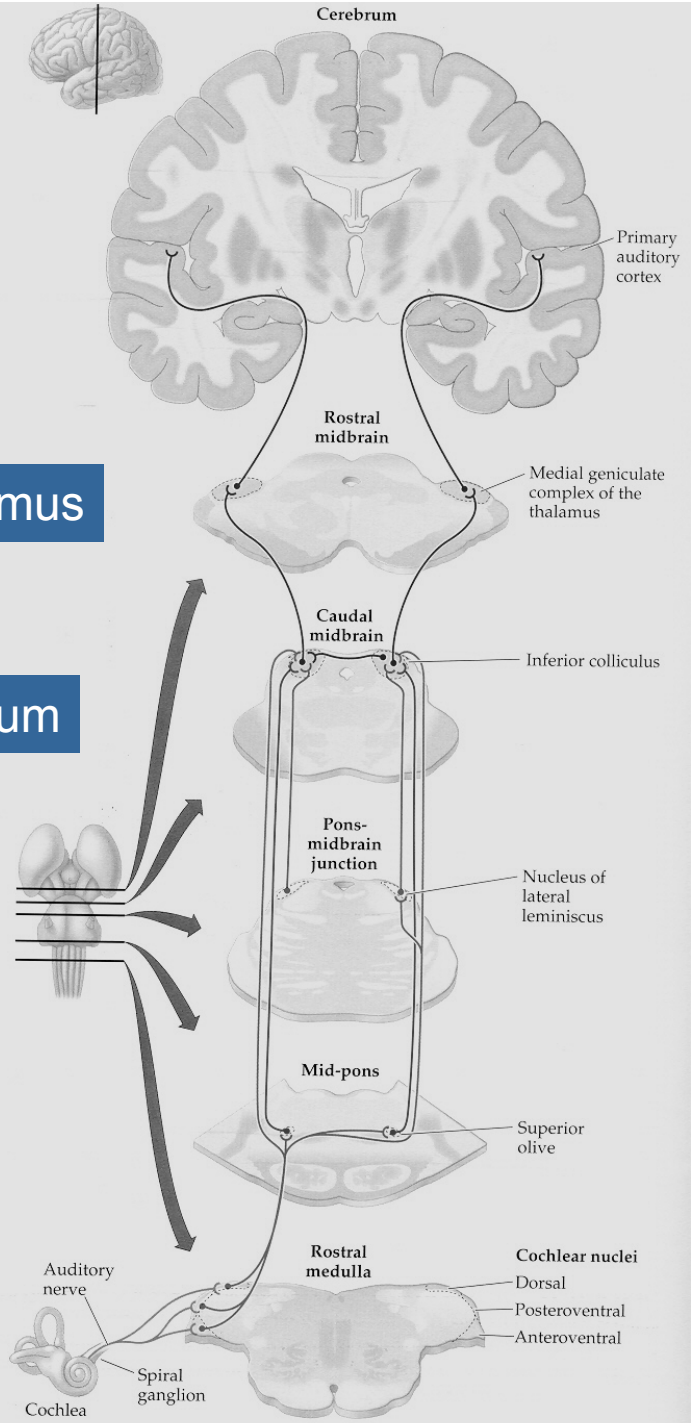

Tonotopická a bilaterální organizace kůry
Neurony citlivé na modulované frekvence nebo volání

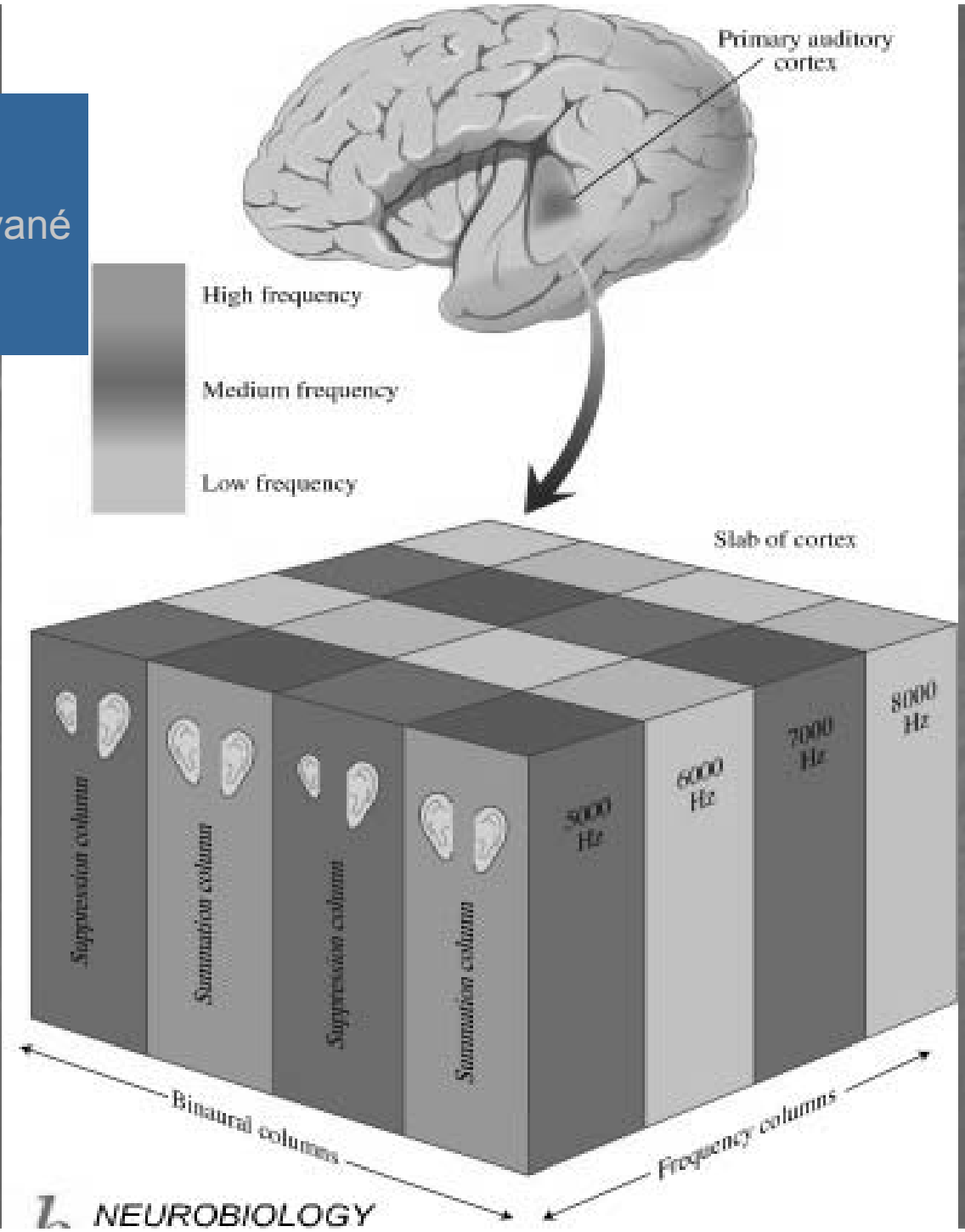

Psychoakustika:
Hlasitost není totéž co intenzita
a frekvence není totéž co výška tónu (nestoupe lineárně)
Izofony

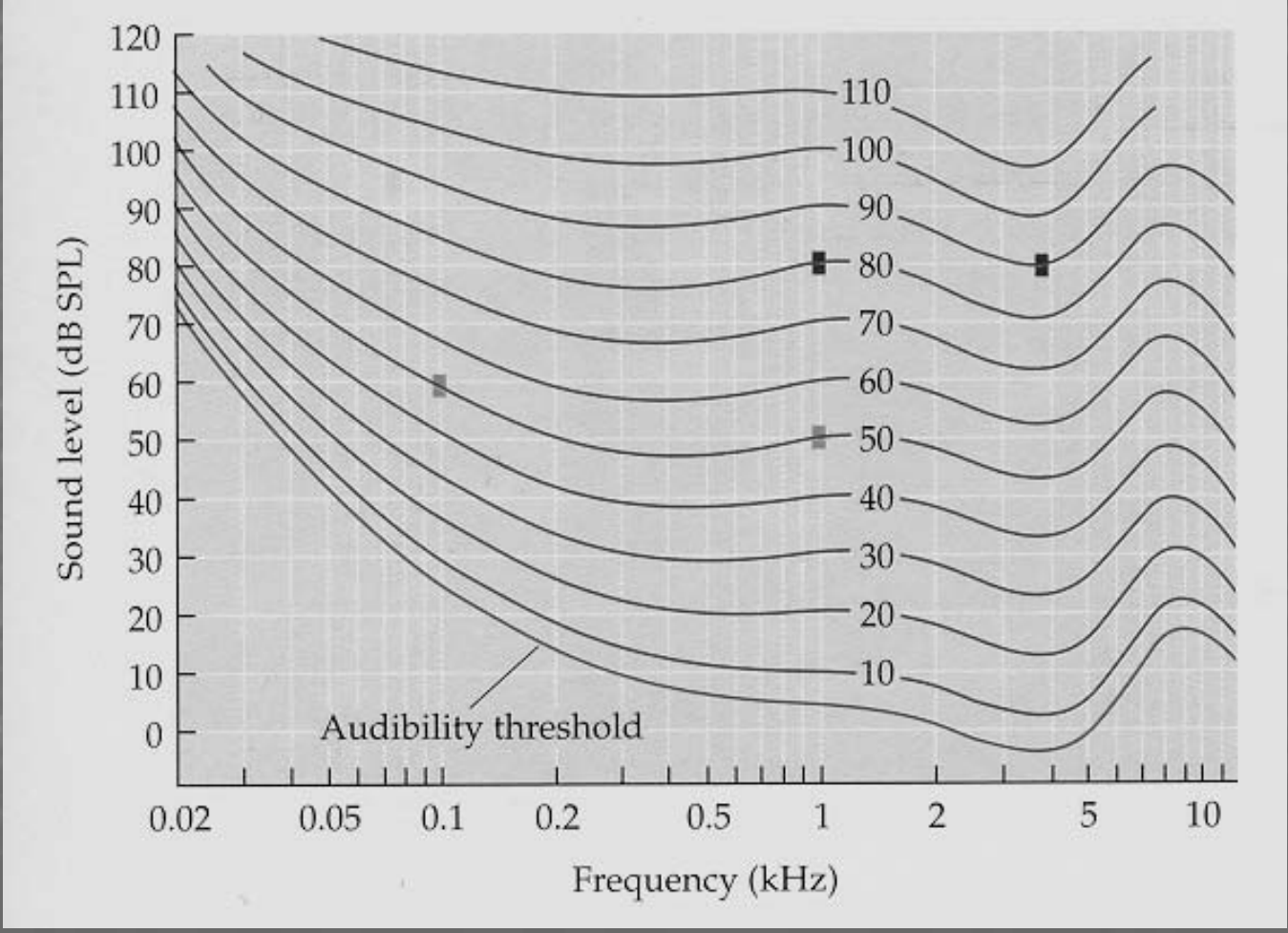

http://www.sinauer.com/wolfe/chap9/equalloudF.htm

Určení hlasitosti zvuku

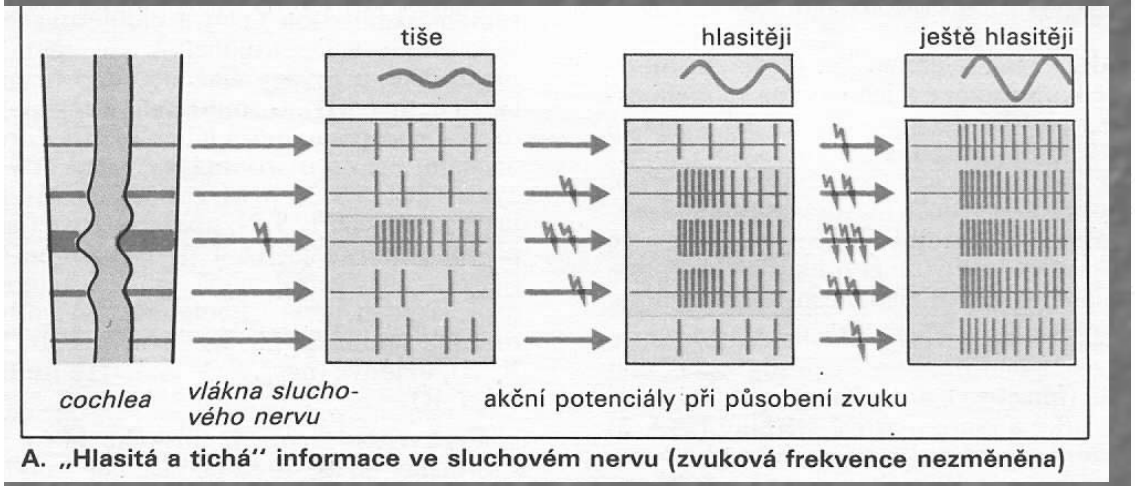

A. „Hlasitá a tichá" informace ve sluchovém nervu (zvuková frekvence nezměněna)

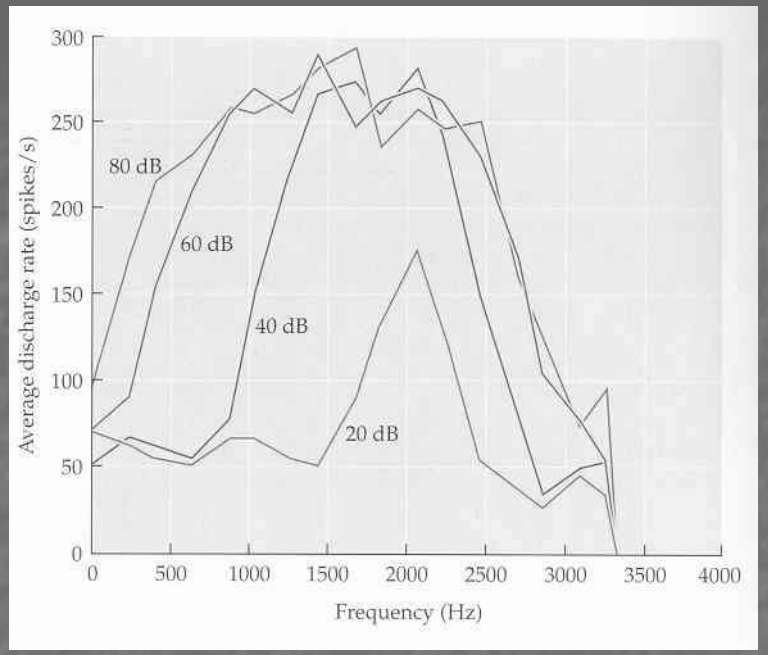

Poznáme 1dB ze 100dB
Důležité-odhaduje se z toho směr zvuku
Čím hlasitější, tím větší rozsah zabere.
Vlákna sl. nervu specializovaná na určitou Hlasitost.

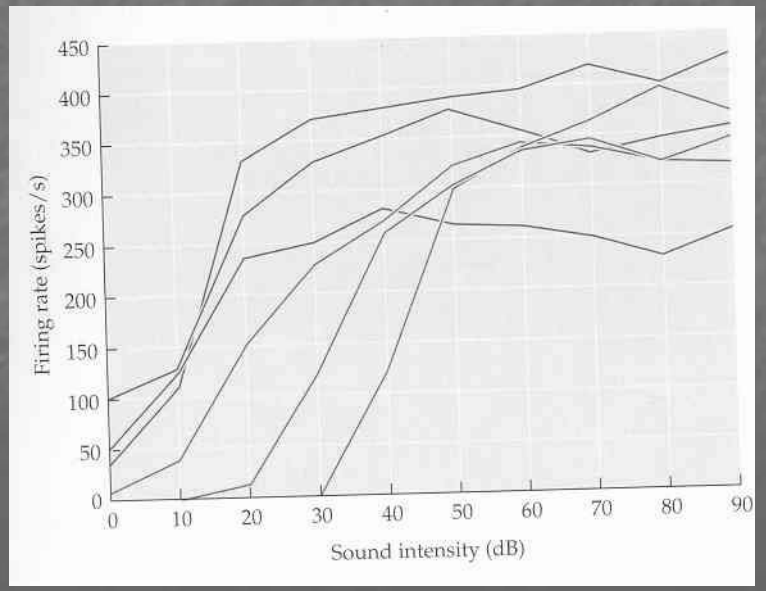

Určení směru zvuku – dva klíče

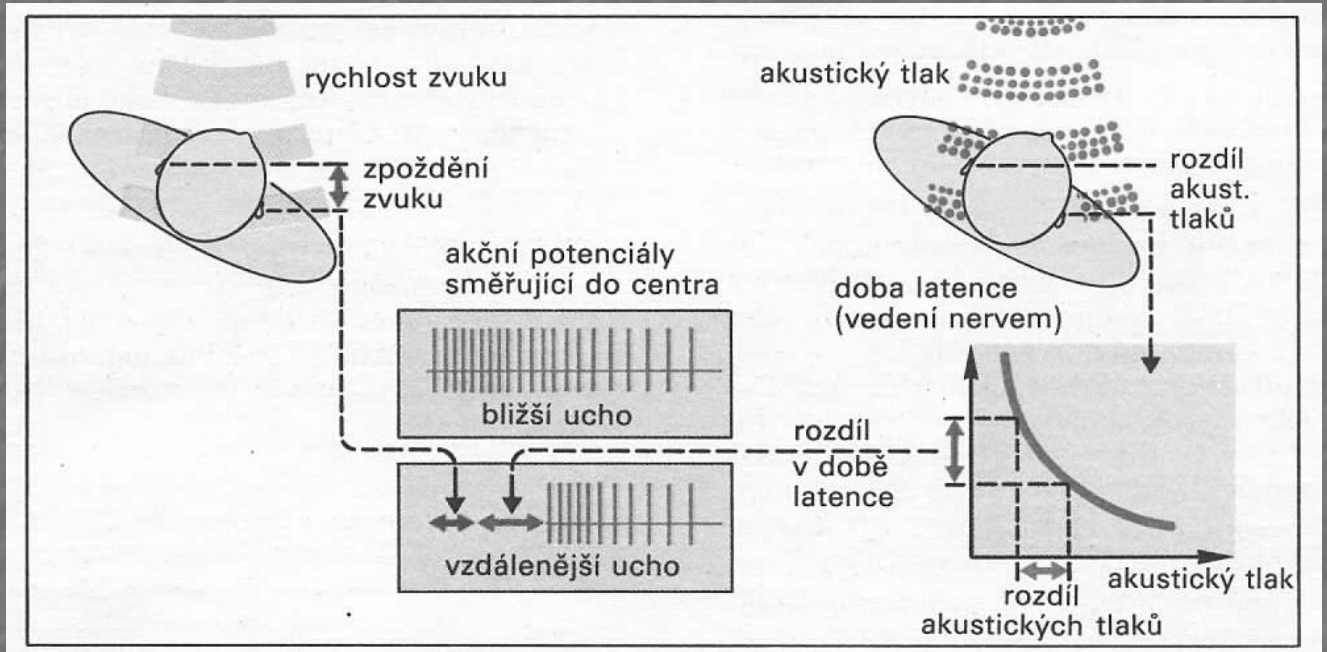

B. Prostorové slyšení: zpoždění zvuku a rozdíl latencí

Koincidenční detektor

Simultánně
Offset

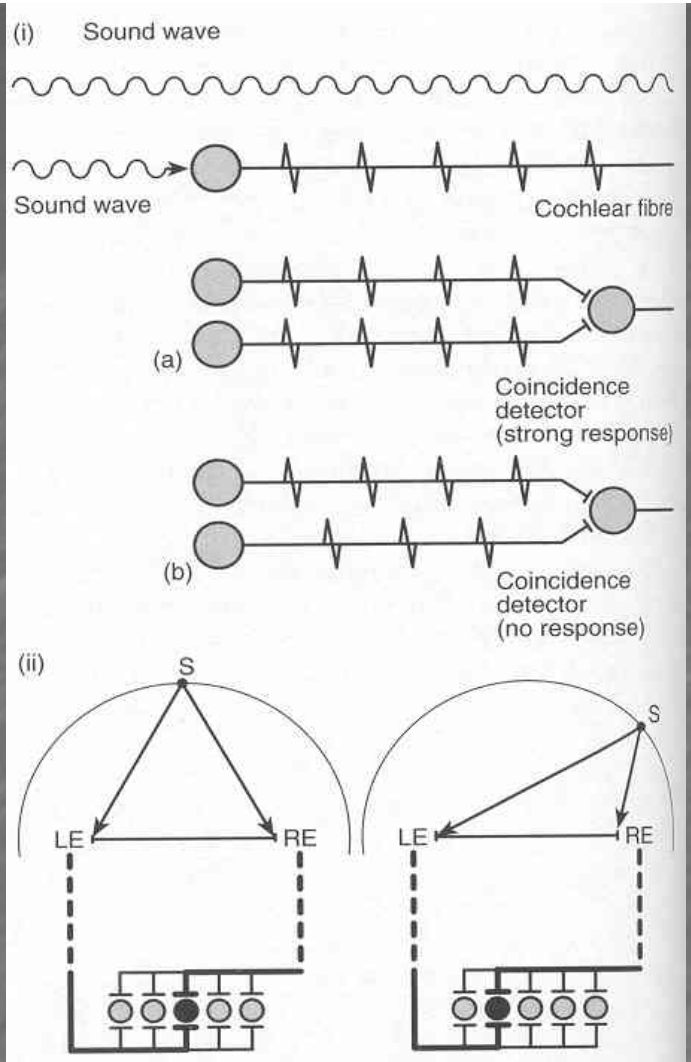

Figure 9.8 (i) Phase locking and coincidence detection. The cochlear fibre fires in response to every second peak in the sound wave. (a) If cochlear fibres from opposite ears converge on a coincidence detector the latter will fire if the two signals are delivered within a few tens of microseconds of each other; (b) if the time differential is greater the detector will respond only weakly or not at all. (ii) The principle of source location by way of interaural time differences (ITDs). A sound source (S) equidistant from the two ears will stimulate a certain coincidence detector (dark circle); a sound source further from one ear than the other will stimulate a different coincidence detector. LE = left ear; RE = right ear. Further explanation in text. After Konishi, 1993

Prostorové slyšení – časový klíč

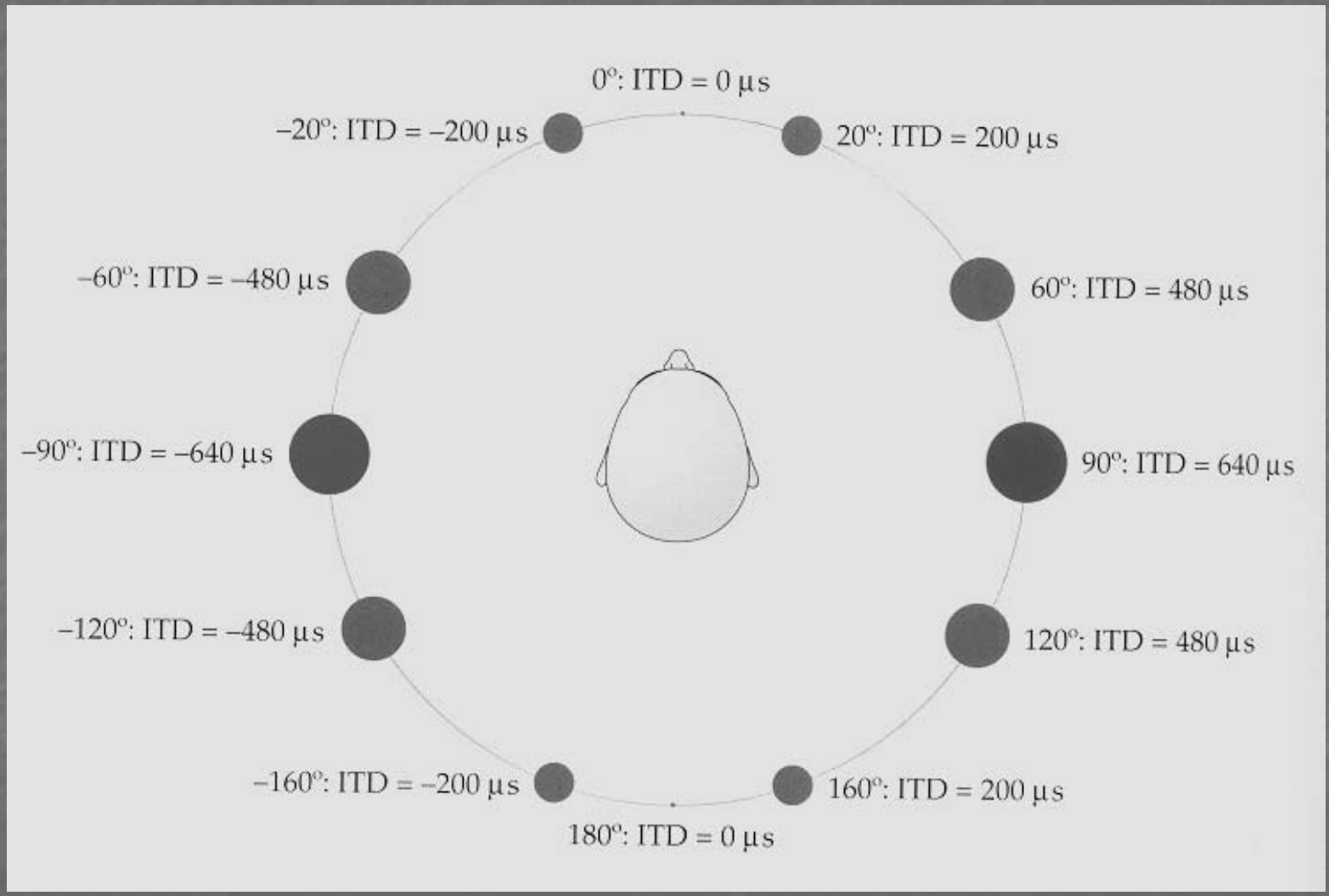

Po jediné synapsi se už dráhy kříží – na rozdíl od zraku. Synapse zdržují.

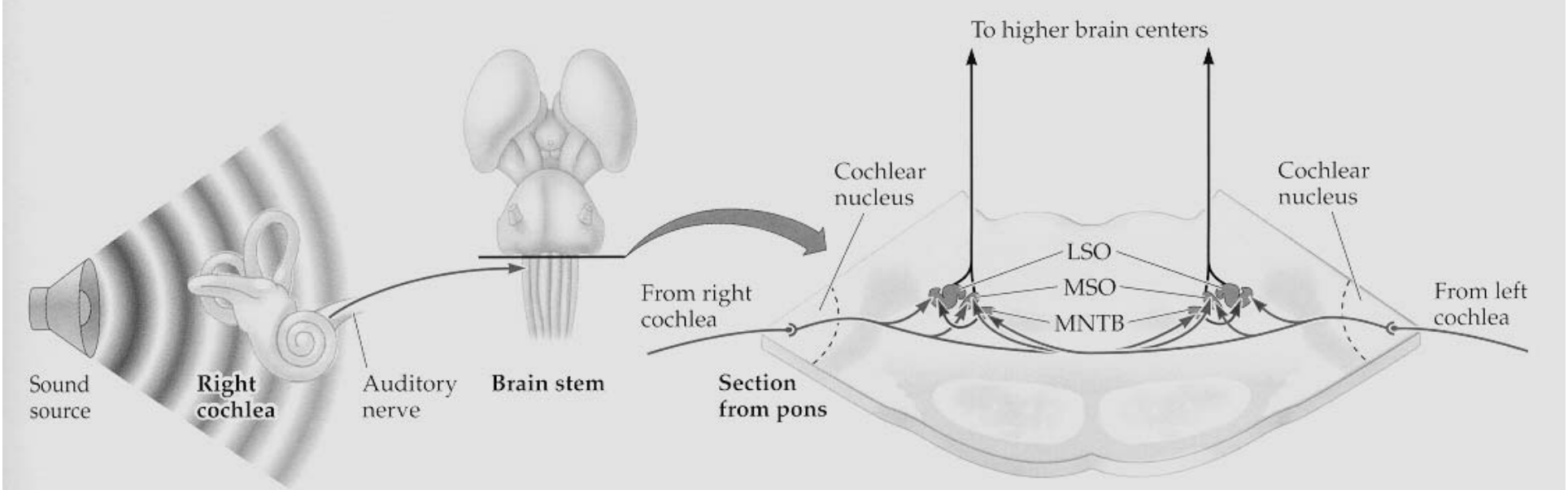

Medial Superior Olives (MSO) – časový rozdíl
Lateral Superior Olives (LSO) – intenzitní rozdíl

Vzdálenost zdroje – hlasitost
spektrální složení zvuku

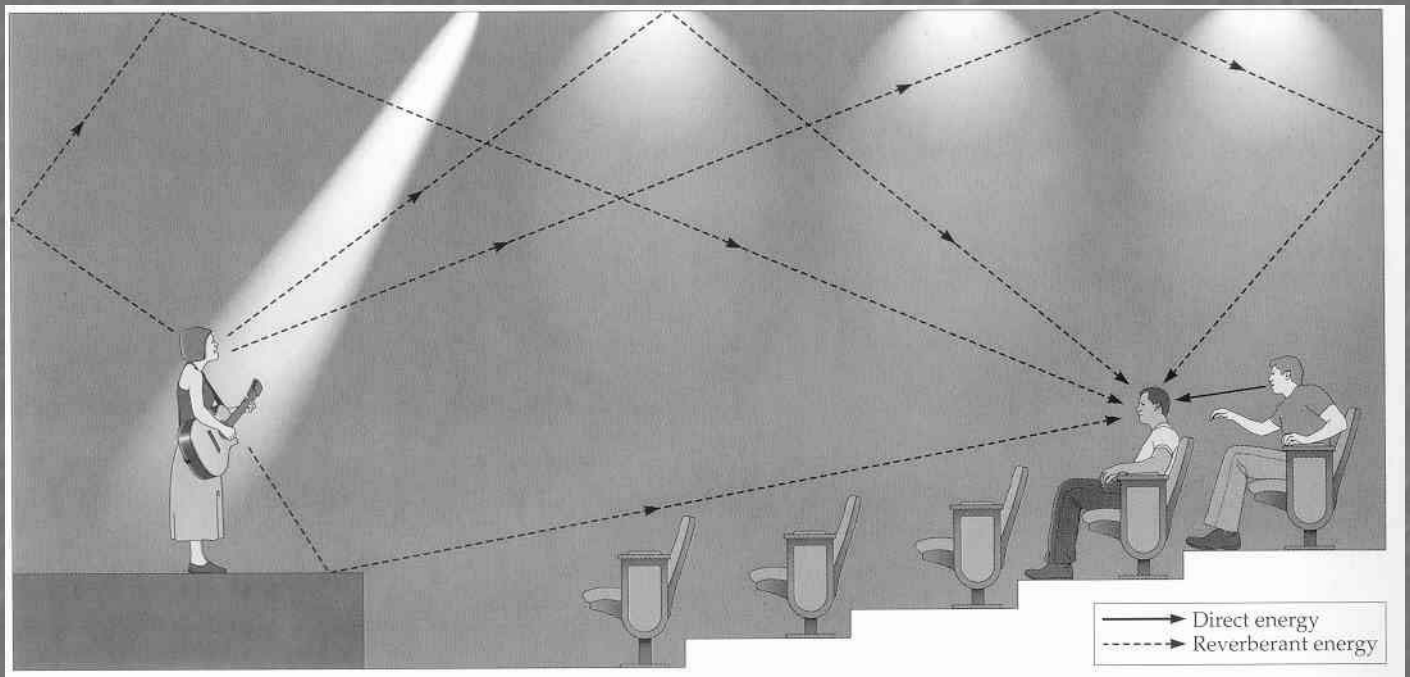

FIGURE 10.11 The relative amounts of direct and reverberant energy coming from the listener's neighbor and the singer will inform him of the relative distances of the two sound sources.

more like a "boom." Note that this auditory cue is analogous to the visual depth cue of atmospheric perspective (more distant objects look more blurry).

A final distance cue stems from the fact that, in most environments, the

Barvy zvuku

Komplexní tóny a
Fourierova analýza zvuku

Barvu tónů určuje spektrum

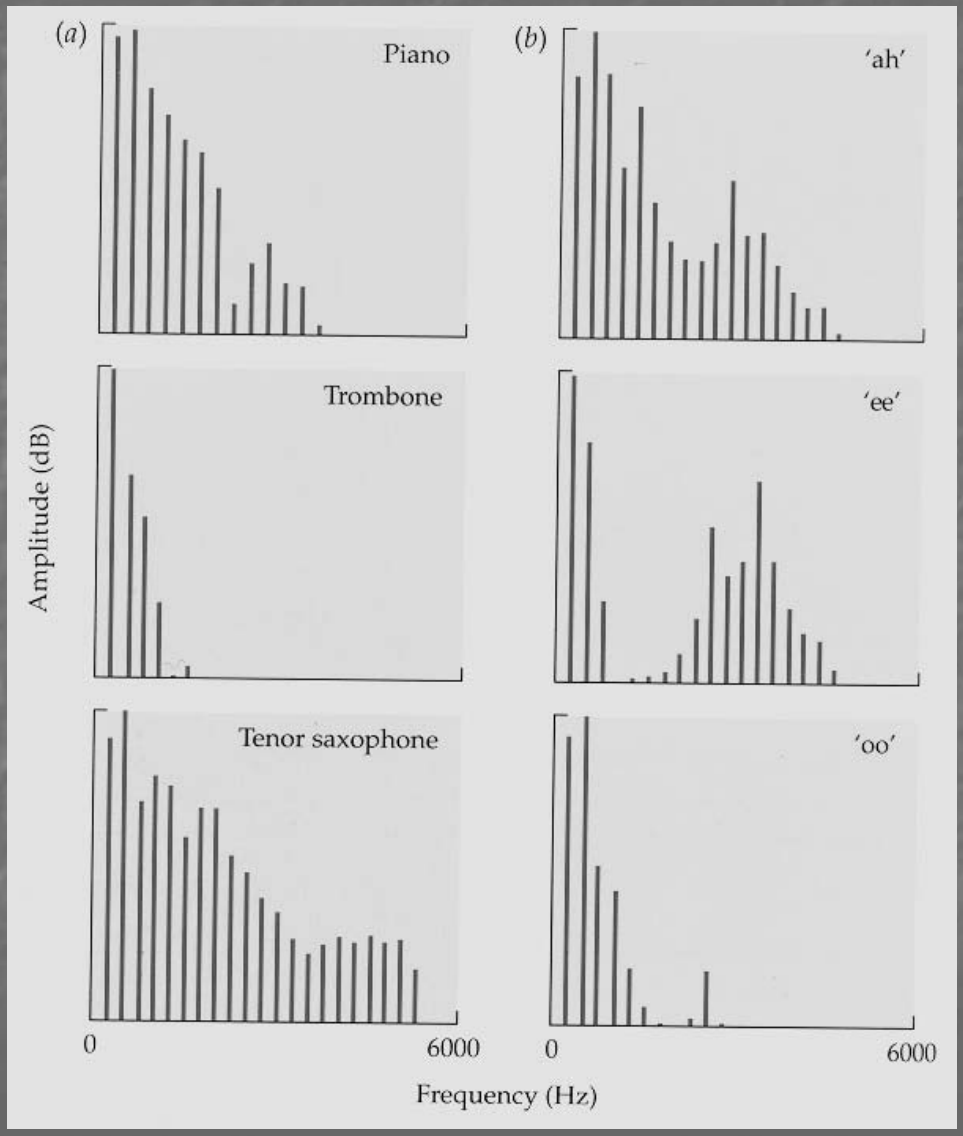

Harmonické frekvence

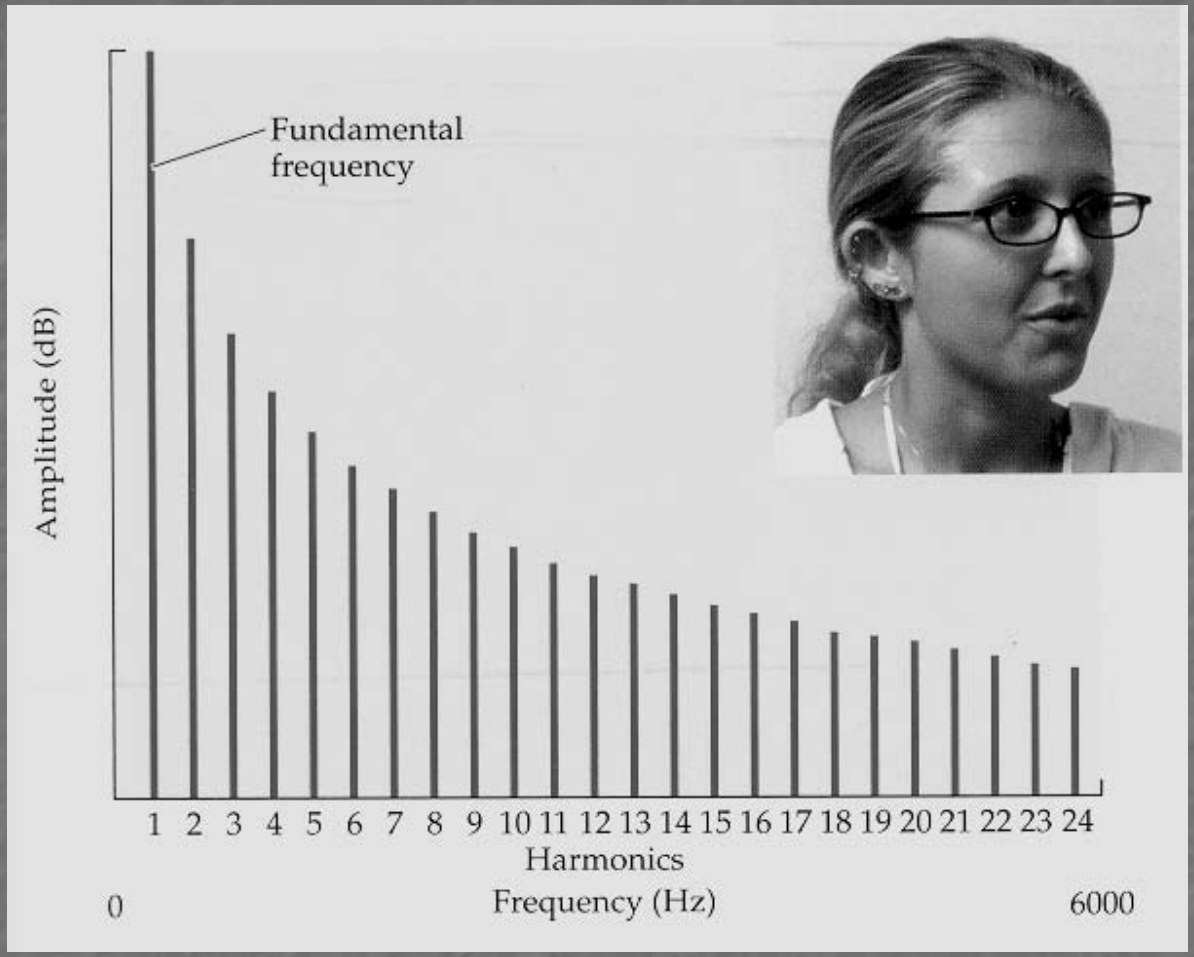

Většina zvuků má harmonické frekvence.

Harmonické frekvence
Výška tónu zůstane beze změny i když hlavní frekvence chybí!
Důležitější je vztah mezi harmonickými.

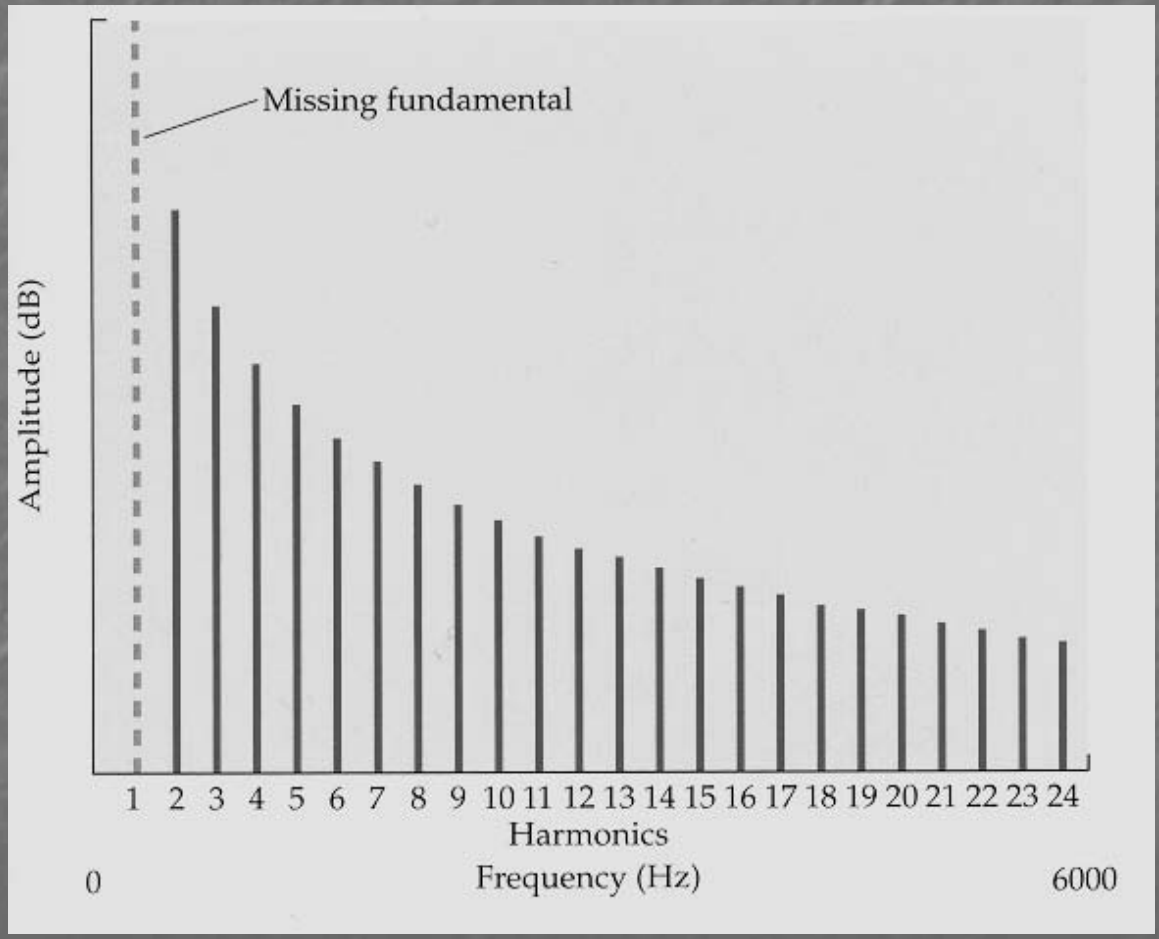

http://www.sinauer.com/wolfe/chap10/missingfundF.htm

Harmonické frekvence
Výška tónu zůstane beze změny i když hlavní frekvence chybí!

Po součtu se hlavní frekvence objeví.

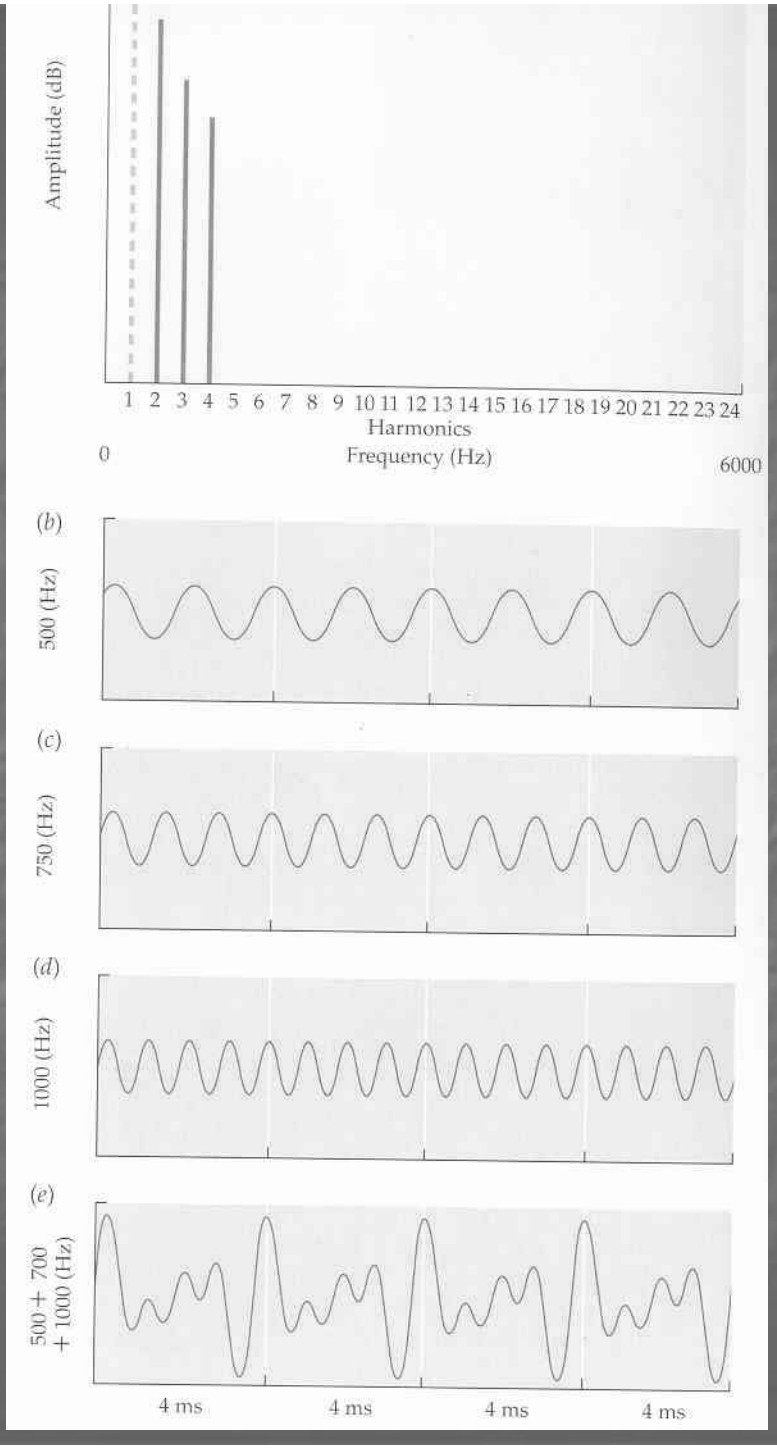

Nástup a konec zvuku rozhodují o vjemu. Jsou velmi důležité pro rozlišení hlásek (bill x will).

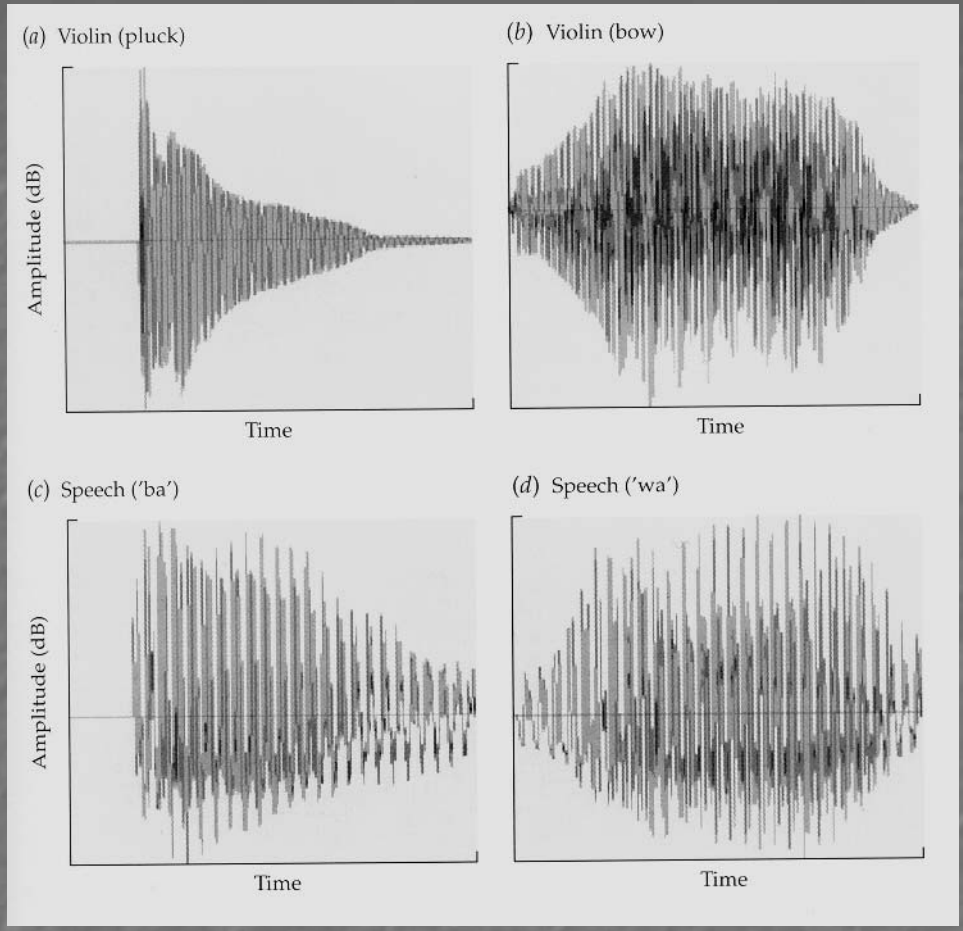

http://www.sinauer.com/wolfe/chap10/timbreF.htm

Přerušení zvuku na krátkou dobu není patrné – efekt doplnění

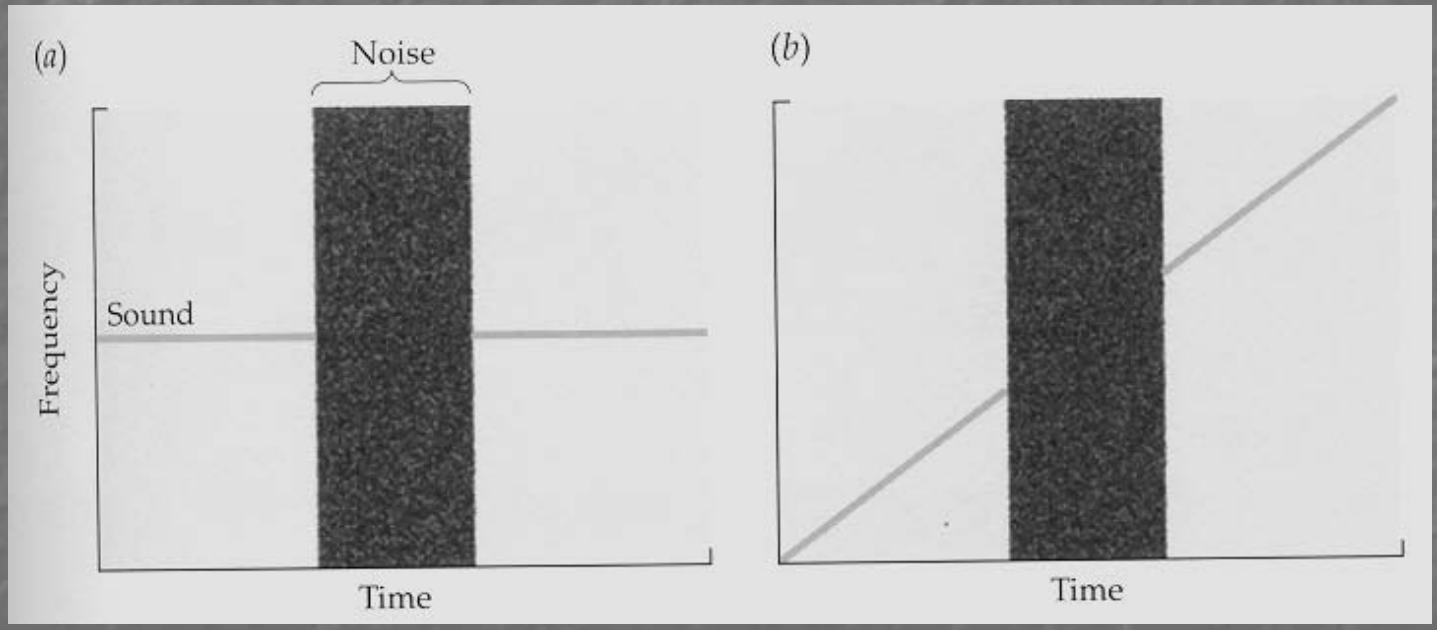

Přerušení věty – šum vadí porozumění méně než ticho. Ticho zvuk „roztrhá“

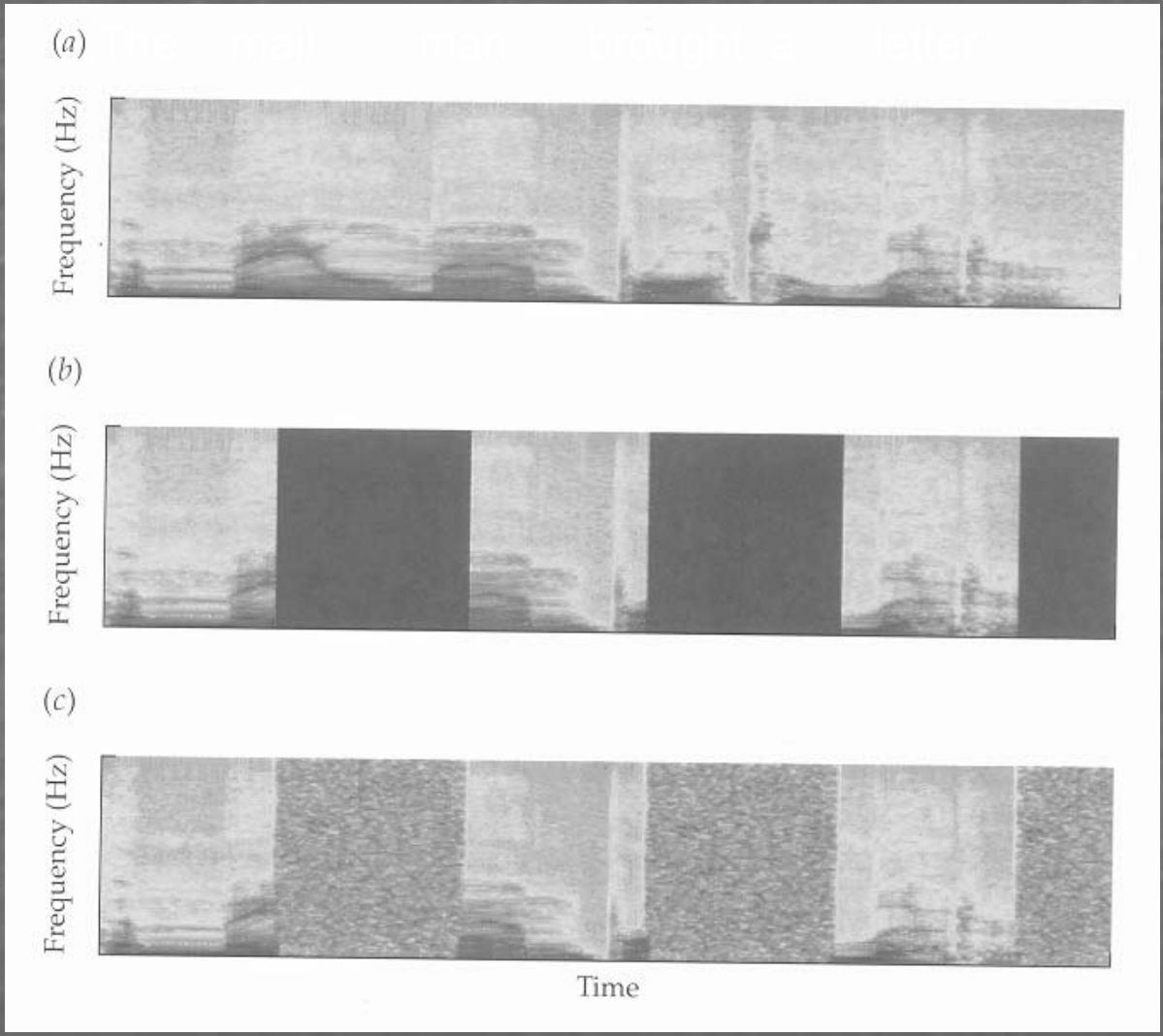

http://www.sinauer.com/wolfe/chap10/restorationF.htm

Rozlišování zdrojů zvuků-segregace.
Těžší než u zraku – vše v jednom.
Prostorové, spektrální a časová segregace.

Dvě samostané „linky“ –
dva samostatné zdroje (proudy) zvuku

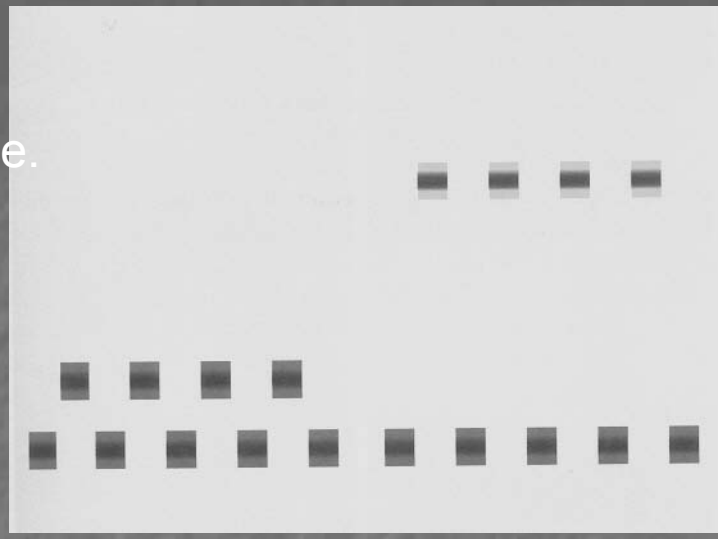

Dvě samostatné melodie

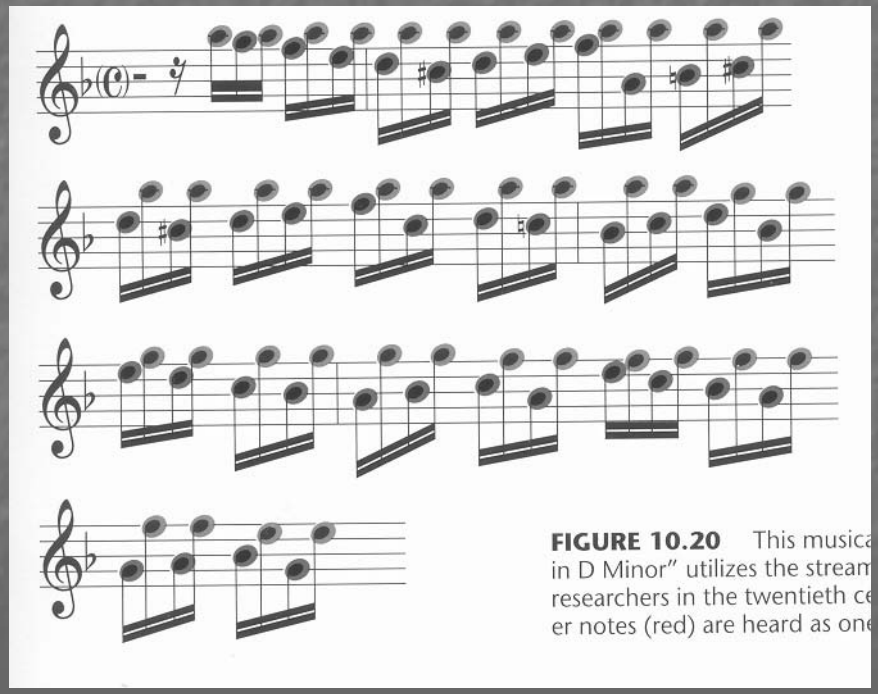

FIGURE 10.20 This musica
in D Minor" utilizes the stream
researchers in the twentieth ce
er notes (red) are heard as one

Percepce různých kategorií

Otoakustické emise, 2008

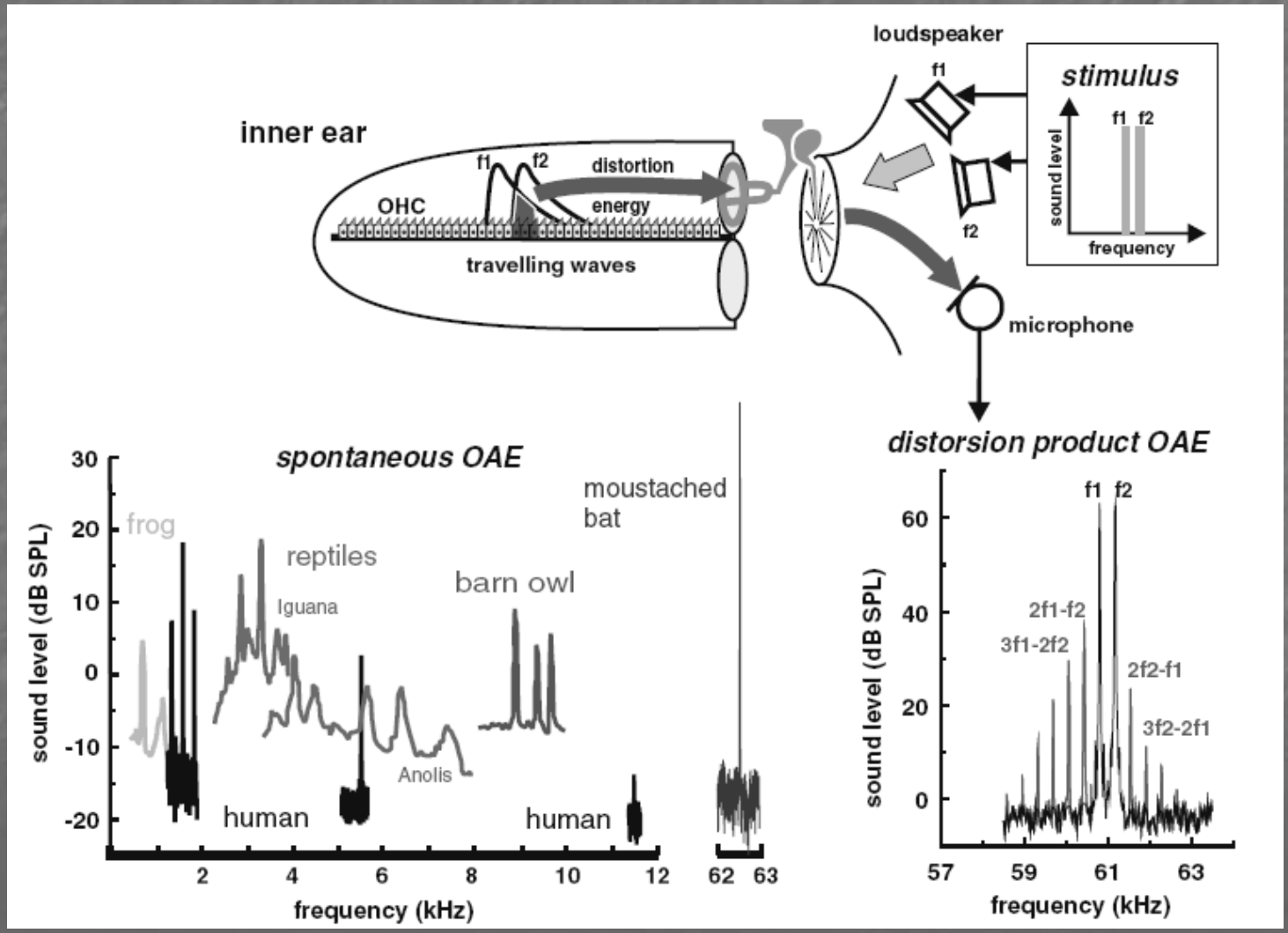

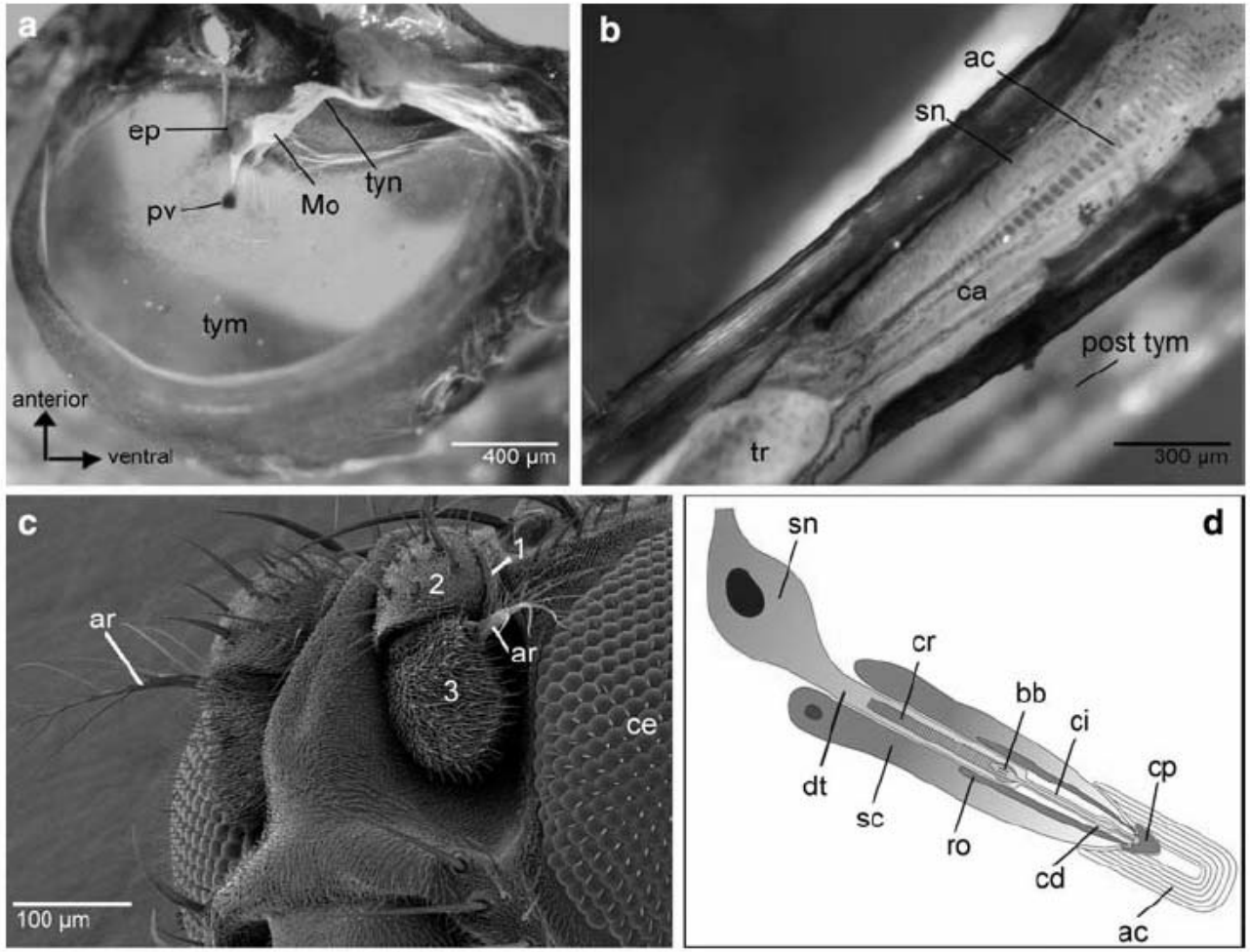

Fig. 2 Important anatomical features of auditory organs in insects. **a** Tympanal organ in the first abdominal segment of the locust (*Locusta migratoria*), inside view. The relatively large tympanum (tym) spans across a cuticular ring. The peripheral sensory ganglion (Müller's organ, MO) lies near the anterior edge, from where sensory dendrites reach out to sclerotized attachment points on the tympanum. The dendrites in the pyriform vesicle (pv) insert in a relatively thin membrane region, those of the elevated process (ep) in a thicker region; *tyn* tympanal nerve. **b** Tympanal organ of tropical bushcricket (*Mecopoda elongata*) in the opened foreleg tibia and after impregnation with methylene blue. The characteristic crista acustica (ca) extends along a branch of the acoustic trachea (tr). It comprises ca. 40 scolopidial sensory neurons and is part of a larger mechanosensory organ complex in the insect leg; *sn* sensory neurons; *ac* attachment cells; *post tym* posterior tympanum. **c** Scanning electronmicrograph of *Drosophila* head showing the two antennal hearing organs next to the compound eyes (ce). The branched arista (ar) is firmly attached to the third antennal segment (3); both oscillate in the acoustic near-field (see also Fig. 7); *1*, *2*, *3* segments of left antenna. **d** Schematic representation of a single scolopidium with bipolar sensory neuron and accessory cells. The dendrite (dt) of the sensory neuron (sn) runs out into a ciliated terminal (ci); *cd* ciliary dilatation; *ac* attachment cell; *sc* scolopale cell; *cr* ciliary root; *bb* basal body; *ro* rod; *cp* scolopidial cap

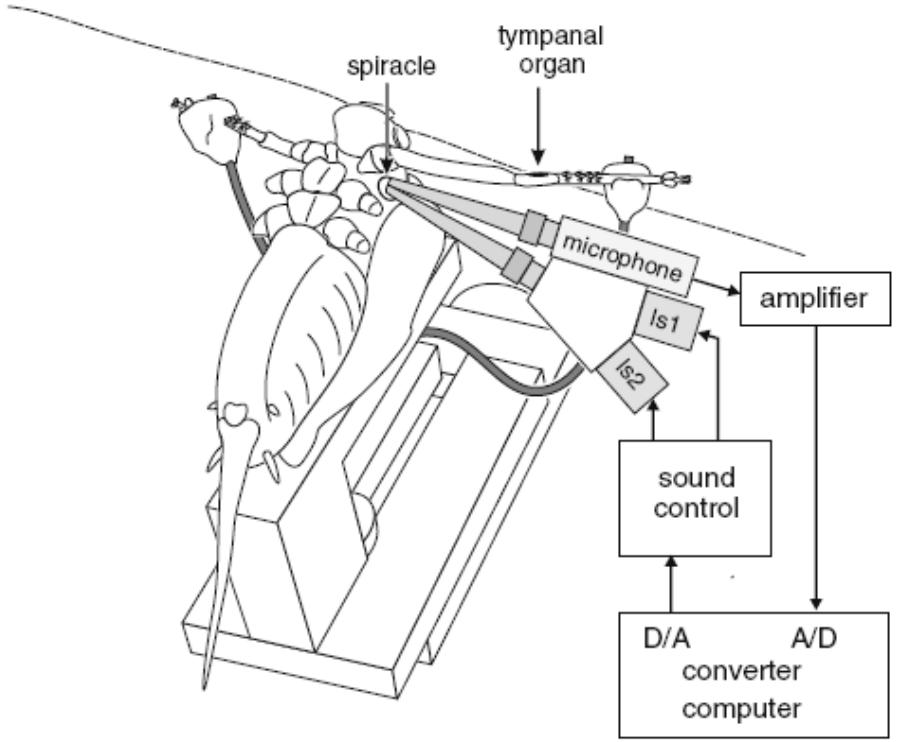

Fig. 3 Recording DPOAEs in the bushcricket *Mecopoda elongata*, experimental setup. The insect is secured to a metal holder and the forelegs fixed to two supports with beeswax. For acoustic stimulation, two pure-tone signals are generated via D/A-conversion and fed into two loudspeakers (ls1, ls2) following calibration and power amplification. Separation of the two stimulus channels is essential to preclude distortions in the technical sound-producing system. The resulting sound signal, which consists of the two stimuli as well as the DPOAE, is recorded via a microphone, then amplified and fed into a A/D converter. Sound-producing and sound-recording channels are gathered into a coupling device, whose tip is adapted to the diameter of the opening of the acoustic trachea (spiracle) in the prothorax of *Mecopoda*. One advantage of this arrangement is that the stimulating/recording device is applied to the prothoracic spiracle while the tympanal organ with its crista acustica remains freely accessible for experimental manipulations

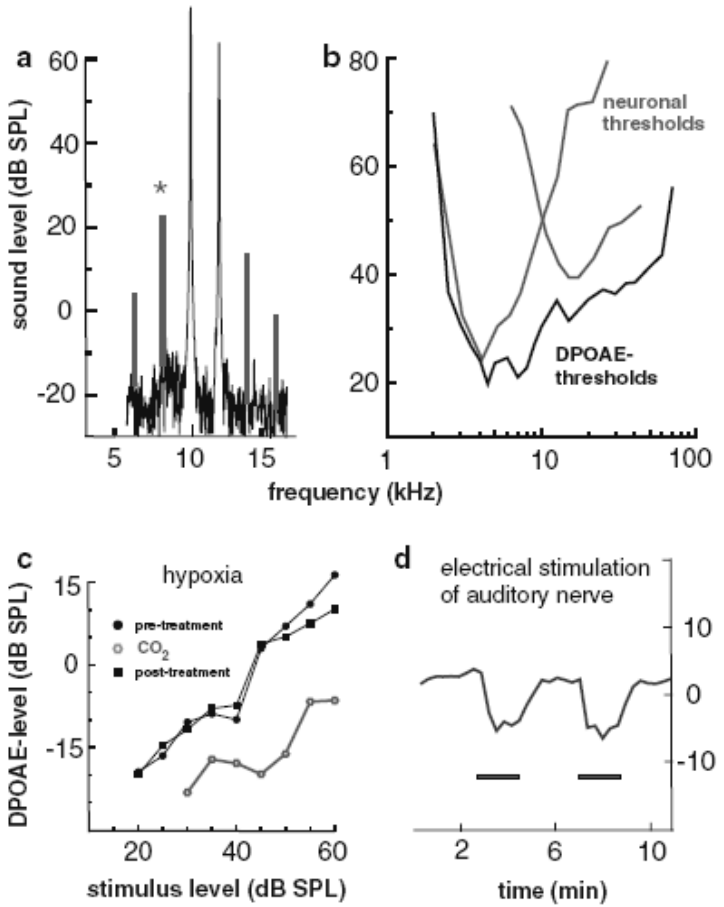

Fig. 4 DPOAE-measurements in the tympanal organ of the locust. **a** DPOAE-spectrum following two-tone stimulation with 10 and 12 kHz; distortion products (*peaks in red*) reach sound intensities that are clearly distinguishable from background noise. Asterisk denotes 2f1 − f2 distortion product. **b** Auditory threshold curves determined electrophysiologically for two groups of neurons (*in red*; adapted from Römer 1976) and expressed as sound intensity sufficient to elicit DPOAEs (*in black*; adapted from Kössl and Boyan 1998b) within the normal hearing range of locusts. **c** Reduction of DPOAE-levels following CO_2-treatment demonstrates the importance of active metabolic processes for generation of otoacoustic emissions (adapted from Kössl and Boyan 1998a, b). **d** Brief electrical stimulation of the auditory nerve (*horizontal bars*) causes transient reduction of emission levels (acoustic stimuli: 10.5/12 kHz with 60/50 dB SPL; electrical nerve stimulation: bipolar pulses of 10 µA, pulse frequency 200 Hz, pulse duration 2 ms; modified from Möckel et al. 2007)

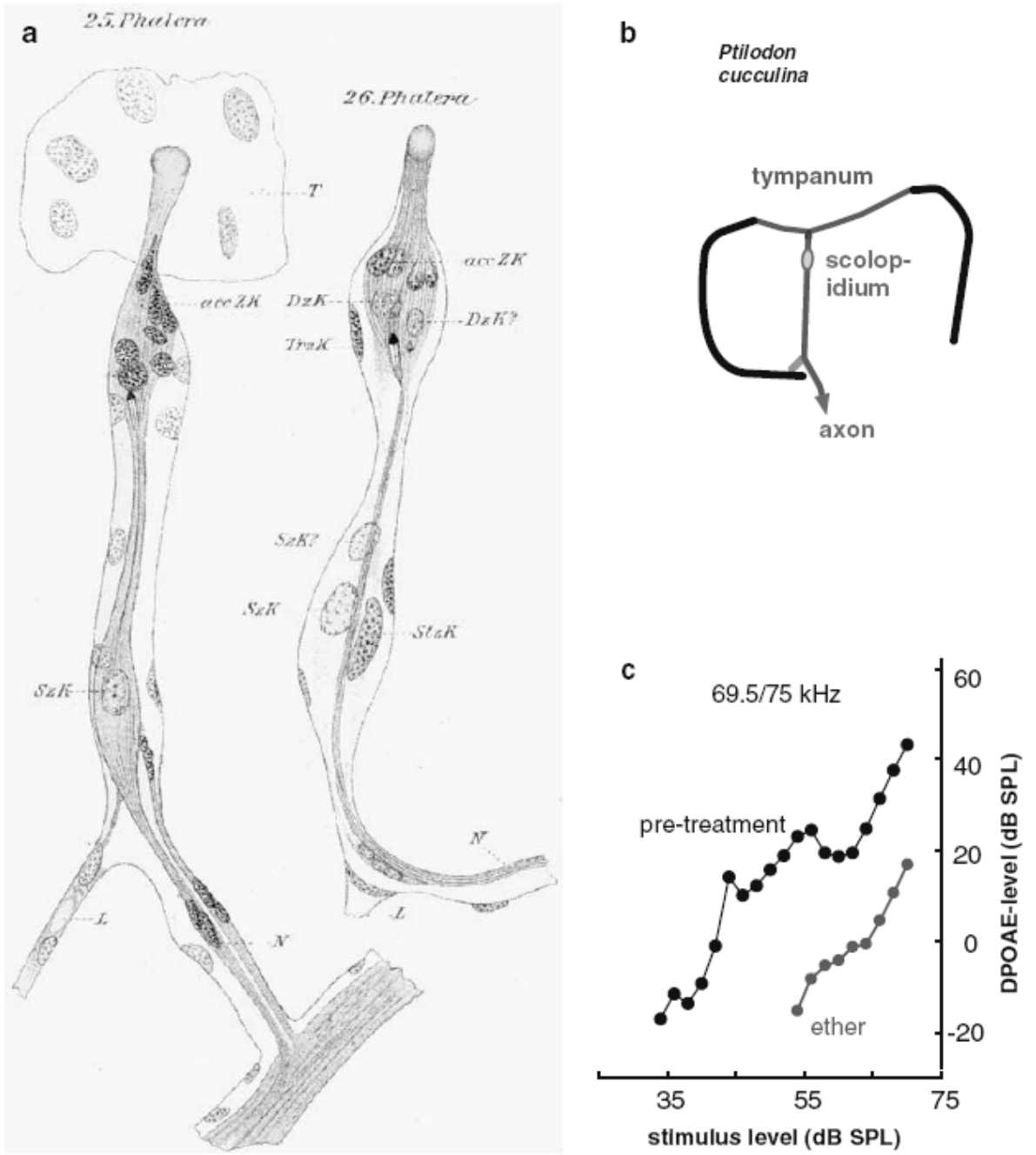

Fig. 5 The metathoracic tympanal organ of notodontid moths has only one auditory neuron; nonetheless, the ear produces distinct DPOAEs in the high frequency range. **a** Detailed drawings of Eggers (1919; plate 23)demonstrate that the tympanal scolopidium of the buff-tip (*Phalera bucephala*) comprises only one sensory neuron (*T* tympanum; *N* tympanal nerve; *L* ligament; remaining labels denote putative cell nuclei). **b** Schematized representation of the tympanal organ of notodontids; the scolopidial dendrite is attached to the tympanum. **c** DPOAE growth-functions in tympanal organ of another notodontid, the maple-prominent (*Ptilodon cucculina*), before and after treatment with ether acting as an anesthetic; the two sound stimuli were at 69.5 kHz (f1) and 75 kHz (f2) (modified from Kössl et al. 2007)

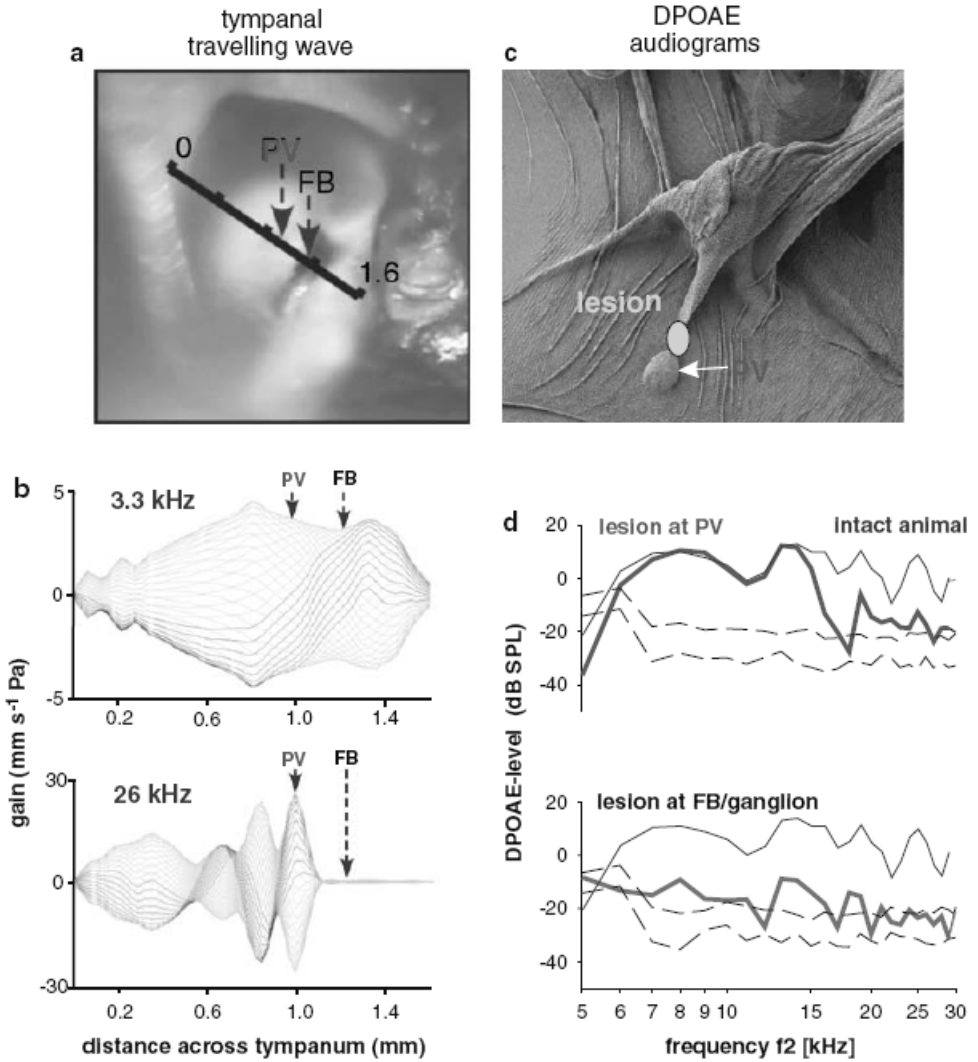

Fig. 6 Müller's organ of *Locusta migratoria*; travelling waves and DPOAEs before and after lesions. **a** External view of tympanum; *diagonal line* indicates measuring points (in mm) for laser-vibrometric recordings of tympanic vibrations. *Arrows* mark position of pyriform vesicle (PV) and of folded body (FB). **b** Stimulation with pure tones generates vibration patterns that resemble travelling waves across measuring points. Low frequency stimulation (at 3.3 kHz) causes displacements of PV and FB, while high-frequency stimulation (at 26 kHz) generates amplitude maxima at the PV without displacing FB. **c** Internal view of locust tympanum showing Müller's organ and PV (scanning electronmicrograph). The PV was severed from Müller's organ by setting a lesion through the dendritic attachments (*yellow spot*). **d** DPOAE-levels at sound stimuli of constant intensity and varying frequency (f2), i.e., so-called DP-gram (f2/f1 ratio maintained at 1.08; L1/L2 of 60/50 dB SPL). *Upper:* following a lesion at PV, DPOAE-levels above ca. 15 kHz (*red curve*) drop nearly to noise level (*dashed black lines* noise level expressed as the average (±1SD). *Lower:* subsequent lesion of FB and of Müller's organ itself (in the same preparation) cause a marked reduction of DPOAE-levels across the entire frequency range. The results indicate that high-frequency DPOAEs are only generated as long as the connection between sensory neurons and PV remains intact (**a**,**b** modified from Windmill et al. 2005; **c**,**d** modified from Möckel et al. 2007)

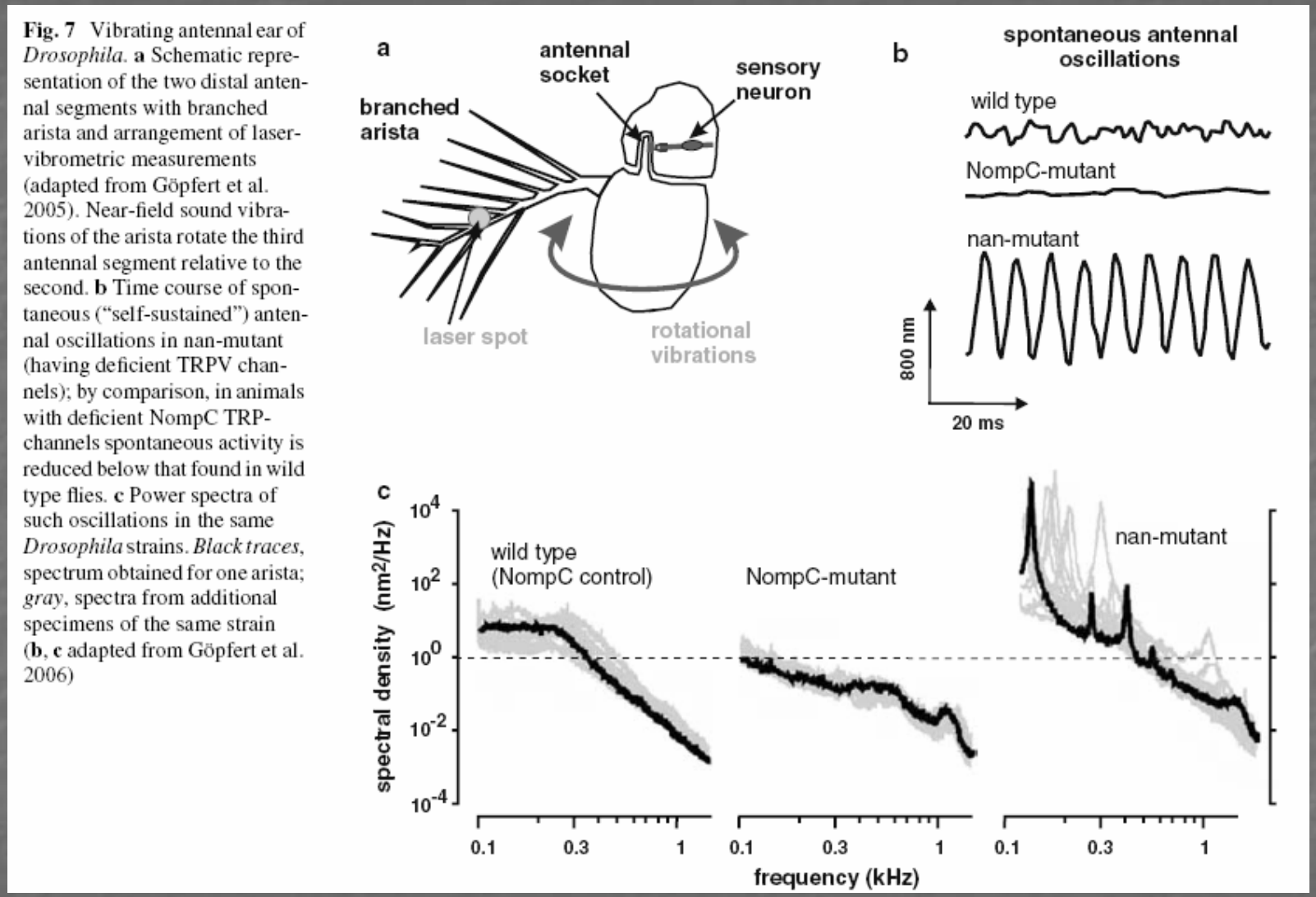

Fig. 7 Vibrating antennal ear of *Drosophila*. **a** Schematic representation of the two distal antennal segments with branched arista and arrangement of laser-vibrometric measurements (adapted from Göpfert et al. 2005). Near-field sound vibrations of the arista rotate the third antennal segment relative to the second. **b** Time course of spontaneous ("self-sustained") antennal oscillations in nan-mutant (having deficient TRPV channels); by comparison, in animals with deficient NompC TRP-channels spontaneous activity is reduced below that found in wild type flies. **c** Power spectra of such oscillations in the same *Drosophila* strains. *Black traces*, spectrum obtained for one arista; *gray*, spectra from additional specimens of the same strain (**b**, **c** adapted from Göpfert et al. 2006)

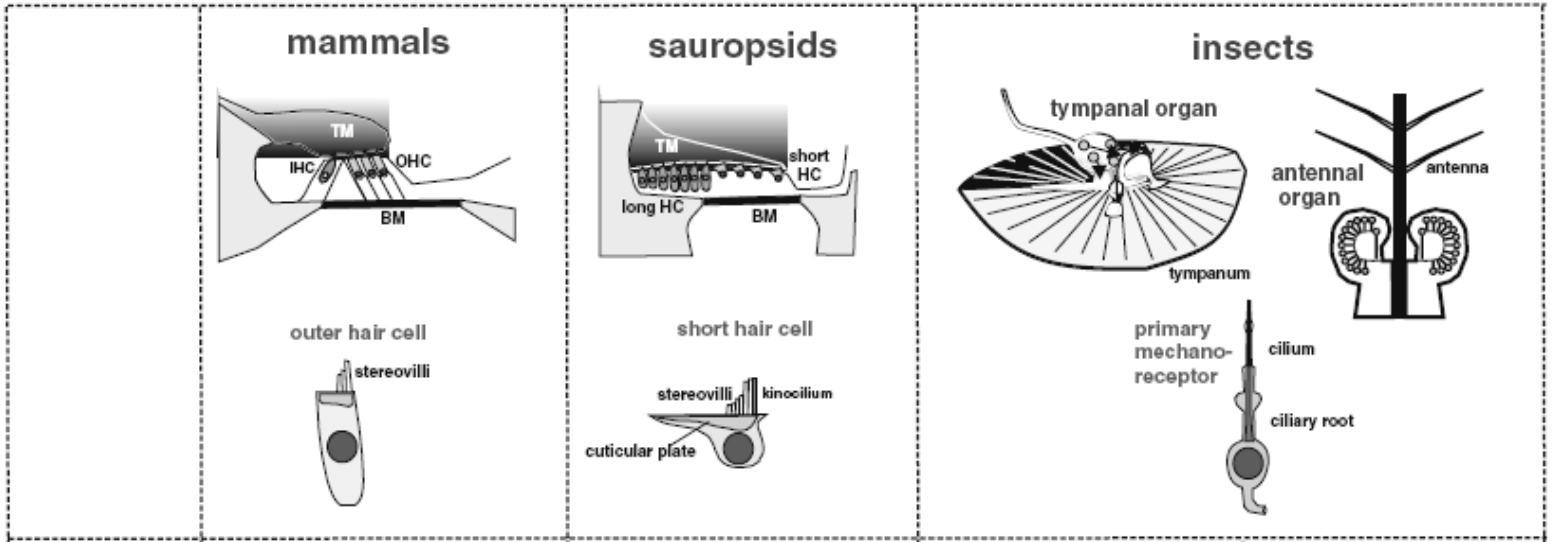

	mammals	sauropsids	insects	
hearing range	10 Hz - >200 kHz	80 Hz - 11 kHz	1 kHz - 100 kHz	100 - 1000 Hz
spontaneous OAE	some species 0.5 - 62 kHz up to 40 dB SPL	some species 0.8 - 11 kHz up to 25 dB SPL	?	spontaneous vibrations 100 - 1000 Hz
DPOAE-sensitivity	ca. -3 dB SPL	ca. 10 dB SPL	ca. 12 dB SPL	?
cell soma motility	70 kHz	negative	?	?
motile cilia/ stereovilli	$\leq$ 3 kHz (force generation)	bis ~3 kHz (electr. evoked OAE)	?	?

Fig. 8 Comparing the ears of mammals, sauropsids, and insects: fundamental anatomical and bio-acoustical parameters. Hearing ranges are indicated without considering infra-sound perception. DPOAE-sensitivities are listed for minimal stimulus-levels that are just sufficient to evoke DPOAEs of −10 dB SPL. *IHC* inner hair cell; *OHC* outer hair cell; *TM* tectorial membrane; *BM* basilar membrane. Data sources: Frank et al. 1999 (motility of OHC-somata); Ricci et al. 2002 (motile stereovilli in mammalian cochlea); Manley et al. 2001 (electrically evoked OAEs in reptiles); Manley et al. 1993 (DPOAEs in lizards). See text for detailed discussion

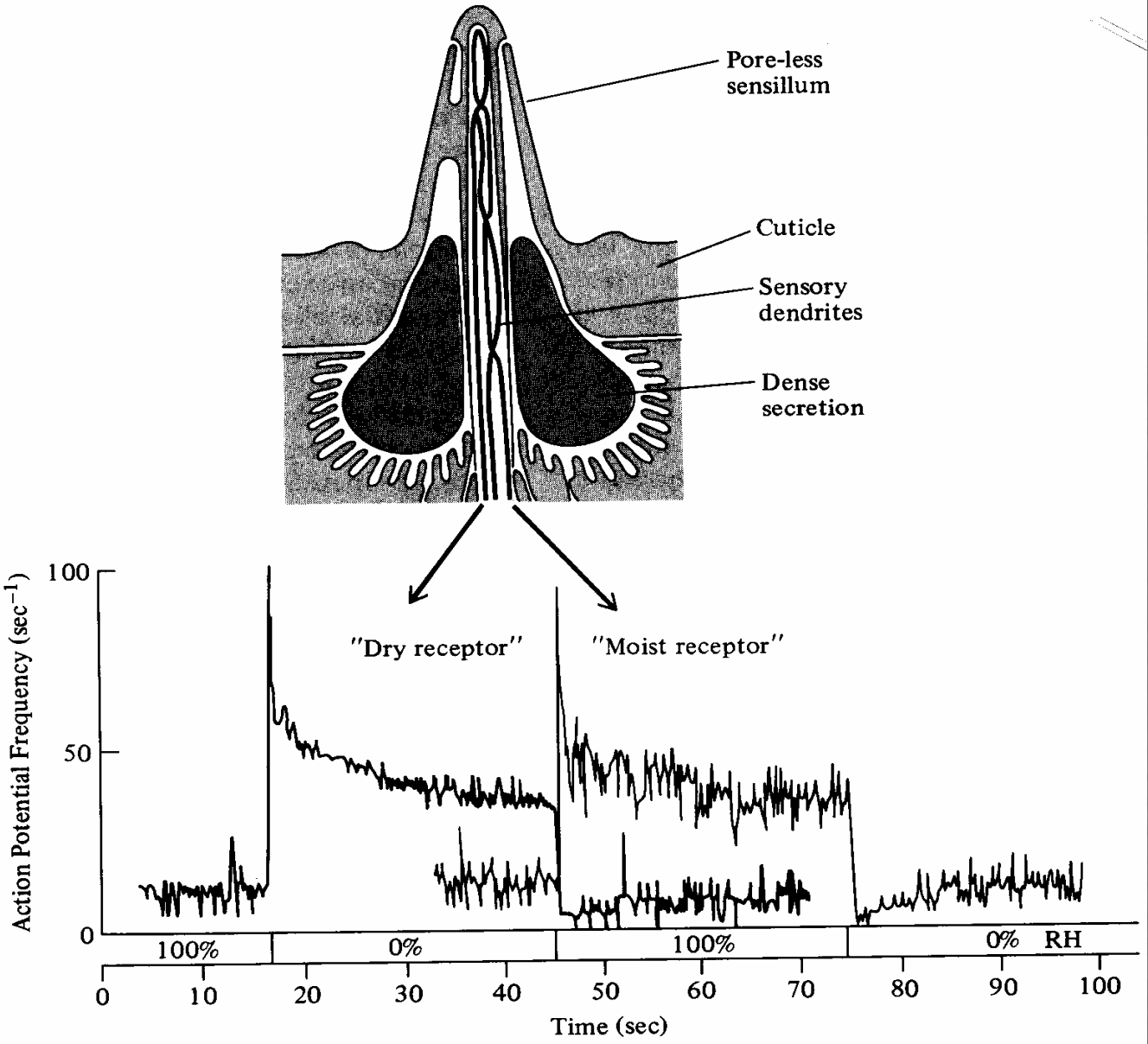

FIGURE 7–18 The "cold-moist-dry" triad sensory sensillum of the cockroach contains three bipolar sensory neurons; one neuron of the hygroreceptor responds to high humidity ("moist" receptor) and one to low humidity ("dry" receptor). The receptor cavity of the poreless sensillum is filled with a dense secretion. *(Modified from Yokohari and Tateda 1976; Schaller 1978.)*